NIH/TR/2021-22

A Technical Report

Evaluation of seasonal extreme rain events across river basins of India in 3D global temperature change scenario

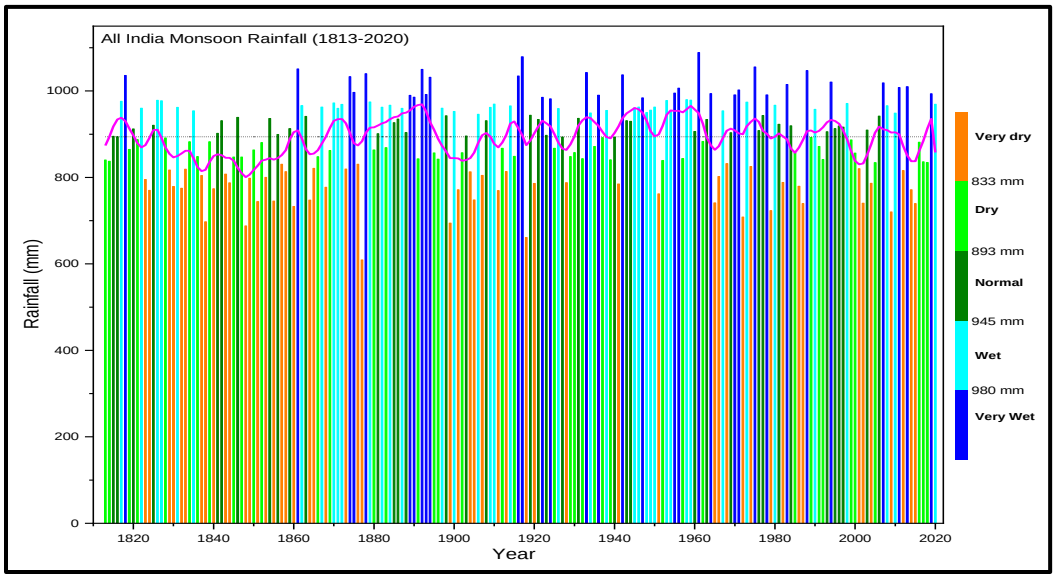

Project Team

Name of PI: Dr. Ashwini Ranade

Name of Co-PI: Dr. Archana Sarkar

आपो हि ष्ठा मयोभुवः

National Institute of Hydrology

Deptt. of WR, RD & GR,

Ministry of Jal Shakti, Govt. of India

Jal Vigyan Bhawan, Roorkee - 247667 (Uttarakhand), INDIA

Year 2018-21

CONTENTS

Summary:

Basin-scale monthly rainfall series for 11 major basins, 9 minor basins, the West Coast Drainage System, and All-India were extended from 1813–2000 (basin-specific start years) to 2020 using 1° gridded daily rainfall (2001–2020) and the ratio method. Annual and seasonal rainfall climatology and variability were analysed for basins and homogeneous zones. Short- (15-year), medium- (31-year), long-term (51-year), and secular (101-year) tendencies were examined using Cramer's t_k statistic. Rainfall was classified into five categories (very dry to very wet) using quintiles, enabling identification of distinct monsoon rainfall epochs. Normal (1901–2000) annual rainfall ranges from 487.7 mm (Luni) to 2519.5 mm (Surma). Over 1920–2020, significant monsoon rainfall increases are observed over Krishna (2.9%), Tapi (4.2%), the West Coast system (2.9%), and All-India (1.3%) relative to the preceding period. In contrast, 2001–2020 shows significant monsoon rainfall declines compared to 1901–2000 over Ganga (−6.6%), Brahmaputra (−7.6%), Cauvery (−18.7%), Brahmani (−12.9%), and Pallar–Ponniyar (−19.7%), while Surma increases (+7.9%). Overall, recent decades indicate reduced monsoon rainfall over northeast and parts of southeast peninsular India, and increased rainfall over central-northwest, north peninsular, and northern India.

At the zonal scale, normal (1901–2000) annual rainfall across seven homogeneous zones ranges from 775.2 mm in Northwest India (NWI) to 2159.6 mm in Northeast India (NEI). During 2001–2020, monsoon rainfall declines significantly over North-Central India (NCI; −9.7%) and NEI (−7.3%), while annual rainfall decreases significantly over NCI (−9.6%), North Mountainous India (NMI; −12.9%), and NEI (−9.4%). The precipitation concentration index (PCI) indicates strong seasonality: rainfall is relatively uniform over South Peninsular India (SPI) but highly concentrated over NWI. While PCI shows no robust long-term trend nationally, recent decades indicate greater concentration of annual rainfall over NMI, NEI and East Peninsular India (EPI), and of monsoon rainfall over NEI, into fewer intense spells. Spectral analysis suggests that interannual variability is dominated by short-term fluctuations (~75%), followed by decadal (~15%) and long-term (~10%) components. Large-scale extreme rainfall events (1–10 days) were also analysed over 1951–2020 using event intensity (ERE-RI) and cumulative amount (ERE-RA). Mean 1-day intensity ranges from 20.3 mm (NWI) to 45.2 mm (NEI), while mean 10-day intensity varies from 9.8 mm (NMI) to 24.5 mm (NEI). Mean 10-day cumulative rainfall ranges from 97.8 mm (NMI) to 245.1 mm (NEI). Significant increases are found in 1-day ERE rainfall over West Peninsular India (WPI), EPI and NMI, whereas 7–10 day ERE intensity and amount decrease significantly over NCI.

Three-dimensional thermal structure changes were analysed at 37 pressure levels using CFSR-2 reanalysis temperatures (1979–2018) across global, hemispheric, zonal (9 climate zones) and regional (54 macro-geodomains) scales. A consistent significant warming is detected in column-mean temperatures of the lower troposphere (1000–700 hPa), upper troposphere (600–250 hPa) and the full troposphere (1000–250 hPa) over the globe, both hemispheres, and all climatic zones. Tropospheric warming is stronger in the Northern Hemisphere (0.30°C/decade) than the Southern Hemisphere (0.20°C/decade), with the fastest increase over the Northern Polar zone (0.37°C /decade) and the weakest over the Southern Polar zone (0.05°C /decade). Over the most recent decade, tropospheric temperature rose by ~0.50°C globally (0.57°C in NH; 0.42°C in SH). Among the 54 geodomains, the largest lower-tropospheric warming occurs over the eastern Northern Polar region (+1.22°C), upper-tropospheric warming over South Africa (+0.96°C), tropopause warming over equatorial Southeast Asia (+0.65°C), and notable stratospheric warming over the Indian subcontinent and adjacent oceans. Enhanced NH tropospheric warming increases inter-hemispheric thermal asymmetry, potentially favouring a westward shift of monsoon circulation, with stronger monsoon activity over northern/northwestern India and weaker conditions elsewhere.

Atmospheric anomaly patterns were examined for the four most extreme wet and dry monsoon months (June–September) during 1979–2015, and for 1–10 day extremes across seven subzones. Wet months are characterised by a warmer, deeper subtropical Asian column (especially over the Tibet–Himalaya) and widespread negative pressure anomalies over the equatorial–tropical Pacific and Asian landmass, extending poleward. In contrast, dry months show a cooler, thinner subtropical Asian column with positive pressure anomalies dominating the Asia–Pacific region. Case studies of 1–10 day extreme rainfall events indicate that rapid monsoon intensification—linked to persistent upper-

tropospheric warming from the Tibet to Turkey sector and a strengthened ridge in the upper-level westerlies—can trigger severe rainfall events of varying spatial and temporal scales across India.

The evolving relationships between rainfall and global climatic indices are underscored. The Southern Oscillation Index (SOI), Arctic Oscillation (AO), Niño3.4 and Pacific Decadal Oscillation (PDO) are most influential indices across basins, mostly show stronger relationship in June and September compared to July and August. Over time, AO and SOI maintained significant positive relationship and Niño3.4 inverse relationship with ISMR while, the AO-ISMR link weakened post-1980s indicating shift in traditional teleconnections with climate change. Northern and eastern basins, exhibit strong correlations with the warming over eastern and central Afro-Asian highlands, while southern basins influenced by equatorial climate dynamics. The findings emphasize the need for region-specific model predictions and localized adaptive water management strategies.

Introduction:

Heterogeneous warming of global troposphere in last few decades are observed to make changes in spatio-temporal characteristics of rainfall across the country. Potential climate change and its impacts on rainfall distribution pose a threat to water resources throughout the world. Changes in patterns of extreme floods and droughts as well increase in the extreme rain events are well documented. events (Senior et al. 2002; IPCC 2007, Goswami et al. 2006; Rajeevan et al. 2008; Guhathakurta 2011; Ranade and Singh 2014). The Intergovernmental Panel on Climate Change in their recent sixth assessment report (IPCC, 2021) projected that i) South Asian summer monsoon precipitation decreased over several areas since the mid-20th century (high confidence) but is likely to increase during the 21st century, with enhanced inter-annual variability; ii) Extreme rainfall are projected to be intensifies by 7% for each additional 1ºC due to acceleration of hydrological cycle in warmer climate across the globe and become more frequent mostly in Africa and Asia; iii) the proportion of intense tropical cyclones (categories 4-5) and peak wind speeds of the most intense tropical cyclones are projected to increase at the global scale with increasing global warming. The report also highlighted that, 'It is indisputable that human activities are causing climate change, making extreme climate events, including heat waves, heavy rainfall, and droughts, more frequent and severe. As reported by the IPCC, the Indian subcontinent will be adversely affected by enhanced climate variation, rising temperature, and substantial reduction in summer rainfall with water stress in some areas by 2020. After general acceptance of global warming a reality, numerous studies have been undertaken to generate information useful for the assessment of water resources and hydro-meteorological disasters in order to comprehend the impact of climate change. It has been seen that, annual, seasonal, and monthly rainfall across India shows strong spatiotemporal variation and large departures from normal. Many of the studies show an overall decreasing trend in monsoonal rainfall over a major part of the country. Earlier we have studied climatological and fluctuation features of parameters of the hydrological wet season in 11 major and 36 minor river basins in India. We did not find any significant long term trends in wet season parameters for any basin, but noticed a declining tendency in wet season rainfall in some major basins of the Central India (Ranade et.al. 2008). Numerous studies have reported the rising frequency in short period extremes especially in Central India and attributed to the significant increase in synoptic activities, convective instabilities' etc. We have studied variations in spatio-temporal extreme rainfall fields over the Indian region. It is shown that small-scale, short-duration EREs are embedded in large-scale, long-period intense wet spells, and rainwater generated during the main monsoon wet period is highly correlated with the Asia-Pacific monsoon intensity (Singh and Ranade 2010). Few intense rain spells, consequently heavy flooding and disasters occur across the country even in dry monsoons. At such times sudden intensification of the monsoon circulation is seen associated with anomalous warming of the upper troposphere between Tibet

and Turkey sector and development of strengthened ridge in upper tropospheric westerlies over there. Few case studies of extreme rain events carried out by us (Ranade and Singh 2019 & 2021) revels that, abrupt warming and cooling in the atmosphere drastically modulates the monsoon circulation and intensify the associated weather systems causing heavier rains over a region. Persistence in temperature and circulation anomalies across the globe are strongly linked to the occurrences of severe rain events over a wide-ranging scale from small-scale short-period heavy rain events to large-scale long-period extreme wet spells. Locations of warming and cooling across the globe are the determinant of the plausible locations for the origin of various type of weather systems. Types of weather systems and general and monsoonal circulation associated with the occurrence of extreme rain events in different parts of the country could be different. There is pressing need to understand the climatic changes in 3-D structure of global temperature. Keeping in mind, recent changes in global atmospheric thermal structure, monsoon circulation pattern, and occurrence of EREs, we have studied the rainfall variability in annual and seasonal rainfall of 11 major basins, 9 independent minor basins and 7 homogeneous zones across India and associated 3-D structure of global temperature.

Major Objectives:

1. To uncover long-term trends and spatio-temporal variability and dominant modes in annual and monsoon rainfall of 11 major, 9 independent minor basins, as well as the West Coast Drainage System (WCDS) and 7 homogeneous zones in India using the longest instrumental rainfall series.
2. Identification of different types of seasonal large-scale extreme rain events concerning rainfall amount, rainfall intensity and duration over seven homogenous rainfall zones of India during 1951-2020.
3. To investigate the influence of global climatic indices on rainfall variability at the river basin scale and analyze the evolving relationships between them under the influence of global warming.
4. Evaluation of 3D global atmospheric parameter changes conducive for the occurrence of large-scale extreme rain events over seven homogeneous rainfall zones during different seasons.
5. To understand the impact of global tropospheric warming on rainfall distribution and variability of each river basin.

Section-I

Statistical and Fluctuation Characteristics of Longest Instrumental Rainfall Series of Major and Minor River Basins.

The longest instrumental area-averaged monthly rainfall series for 11 major river basins and 36 minor river basins earliest available from 1813 to 2000 (Sontakke and Singh, 1996) are used in this study. Preparation of the series has been done based upon the classification of the country's river systems into major and minor basins by K. L. Rao (1975). Longest rainfall series is available for 11 major basins and 36 minor basins and the west coast drainage system. Twenty-seven of the 36 minor basins are the sub-basins of five major basins- the Indus 3 (Chenab, Beas and Satluz), the Ganga 13 (Yamuna, Ramganga, Gomati, Ghaghara, Gandak, Kosi, Mahananda, Chambal, Sind, Betwa, Ken, Tons and Son), the Brahmaputra 3 (Tista, Brahmaputra and Dhansiri), the Godavari 5 (Wainganga, Wardha, Penganga, Godavari and Indravati) and the Krishna 3 (Bhima, Krishna and Tungabhadra). The other nine minor basins are Luni, Surma, Kasai, Damodar, Suvarnarekha, Brahmani, Penner, Palar & Ponnaiyar and Vaigai. The Sabarmati, the Mahi, the Narmada, the Tapi, the Mahanadi and the Cauvery are the major basins without any distinct minor basin on the 1:1M scale map of India. For the updation of the monthly rainfall series 11 major basins and 9 independent minor basins were selected. 1º X 1º gridded daily rainfall data from India Meteorological Department from 1951-2020 is used for the updation of the monthly rainfall series of river basins up to 2020.

1. Brief Physical and Climatological information of river basins

Brief physical features, physiographic characteristics and climatological information of 11 major basins and 9 independent minor basins till 2020 are given in order. The WCDS is given thereafter. Table 1.1 lists important information (e.g. drainage area, river length, no. of rainguages considered, mean annual and monsoonal rainfall, annual water potential, utilizable water, storage capacity of the basin, no. of dams and other water assets) about all the basins, the WCDS and the whole country. Table 1.2 describes the land-use land-cover statistics (e.g Buildup land, Agricultural land, forest, grassland, wasteland, waterbodies, snow/glacier coverage etc.) for all major river basins, WCDS and country as a whole. Table 1.3 and 1.4 documents the basic statistical parameters (e.g. mean, sd, median, cv, highest and lowest) calculated for the period 1901-2000 for annual and monsoon rainfall respectively.

1.1 The Indus Major Basin:

The Indus rises in the Tibet near the Mansarovar Lake at an elevation of 5,180 m, passes through northern Kashmir and Gilgit, enters Pakistan and emerges out of the hills near Attock. The major tributaries are the Kabul, the Swat and the Kurram from the west and the Jhelum, the Chenab, the Ravi, the Beas and the Satluz from the east. Earliest rainfall record for Sirsa and Ferozepur is available from 1844 and for all the 19 raingauges of the selected network from 1901 onwards. Mean annual and monsoonal rainfall over the basin is 860.4(±172 mm) and 619.5(±164.7 mm) respectively. The coefficient of variation (CV) is 20% and 26.6% for annual and monsoon rainfall respectively. The highest rainfall in a year is 1399.5mm and lowest is 508.4mm.

1.2 The Ganga Major Basin:

The Ganga originates near the Gangotri glacier (Uttar Kashi district, Uttarakhand) at an elevation of 7,010 m. The river flows through 250 km in the rugged terrain of Himalaya before descending into the plains at Rishikesh. After traversing through Uttar Pradesh and Bihar the Ganga bifurcates into Bhagirathi and Padma in West Bengal. The Bhagirathi is known as Hoogly beyond Kalna and up to '*Mouths of Ganga*' in the Bay of Bengal. The Padma enters Bangladesh and joins Brahmaputra and later Meghna in the downstream. The river further flows as Meghna. It breaks into number of estuaries that pass through Sunderban to join the Bay of Bengal. The total length of the Ganga along the Hoogly is 2,525 km- 1,450 km in Uttar Pradesh, 445 km in Bihar and 520 km in West Bengal. The important tributaries from north are Yamuna, Ramganga, Gomati, Ghaghara, Gandak and Kosi and from south Chambal, Ken, Betwa, Sind, Tons and Son. The Damodar joins the river in the last reaches along the Bhagirathi and the Hoogly. The drainage area of the Ganga system of rivers accounts 26.3% of India's geographical area. The drainage area is spread over the states of Uttar Pradesh, Uttarakhand, Himachal Pradesh, Punjab, Haryana, Rajasthan, Madhya Pradesh, Chhattisgarh, Bihar, Jharkhand and West Bengal and Union Territory of Delhi. Earliest rainfall record from Kolkata is available from 1829, Bankura was added in 1831, Darjeeling in 1837 and Patna in 1842. Data for 32 stations is available from 1844 and for all 131 stations of the selected network from 1889. Mean annual and monsoonal rainfall over the basin is 1083.5(±125.8 mm) and 919.1(±110.7 mm) respectively. The coefficient of variation (CV) is 11.6% and 12% for annual and monsoon rainfall respectively. The highest rainfall in a year is 1405.5mm and lowest is 807.5mm.

1.3 The Brahmaputra Major Basin:

The Brahmaputra River rises at an elevation of 5,150 m in the Kailas range of the Himalayas. After flowing 1,700 km in the Himalayas it enters India across the Sadiya frontiers. It flows 720 km in Assam to enter Bangadesh. The main tributaries are the Ngangchu, the Dibang, the Luhit, the Subansiri, the Kameng, the Manas, the Buri Dihing, the Dhansiri, the Kopilli, the Tista, the Jaldhaka, the Torsa, the Kalyani and the Raidok. Earliest rainfall record is available from 1848 for four stations (Nowgong, Guwahati, Dibrugarh and Sibsagar). The data for all 11 stations of the selected network is available from 1871. Mean annual and monsoonal rainfall over the basin is 2478.3(±237.1mm) and 1706.6(±1684.9 mm) respectively. The coefficient of variation (CV) is 9.6% and 10.6% for annual and monsoon rainfall respectively. The highest rainfall in a year is 3161.6mm and lowest is 1979.2mm.

1.4 The Godavari Major Basin:

The Godavari rises in the Nasik district (Maharashtra), flows for 1,465 km and falls into the Bay of Bengal. Its vast catchment area is spread over five states, the Maharashtra (48.6%), Madhya Pradesh (20.7%), Karnataka (1.4%), Orissa (5.5%) and Andhra Pradesh (23.8%). The important tributaries are the Wainganga, the Wardha, the Penganga, the Manjra and the Indravati. Earliest rainfall record from 1826 is available from Nagpur; Nasik and Seoni were included in 1844 and Amraoti in 1859. The data for all 22 raingauges of the selected network is available from 1871. Mean annual and monsoonal rainfall over the basin is 1068.3(±167.5 mm) and 901.7 (±146.3mm) respectively. The coefficient of variation (CV) is 15.7% and 16.2% for annual and monsoon rainfall respectively. The highest rainfall in a year is 1433.4mm and lowest is 604mm.

1.5 The Krishna Major Basin:

The river rises at an elevation of 1,360 m from a water spring near Mahabaleshwar. It flows 1,400 km to join the Bay of Bengal. The drainage area is spread over three states as Maharashtra 26.8%, Karnataka

43.8% and Andhra Pradesh 29.4%. The important tributaries are the Ghatprabha, the Bhima and the Tungabhadra. The earliest rainfall record for Pune is available from 1826; Satara was added in 1836 and Shimoga in 1837. The data for 25 stations of the selected network is available from 1871. Mean annual and monsoonal rainfall over the basin is 825.7(±122.5 mm) and 581.4 (±101.9mm) respectively. The coefficient of variation (CV) is 14.8% and 17.5% for annual and monsoon rainfall respectively. The highest rainfall in a year is 1116.4mm and lowest is 555.7mm.

1.6 The Sabarmati Major Basin:

The river rises in the Aravalli hills and flows 300 km through the Rajasthan and the Gujarat states to join the Arabian Sea. The Sei, the Wakul, the Harnar, the Hathmati and the Watrak are the main tributaries. Earliest rainfall record for Ahmedabad is available from 1843; Kaira was included in 1861. The data for four stations of the selected network is available from 1871. Mean annual and monsoonal rainfall over the basin is 742.8(±269.1 mm) and 708.3 (±264.1mm) respectively. The coefficient of variation (CV) is 36.2% and 37.3% for annual and monsoon rainfall respectively. The highest rainfall in a year is 1622.9mm and lowest is 248.9mm.

1.7 The Mahi Major Basin:

The river rises in the Vindhyas at an elevation of 500 m. It flows through the Madhya Pradesh, the Rajasthan and the Gujarat states a length of 533 km and falls eventually in the Arabian Sea. The Son, the Anas and the Panam are the main tributaries. Earliest rainfall record for Udaipur is available from 1857; Neemuch was included in 1860 and Baria in 1869. The data for all eight raingauges of the selected network is available from 1871. Mean annual and monsoonal rainfall over the basin is 825.4(±225.4 mm) and 772.4 (±218.4mm) respectively. The coefficient of variation (CV) is 27.3% and 28.3% for annual and monsoon rainfall respectively. The highest rainfall in a year is 1433.3mm and lowest is 383.7mm.

1. 8 The Narmada Major Basin:

The river rises at an elevation of 900 m near Amarkantak (Madhya Pradesh). It flows through the Madhya Pradesh, the Maharashtra and the Gujarat states for a length of 1,312 km before falling into the Arabian Sea. The Burhner is the major tributaries. Rainfall data from 1844 is available for four stations Mandla, Jabalpur, Narsinhapur and Hoshangabad. The data for all eight raingauges of the selected network is available from 1871 onwards. Mean annual and monsoonal rainfall over the basin is 1107.3(±199.1 mm) and 997.2 (±182.7mm) respectively. The coefficient of variation (CV) is 18% and 18.3% for annual and monsoon rainfall respectively. The highest rainfall in a year is 1588.7mm and lowest is 727mm.

1.9 The Tapi Major Basin:

The river rises near Multai (Betul district, Madhya Pradesh) at an elevation of 730 m. It flows 724 km through the Madhya Pradesh, the Maharashtra and the Gujarat states before falling into the Arabian Sea. The Purna, the Vaghur, the Girna, the Bori, the Panjhra and the Aner are the important tributaries. Earliest rainfall record is available from 1844 for Betul; Amraoti and Buldhana were included in 1861. The data for all seven raingauges of the selected network is available from 1871. Mean annual and monsoonal rainfall over the basin is 894.4(±183.3mm) and 781.8 (±172.3mm) respectively. The coefficient of variation (CV) is 20.5% and 22% for annual and monsoon rainfall respectively. The highest rainfall in a year is 1323.9mm and lowest is 457mm.

1.10 The Mahanadi Major Basin:

The river originates from a pond near a village called 'Pharsiya' (Raipur district, Jharkhand). It flows for 587 km and beaks into two branches, the Katjuri and the Birupa, that fall into the Bay of Bengal. Its drainage area is spread over the Jharkhand, the Orissa, the Bihar and the Maharashtra states. Earliest rainfall record from 1848 is available for Puri; Sambalpur was included in 1861. The data for all 11 raingauge stations of the selected network is available from 1871. Mean annual and monsoonal rainfall over the basin is 1410.4(±202.2mm) and 1185.4 (±175.9mm) respectively. The coefficient of variation (CV) is 14.3% and 14.8% for annual and monsoon rainfall respectively. The highest rainfall in a year is 1915.8mm and lowest is 942.3mm.

1.11 The Cauvery Major Basin:

The Cauvery rises at an elevation of 1,340 sq. km in the Brahmagiri range of the Western Ghats in the Coorg District of Karnataka. It flows 800 km and joins the Bay of Bengal at Kaveripatnam. State-wise drainage area of the basin is distributed as 3.3% in Kerala, 41.2% in Karnataka and 55.5% in Tamil Nadu. The Cauvery splits into two branches, the Cauvery and the Vennar, which feed the Tanjore delta. The important tributaries are the Harangi, the Hemavati, the Shimsha, the Arkavati, the Lakshmanatirtha, the Kabini and the Suvarnavati in Karnataka and the Bhavani, the Noyli and the Amaravati in Tamil Nadu. Earliest rainfall record from 1829 is available for Ootacamund; Tumkur and Mysore were included in 1837. The data for all 13 stations of the selected network is available from 1871. Mean annual and monsoonal rainfall over the basin is 1265.5(±152.1mm) and 767 (±114.7mm) respectively. The coefficient of variation (CV) is 12% and 15% for annual and monsoon rainfall respectively. The highest rainfall in a year is 1739.7mm and lowest is 926.4mm.

1.12 The Luni Independent Minor Basin:

The River drains 79,456 sq. km area in Rajasthan and Gujarat. Earliest rainfall record from 1856 is available for Deesa and Ajmer; Pali was included in 1867. The data for all eight stations of the selected network is available from 1871. Mean annual and monsoonal rainfall over the basin is 487.7(±182.2 mm) and 445.4 (±170.8mm) respectively. The coefficient of variation (CV) is 37.4% and 38.3% for annual and monsoon rainfall respectively. The highest rainfall in a year is 1097.7mm and lowest is 167.5mm.

1.13 The Surma Independent Minor Basin:

The River drains 47,216 sq. km area in Assam, Meghalaya, Manipur, Mizoram and Tripura. There are three raingauges in the basin. The data for *Silchar* is available from 1948, for Shillong from 1866 and for *Agartala* from 1871. Reliable monthly rainfall sequence could be developed for the period 1848-2006. Mean annual and monsoonal rainfall over the basin is 2519.5(±306.1mm) and 1586.7 (±222.3mm) respectively. The coefficient of variation (CV) is 12.1% and 14% for annual and monsoon rainfall respectively. The highest rainfall in a year is 3352.5mm and lowest is 1835.2mm.

1.14 The Kasai Independent Minor Basin:

The drainage area is confined to the West Bengal state. Earliest rainfall record for *Bankura* is available from 1931; observation at *Purulia* started in 1848 and at *Midnapore* in 1854. Mean annual and monsoonal rainfall over the basin is 1442.6(±242.7mm) and 1114.2 (±189.4mm) respectively. The coefficient of variation (CV) is 16.8% and 17% for annual and monsoon rainfall respectively. The highest rainfall in a year is 2046.6mm and lowest is 963.2mm.

1.15 The Damodar Independent Minor Basin:

The River originates in the Palamau district (Jharkhand) and after flowing 541 km through Bankura and Burdwan districts it joins the Hoogly near Fulta point. Earliest rainfall record for Kolkata is available from 1829; Hazaribagh, Suri and Berhampore were included in 1848 and Hooghly was included in 1854. The data for all 11 stations of the selected network is available from 1871. Mean annual and monsoonal rainfall over the basin is 1473.4(±222.5 mm) and 1123.3 (±176mm) respectively. The coefficient of variation (CV) is 15.1% and 15.7% for annual and monsoon rainfall respectively. The highest rainfall in a year is 2080.8mm and lowest is 978.1mm.

1.16 The Suvarnarekha Independent Minor Basin:

The River originates in the Jharkhand State, flows 395 km through the states of Jharkhand, Orissa and West Bengal before falling into the Bay of Bengal. The Kanchi, the Karffari and the Karkai are its important tributaries. There are four raingauges in the basin- rainfall record for *Ranchi* is available from 1848, for *Balasore* from 1859, for *Chaibassa* from 1869 and *Baripada* from 1871. Mean annual and monsoonal rainfall over the basin is 1509.5(±214.7 mm) and 1146.7 (±163.4mm) respectively. The coefficient of variation (CV) is 14.2% and 14.3% for annual and monsoon rainfall respectively. The highest rainfall in a year is 2083mm and lowest is 1080.2mm.

1.17 The Brahmani Independent Minor Basin :

The River originates in the Ranchi district (Jharkhand) at an elevation of 600 m. It flows 800 km through the Jharkhand, the Chhattisgarh and the Orissa states before joining Bay of Bengal. The Kara, the Sankhad and the Tikra are the important tributaries. There are three raingauges (*Rajgangapur, Keonjhargarh and Dhenkanal*) in the basin with data from 1871. Mean annual and monsoonal rainfall over the basin is 1434.3(±205.6mm) and 1140.2 (±183.1mm) respectively. The coefficient of variation (CV) is 14.3% and 16.1% for annual and monsoon rainfall respectively. The highest rainfall in a year is 1930.7mm and lowest is 1008.5mm.

1.18 The Penner Independent Minor Basin:

The River rises in the Chennakesava Hills (Karnataka state), flows through the Karnataka, the Andhra Pradesh and the Tamil Nadu states for 597 km and falls into the Bay of Bengal. The tributaries are the Jayamangdi, the Kunderu, the Sagileru, Chitravati, Papagni and Cheyyeru. Earliest rainfall record for *Chennai* is available from 1813; *Cuddapah* was included in 1852, *Nellore* in 1863, *Ongole* and *Chitradurg* in 1870 and *Anatapur* in 1871. Mean annual and monsoonal rainfall over the basin is 870.2(±170.8mm) and 368.2 (±94.5mm) respectively. The coefficient of variation (CV) is 19.6% and 25.7% for annual and monsoon rainfall respectively. The highest rainfall in a year is 1328.5mm and lowest is 469.8mm.

1.19 The Palar & Ponnaiyar Independent Minor Basin:

The system of Palar and Ponnaiyar rivers drains 48,084 sq. km area in the Karnataka, the Andhra Pradesh and the Tamilnadu states. There are three raingauges in the catchment. Earliest rainfall record for *Cuddalore* is available from 1853; *Vellore and Chingleput* were included in 1863. Mean annual and monsoonal rainfall over the basin is 1194.4(±266.7mm) and 434.3 (±108.5mm) respectively. The coefficient of variation (CV) is 22.3% and 25% for annual and monsoon rainfall respectively. The highest rainfall in a year is 1916.5mm and lowest is 650.5mm.

1.20 The Vaigai Independent Minor Basin:

The catchment area of the Vaigai River is confined to Tamilnadu state. Earliest rainfall record for *Madurai* is available from 1846; *Tirunelvelli* was included in 1854; and *Pudukottai, Nagarcoil and Ramnathapuram* in 1871. Mean annual and monsoonal rainfall over the basin is 904.2(±144.3 mm) and 255.3 (±65.9mm) respectively. The coefficient of variation (CV) is 16% and 25.8% for annual and monsoon rainfall respectively. The highest rainfall in a year is 1245.4mm and lowest is 590.9mm.

1.21 The West Coast Drainage System:

Twenty five small rivers originate in the Sahayadri Range and flow into the Arabian Sea. On any small size map it's difficult to delineate the catchment's area of all these rivers. The combined area of different catchments of the Sahayadri is referred to as the West Coast Drainage System (WCDS). Earliest record of the Mumbai station in the WCDS is available from 1817; Tiruvanthapuram was included in 1838 and Cochin 1842. The data for all 21 raingauges of the selected network is available from 1871. Mean annual and monsoonal rainfall over the basin is 2528.5(±284.4 mm) and 1957 (±273.3mm) respectively. The coefficient of variation (CV) is 11.2% and 14% for annual and monsoon rainfall respectively. The highest rainfall in a year is 3340.6mm and lowest is 1857.7mm.

1.22 The All India

With three large watersheds, the Himalayas, the Vindhyas and the Western Ghats, the country is drained by 11 major and 43 minor rivers and numerous rivulets. The geographical area of the country considered in the study is 3,188,111 sq. km^2 (excluding Sikkim, Arunachal Pradesh, Andaman Nicobar islands and Lakshadweep islands due to non-availability of long period data). Longest rainfall series could be prepared using well spread network of 316 raingauge stations from earliest available year up to 2000. The earliest available record is for Chennai in 1813, Mumbai included in 1817, and Pune and Nagpur were added in 1826. Mean annual and monsoonal rainfall over the country is 1165.9(±106.2 mm) and 906.5(±88.3mm) respectively. The coefficient of variation (CV) is 9.1% and 9.7% for annual and monsoon rainfall respectively. The highest rainfall in a year is 1435.3mm and lowest is 895.7mm.

2. The methods of development and update of river basin rainfall series:

Longest instrumental area averaged basin-scale monthly rainfall dataset of 11 major basins, 9 minor basins, west coast drainage system and for the whole country available from 1813 to 2000 (Sontakke and Singh, 1996 & 2008) has been updated from 2001 to 2020. The starting year of the dataset varies from one basin to another. For the major basins the starting years are: The Indus 1844; The Ganga 1829; The Brahmaputra 1848; The Sabarmati 1861; The Mahi 1857; The Narmada 1844; The Tapi 1859; The Godavari 1826; The Krishna 1826; The Mahanadi 1848; The Cauvery 1829; The West coast drainage system 1817; and All India 1813. For independent minor basins the start is: Luni 1856; Surma 1848; Kasai 1831; Damodar 1829; Subarnarekha 1848; Brahmani 1871; Penner 1813; Palar & Ponnaiyar 1853; Vagai 1846 and The West Coast Drainage System (WCDS) 1817.

Longest instrumental area-averaged monthly rainfall sequence of the basins has been developed and updated in three phases. In the first phase, station dataset for the period 1901-2000 from National Data Center and Hydrology Section of the IMD, Pune is used (Mooley and Parthasarathy, 1984). In second phase, data up to 1900 is obtained from the India Meteorological Department (IMD) publication 'Monthly and Annual Rainfall of 457 Stations in India to the End of 1900' (Eliot, 1902). While in third phase, each station value has been extracted from the corresponding value of the grid from the 1º X 1º gridded rainfall dataset obtained from India Meteorological Department.

(i) In the first phase, for the period 1901 to 2000, simple arithmetic mean of all available gauges in the basin from fixed well spread instrumental network of 316 raingauge stations were used.
(ii) In second phase the dataset been extended backward from 1900 to 1813 (starting year is different for each basin) when lesser number of observations were available, by applying theoretically vindicated numerical method on limited available observations (Sontakke and Singh, 1996); and
(iii) In the third phase, the dataset has been updated from 2001 to 2020 by using 1-deg gridded daily rainfall with the ratio method suggested by Rainbird (1967) and approved by WMO.

The detailed procedure and the computational steps for the reconstruction of the dataset in first two phases were described in Sontakke and Singh (1996), Sontakke et.al. (2008) and Wigley et al (1984). Prior to 1900, density of the raingauge network decreases drastically non-monotonically back in time. As stated earlier, the earliest available record is for Chennai in 1813, Mumbai was included in 1817, and Pune and Nagpur were added in 1826. Up to year 1900, 314 stations were available. Reliability of the data was checked by Blanford (1886) and Eliot (1902) and did not find any serious error. All reconstructions have been made by considering 1901-2000 as the reference period. Linear regression is calculated between M-gauge mean series and m-gauge mean series during reference period (M is no. of gauges in reference period and m in the year considered for the reconstruction). It is then used to estimate the representative mean rainfall for the construction year. Theoretically derived mathematical expression given by Wigley et al.(1984) is adopted for the calculation of correlation (Rm ,M) between M-gauge mean rainfall series and m-gauge mean series (m is a subset of M). The correlation coefficient then used to inflate the variance of estimated rainfall of the construction year to get the reconstructed rainfall. The process is repeated backward for each year under consideration of reconstruction.

3. Chief statistical features of seasonal rainfall

Area-averaged monthly, seasonal (Jan-Feb, March-April-May, June-July-Aug-Sept and Oct-Nov-Dec) and annual rainfall series for all basins, WCDS and All India have been developed and analyzed. Climatological and fluctuation features of all the time series have been calculated and documented (table 1.2). Normally (1901-2000) the mean annual rainfall of all major river basins varies from 742.8mm over Sabarmati to 2478.3mm over Brahmaputra. The WCDS gets 2528.5 mm annual rainfall in normal year. The coefficient of variation of the annual rainfall varies from 9.6% (Brahmaputra) to 36.2% (Sabarmati). The year-wise highest rainfall normally varied between 1116.4 mm (Krishna) and 3161.6mm (Brahmaputra), while that of lowest from 248.9mm (Sabarmati) to 1979.2mm (Brahmaputra). For the country as whole, All India gets 1165.9mm rainfall annually with the highest rainfall as high as 1435.3mm and as low as 895.7mm. For independent minor basins, the mean annual rainfall varies form 487.7mm over luni to 2519.5mm over Surma. The coefficient of variation varies from 12.1% (Surma) to 37.4% (Luni). The year-wise highest annual rainfall was for Surma (3352.5mm) and the lowest for Luni 9167.5mm).

Inter-annual variations in annual, seasonal and monthly rainfall are filtered with 9-point filtering technique in order to suppress the high frequency components and understand the variability in low frequency mode. The smoothed series display many aperiodic fluctuations. Epochs with persistently large-or smaller period under wet or dry condition (with respect to climatological normal) can be seen in the graphs. Seasonal and annual rainfall condition of a particular year are categorized as *very dry, moderately dry, normal, moderately wet and very wet* by using quintiles as a threshold calculated from the dataset of 1901-2000. Categorized rainfall time series for all major and minor basins have been prepared and analyzed. The inter-

annual variation in the categorized monsoonal rainfall during 1813 to 2020 for the country as a whole is shown in fig.1.1a. For All India monsoon rainfall series rainfall less that 833mm is considered as very dry, 834-894mm dry, 895-945mm normal, 945-980mm wet and more than 980mm very wet. Distinct epochs can be identified in the rainfall fluctuations of all India monsoon rainfall. From the visual examination, major epochs noticeable in the monsoon rainfall fluctuations are: 1821-1861 dry, 1862-1897 wet, 1898-1931 dry, 1932-1964 wet, 1965-1988 dry, 1989-1999 wet, 2000-2020 dry. The inter-annual variation in categorized rainfall for major river basins are given in panel 'a' of figure 1.2 to 1.13.

4. Short-term and Long-term rainfall fluctuations

The Cramer's t_k statistics (WMO 1966) has been applied to moving averages of each of the time series to determine the broad nature of (+ve and –ve) short-term tendencies (15-year), medium-term fluctuations (31-year), long-term trend (51-year), and secular trend (101-year). The t_k is calculated and significance is tested for times series of all major and independent minor river basins. The test compares the means of the sub-periods to the mean of the entire record. Visual examination revels that the monthly, seasonal and annual rainfall is found to exhibit wide range of fluctuation characteristics across the country. The major epochal patterns and significant highest and lowest values in running means for monsoonal rainfall of All India and major basins are listed below.

All India: Fig.1.1b represent the Cramer's t_k statistics for All India annual and monsoon rainfall during 1813-2020. The 15-year running mean of monsoonal rainfall first decreased and attain a low value (significant at 1%) centered around 1844 during 15-year period. The means then increases continuously and becomes significantly larger than the overall mean (at 5% level) during the 15-year period centered around 1888. Afterwards it fluctuates within normal limit first decrease and then increase significantly (5% level) up to year centered around 1949. After that, it shows continuous decrease within the normal limit up to 2020. On broader scale five period can be identified in 15-year running means: 1825-1867 dry, 1868-1898 wet, 1999-1815 dry, 1916-1972 wet, 1972-1996 stationary and 1997-2013 dry. 31-year running mean shows five epochal patterns: 1828-1871 dry, 1872-1905 wet, 1906-1919 dry, 1920-1987 wet, 1988-2005 stationary. The lowest significant (1% level) decrease in 31 year running mean is centered on 1845, however the highest significant (1% level) increase is centered on 1948. In 51-year, two epochal patterns can be seen. 1838-1973 is dry, 1974-1989 is wet. The significant lowest (1% level) is centered on 1844 and significant (1% level) highest on 1939. In 101 year cycle only two epochs are identified. 1862-1896 dry, 1897-1964 wet, significant at 1% level up to 1936 and then it is significant at 5%.

Indus Major: Cramer's t_k statistics for Indus major basin during 1844-2020 is given in Fig1.2b. In 15-year window, the running mean attain lowest values (significant 5% level) centered around 1906, 1908 and 1986 while the highest values are centered on 1960 and 1964 (5% level). In recent period, the means are fluctuating. Three broad epochs can be identified. 1859-1946 dry, 1947-1975 wet and 1976-1990 dry. The lowest significant (5% level) decrease in 31 year running mean is centered on 1926, however the highest significant (1% level) increase is centered on 1962. Two epochal patters (1862-1845 dry and 1846-1978 wet) can be identified. In 51-year two epochal patterns can be seen. 1873-1938 is dry, 1939-2005 is wet. The significant lowest (1% level) is centered on 1921 and highest on 1955. In 101 year cycle, epochs are not identified. The running mean series shows continuous increase but still below normal up to 1957, afterwards it show increase above normal.

Ganga Major: Fig 1.3b shows t_k statistics for Ganga major basin during 1829-2020. During the entire period, the 15-year running mean of monsoon rainfall attain the lowest significant decrease centered

around 1843 (5% level) and highest around 1891 (5% level). In recent period, sharp decline is noticeable. During entire record three dry epochs (1836-1856, 1898-1915, 1998-2013) and two wet epochs (1857-1898 and 1916-1997) are observed. In 31-year window, lowest values are not significant while the highest significant increase is centered around 1885 (5% level). Broadly two wet epochs are noticeable (1863-1905 and 1921-1987). 51-year running window shows only one wet epoch from 1864-1980. The significant highest increase is observed around 1939 (5% level). The 101 year means also show only one wet epoch starting from 1880.

Brahmaputra Major: Fig. 1.4b shows Cramer's t_k statistics for annual and monsoonal rainfall of Brahmaputra basin. The highest significant increase (1%) in 15-year running mean is centered around 1865 and lowest significant decrease (1 %) around 2008. Two major epochs can be noticed. The 1855 to 1947 is wet and 1948 to 2013 is dry. In 31-year running mean also two major epochs are seen: 1863-1944 wet, 1845-2005 dry. The highest increase is centered around 1872 (1% level) and lowest decrease around 2000(5% level). In 51-year cycle, the highest significant increase is noticed around 1882 (1% level) and lowest around 1995 (1% level.) In 101 year running mean the highest significant increase is centered on 1907 and lowest decrease around 1970. In both 51-y and 101-y running means, no epochal pattern is seen. There is continuous decrease is observed throughout the entire record.

Godavari Major: Cramer's t_k statistics for Godavari river basin is shown in Fig 1.5b. 15-year running means shows two major wet epochs (1876-1898 and 1929-1966) and two dry epochs (1899-1928 and 1967-2007). The highest increase is centered around 1888 (1% level) and lowest decrease is around 1925 (5% level). In 31-year running means, four periods can be identified (1874-1907 wet, 1908-1920 dry, 1921-1974 wet and 1975-2005 dry. The highest significant increase is centered around 1946 (1% level) while lowest decrease is not significant. In 51-year window, only one epoch is observed. Staring from 1859 to 1978 the period was wet and afterwards decrease can be seen. The highest increase is noticed around 1956 (significant at 5% level) while lowest is not significant. In 101 year window, the values entire statistics is above normal. The highest increase is centered around 1920 (at 1% level).

Krishna Major: Cramer's t_k statistics for Krishna major basin during 1826-2020 is given in Fig 1.6b. In 15-year window, the running mean attain lowest values (significant 1% level) centered around 1852 and 1961 while the highest increase centered on 1960 (1% level). Four broad epochs can be identified. 1843-1876 dry, 1877-1915 wet and 1916-1946 dry and 1947-2013 wet. The lowest significant (1% level) decrease in 31 year running mean is centered on 1851, however the highest significant (1% level) increase is centered on 1968. Four epochal patters (1851-1878 dry, 1879-1907 wet, 1908-1939 dry and 1940-2005 wet) can be identified. In 51-year two epochal patterns can be seen. 1861-1931 is dry, 1932-1995 is wet. The significant lowest (1% level) is centered on 1861 and highest on 1975. In 101-year cycle, epochs are not identified. The running mean series shows continuous increase from lowest centered around 1886 (significant at 1%) to highest increase around 1970 (significant at 1%).

Sabarmati Major: Fig 1.7b shows t_k statistics for Sabarmati major basin during 1861-2020. During the entire period of 15-year running mean the lowest significant decrease is not found significant however the highest significant increase is centered around 1949 (at 5 % level) . On broader scale four major epochs can be identified: 1873-1893 wet, 1894-1925-dry, 1926- 1962 wet, 1963- 2000 dry. In 31-year window, lowest values are not significant while the highest significant increase is centered around 1941 (5% level). Two dry epochs (1898-1927 and 1971-2005) and one wet epoch (1828-1970) are noticeable. 51-year running window shows only two epochs: from 1886-1926 dry and 1927-1967 wet. After 1968 continuous

decrease can be seen. The highest increase and lowest decrease are not significant. The 101 year means also show two epochs: 1911-1936 wet and 1937-1965 dry.

Mahi Major: Cramer's t_k statistics for Mahi river basin is shown in Fig 1.8b. 15-year running means shows two major wet epochs (1864-1893 and 1930-1978) and two dry epochs (1894-1929 and 1979-2007). The highest increase is centered around 1948 and 1952 (5% level) and lowest decrease is around 1904 (5% level). In 31-year running means, four periods can be identified (1872-1892 wet, 1893-1929 dry, 1930-1970 wet and 1971-2005 dry. The highest significant increase is centered around 1948 (5% level) while lowest decrease around 1910 (5% level). In 51-year window, only two epoch are observed: 1890-1929 dry and 1930-1971 wet. After 1972 continuous decrease is seen. The highest increase or lowest decrease is not significant. In 101 year window, continuous decrease is noticed which is not significant.

Narmada Major: Fig. 1.9b shows Cramer's t_k statistics for annual and monsoonal rainfall of Narmada basin. The highest significant increase (1%) in 15-year running mean is centered around 1887 and 1941 and lowest significant decrease (1%) around 1906. Four major epochs can be noticed: 1886-1897 wet, 1898-1926 dry, 1927-1956 wet and 1957-2013 dry. In 31-year running mean also four major epochs are seen: 1865-1898 wet, 1899-1922 dry, 1923-1963 wet and 1964-2005 dry. The highest increase is centered around 1888 and 1946 (1% level) and lowest decrease around 1914 (5% level). In 51-year cycle, the highest significant increase is noticed around 1939 and 1953 (5% level) and lowest not significant. Only one prominent wet epoch from 1921-1970 is noticed. In 101 year running mean the highest significant increase is centered from 1911-1915 and lowest decrease is insignificant. In 101-y running means, also one wet epoch can be noticed from 1894-1944.

Tapi Major: Fig 1.10b shows t_k statistics for Tapi major basin during 1845-2020. During the entire period, the 15-year running mean of monsoon rainfall attain the lowest significant decrease centered around 1905 (5% level) and highest around 1938 (5% level). During entire record two wet epochs (1876-1894 and 1927-2013) and one dry epochs (1895-1926) are observed. In 31-year window, lowest decrease is centered around 1914 (1% level) while the highest significant increase is centered around 1946 (1% level). Broadly two epochs are noticeable (1894-1927 dry and 1928-2005 wet). 51-year running window shows increasing tendency from 1885 to 1954 and decrease thereafter. The significant highest increase is observed around 1954 (1% level). The 101 year means also show continuous increase starting from 1911 and significant around 1964 (1% level).

Mahanadi Major: Fig 1.11b shows t_k statistics for Mahanadi major basin during 1848-2020. During the entire period of 15-year running mean the lowest significant decrease is found around 1971 and 1972 (1% significant) and the highest significant increase is centered around 1940 (at 1% level) . On broader scale three major epochs can be identified: 1863-1877 dry, 1878-1961wet, and 1962- 2013 dry. In 31-year window, significant lowest value is centered around 1977 (1% level) while the highest significant increase is centered around 1932 (1% level). Two epochs (1880-1958 wet and 1959-2005 dry) are noticeable. 51-year running window shows only one wet epoch from 1893-1962 and sharp decline afterwards. The highest increase are found from 1932 to 1942 (1 % significance) and lowest decrease around 1990 (1% level). The 101 year means also show smooth decline centered from 1965.

Cauvery Major: Cramer's t_k statistics for Cauvery major basin during 1830-2020 is given in Fig1.12b. In 15-year window, the running mean attain lowest value (significant 1% level) centered around 2013 while the highest values centered on 1902 (5% level). In recent period, sharp decline is seen. Two broad epochs can be identified. 1837-1876 dry, 1988-2005 wet. The lowest significant (5% level) decrease in 31 year

running mean is centered on 2005, however the highest significant (5% level) increase is centered on 1985. Two epochal patters (1845-1881 dry and 1882-1995 wet) can be identified. In 51-year only one wet epochal pattern is identified from 1882-1987. The significant lowest (5% level) is centered on 1855 and highest on 1971 (1% level). In 101 year epochal pattern is not identified. The running mean series shows continuous increase from start up to highest centered around 1946 (1% level) and then decrease thereafter.

West Coast Drainage System: Fig1.13b shows t_k statistics for WCDS during 1817-2020. During the entire period, the 15-year running mean of monsoon rainfall attain the lowest significant decrease centered around 1851 (5% level) and highest increase in 2013 (1% level). During entire record two epochs (1835-1919 dry and 1920-2013 wet) are observed. In 31-year window, lowest significant decrease is noticed form 1845 to 1855 (5% level) while the highest significant increase is centered around 1968 (5% level). Broadly two epochs are noticeable (1832-1931 dry and 1932-2005 wet). 51-year running window shows only two wet epoch from 1842-1931 dry and wet thereafter. The significant highest increase is observed around 1968 (5% level) and significant lower decrease from 1857 to 1881 (5% level). The 101 year means does not show epochal pattern. There is continuous increase from lowest observed around 1895 (5% level) to 1964 highest significant increase centered around 19705 (1% level).

5. Recent changes in seasonal rainfall

5.1 Recent 15-, 31-, 51-, 101-year change relative to entire record:

Recent 15-, 31-, 51- and 101-year percent changes in summer monsoon rainfall of 11 major basins, 9 independent minor basins, west coast drainage system and All India relative to entire rainfall records are documented in table 1.5. Significance has been tested using Cramer's t_k test. For most of the basins the changes are not significant. But few of them shows consistent significant changes from 15-year to 101-year window. E.g. In Brahmaputra major basin, recent 15 year monsoon rainfall change by -7.1% (significant at 1% level); for 31-year -5.2% (5% level) and for 51-year -4% (1% level). Krishna, Tapi and WCDS major basins in recent 101 years shows significant increase in Rainfall by +2.9% (significant at 5% level), +4.2% (1% level) and +2.9% (5% level) respectively. Mahanadi major basin shows significant decrease in rainfall of -5.2% (1% level) in recent 51-years. While Cauvery shows significant decrease of -15.2% (at 1% level) and -8.1% (at 5% level) in recent 15-year and 31-years respectively. For independent minor basins, Brahmani shows significant decrease of -11.4%, -9.2% and -7.8% (significant all at 1% level) in recent 15-years, 31-years and 51-years. Pallar and Ponniyar also shows significant decrease in monsoon rainfall of -15.3% and -14.2% (both significant at 1%) during recent 15-year and 31-years respectively. Overall for the country as a whole, there is decrease in monsoon rainfall in recent 15-, 31- and 51-years but not statistically significant. However in recent 101 years surprisingly All India monsoon rainfall is showing increasing tendency (+1.3% significant at 5%).

5.2 Recent 20-year change compare to last century (1901-2000)

Changes in annual and monsoon rainfall of basins during 2001-2020 have been tested in relation to more reliable instrumental monthly rainfall records of last 100 years (1901-2000). Table 1.6 documents the recent changes expressed in percentages. The significance of the changes have been tested by using students' t test for the difference between the two sub-period means. It has been seen that, in recent years most of the basins shows negative percentage change compare to last century. Most significant change in annual and monsoon rainfall recorded for Ganga, Brahmaputra, Cauvery, Surma, Brahmani and Pallar & Ponniyar river basins. The annual and monsoonal rainfall of Ganga basin has been decreased significantly by -6.3% and -

6.6% (5% level of significant); Brahmaputra basin -8.4% and -7.6% (1% level) and Cauvery basin: -13.6% and -18.7% (1% level) respectively in recent years. For independent minor basins also significant decrease in annual as well monsoonal rainfall has been noticed. For Brahmani basin: -13.6% and -12.9% (15 level); Pallar & Ponniyar basin: -16.0% and -19.7% (1% level) respectively. For Surma basin the annual and monsoon rainfall decreased by 3.9% and 7.9% (1% level) respectively; For the country as whole the ALL India annual and monsoon rainfall has been decreased by -1.1%, but statistically not significant. The spatial distribution of recent 20 changes in monsoon rainfall compare to 20th century (1901-2000) are given in figure 1.14.

6. The Spectral analysis of longest rainfall series

We observe that, basin-scale longest instrumental rainfall series does not show any significant long-term trend however Interannual variations at different time-scales (annual, seasonal and monthly) does show a mixture of various periodic and random oscillations. Classical harmonic analysis has been used to understand the relative strength of periodic cycles in longest rainfall series.

In harmonic analysis, the time series is transformed into finite number of sine and cosine waveforms combinedly equal to the number of data points of the time series. The number of sine and cosine waves depends upon the total length of time series 'N' is even or odd. If N is even the number of sine coefficients are N/2-1 and cosine are N/2+1. If N is odd then number of sine waves are (N-1)/2 and cosine are (N-1)/2+1. The total variance of the time series is explained by sum of the variances of individual waveform. The wavelength of the waveform is an integer multiple of the 'N'. The amplitudes (Fourier coefficients) of the sine and cosine waves are calculated depending upon whether the record length N is even or odd. The linear combination of the sine and cosine waveform at a particular wavelength forms the harmonic. The variance contained or power of each harmonic is determined from the Fourier coefficients. The detailed mathematical expressions for the calculation of sine and cosine Fourier coefficients and their variances is given in Singh et.al. (2002).

The annual and seasonal mean is excluded from its respective individual time-series to reconstruct the power spectra for annual and monsoonal rainfall of All India and major basins. The power spectra display the normalized spectral density (percentage of variance) against the wavelength of the waveform. Top panels of Fig 1.15 shows the power spectra of annual and monsoon rainfall of All India. In order to easily identify the dominant peaks, the spectra are smoothed by 3-term running mean. The bottom panels of the figure shows the power spectra generated of 9-point filtered annual and monsoonal rainfall series. It has been seen that when high frequency components are removed from the series, prior to reconstruction of power spectra, sum total of variance of all the waveforms could explain only 18.2% variance of actual All India annual rainfall series and 17.4% of variance of Monsoon series. This shows that the inter-annual variability of the All India rainfall series is highly dominated by the short term fluctuations contributed by high frequency components. The results are more or less similar for the individual river basins as well (Fig 1.15). The highest amount of variance explained by filtered series is for Godavari basin (40%) followed by Cauvery (26.3%) and WCDS (24.9%).

Visual examination of power spectra revels that, the significant peaks in the range of 1-10 years, 10-30 years and more than 30 years are consistently observed for all river basins. In order to understand the detailed picture of the distribution of variance in these wavelength ranges, the waves are combined in three bands: (i) waves with a periodicity less than 10 years (short-term fluctuations); (ii) waves with a periodicity of 10–30 years (decadal variations); and (iii) waves with a periodicity of more than 30 years

(long-term variability). The combined percentage of variance explained by these three wavelength bands for annual and monsoonal are given in Fig. 1.16. The combined variance of short-term variations in annual rainfall across the basins varies from 54.3% (Godavari) to 79.4% (Ganga). The decadal variability varies form 14.4% (Ganga and Mahanadi) to 19% (Krishna and Brahmaputra). The long-term variability ranges from 4.8% (Sabarmati) to 21.1% (Godavari). For the monsoon rainfall, the combined variance across the basins varies as follows: short-term variations from 53.9% (Godavari) to 79.5% (Ganga); decadal changes from 10.3% (WCDS) to 25% (Godavari); and long-term variability from 5% (Sabarmati) to 22% (Godavari). For the country as whole the combined variances of short-term variations of annual and monsoon rainfall are 79% and 80%, those of decadal fluctuations are 10.6% and 9.4% and for long-term variations from 10.1% and 10.2% respectively. It can be seen that, the largest contribution to the variance is from short-term variability followed by decadal and long-term variability in the annual and monsoonal rainfall of all river basins.

The success of extrapolation of rainfall time series using harmonic analysis depends upon the degree of regularity present in that series. Ideally in any regular time series, the fewer number of waveforms represent larger portion of total variance. If variance contribution of many oscillations found through harmonic analysis show comparable values, the reliability of prediction by this method is observed to be weak. The results from the study revel that, the seasonal/annual rainfall extrapolation of river basins is not possible using simple classical harmonic analysis. More sophisticated techniques like appropriate filtering of the dataset in order to retain predictable components and removal of noise by using singular spectrum analysis, variable/non-integer harmonic analysis in order to capture realistic periodicities etc. will be used and taken as a separate study.

Section- II

Time series analysis of Seven homogeneous rainfall zones using longest instrumental monthly rainfall records

Based upon the similarity in the summer monsoon rainfall fluctuations, normal start and end of the monsoon rains, area-averaged monsoon rainfall etc. the country has been divided in to optimum (seven) number of homogenous zones (Sontakke and Singh 1996) as shown in fig 2.1. (i) South Peninsular India (SPI); ii) West peninsular India (WPI); iii) East Peninsular India (EPI); iv) North west India; v) North Central India (NCI); vi) North East India (NEI); and North Mountainous India (NMI). The longest instrumental area-averaged monthly rainfall series for seven homogeneous subzones earliest available from 1813 to 2000 (Sontakke and Singh 1996) is updated using IMD gridded 0.5 degree rainfall data upto 2020. Daily 0.5X0.5 degree gridded rainfall data form India Meteorological department is used to develop area averaged daily rainfall series of seven zones of the county for the period 1951-2020. The method for the development of the longest series and its updation is described as follows.

Longest instrumental area averaged monthly rainfall dataset of seven homogeneous zones of the country available earliest from 1813 to 2000 (Sontakke and Singh, 1996 & 2008) has been updated from 2001 to 2020. The starting year of the dataset varies from one zone to another. For each homogeneous zone, the starting years are: The SPI 1813; The WPI 1817; The EPI 1848; The NCI 1831; The 1826; The NMI 1844; The NEI 1829. Longest instrumental area-averaged monthly rainfall sequence has been developed and updated in three phases as per described in Part I for river basins.

1. Brief Physical and climatological information of seven homogeneous rainfall zones

Brief physical features, physiographic characteristics and climatological information of seven homogeneous zones are given in order. Table 2.1 lists important climatological information (e.g. Area, no. of rain gauges, earliest rainfall record, start and end of rainy season, and annual rainy days) for development of the longest rainfall series.

1.1 The South Peninsular India (SPI): It is area of the country south of 15ºN. This zone includes Kerala, Tamilnadu and part of Karnataka and Andhra Pradesh states. Earliest record for Chennai is available from 1813; the data for all 41 stations of the selected network is available from 1871. The longest rainfall series could be developed for the period 1813-2000. The series form 2001-2020 has been updated using gridded dataset.

1.2 The West Peninsular India (WPI): It is portion of the country between 15ºN and 21ºN and west of 79ºE. Maharashtra and part of Karnataka are included in this zone. Earliest record for Mumbai is available from 1817; the data for all 37 stations of the selected network is available from 1871. The longest rainfall series could be developed for the period 1817-2000. Rainfall series from 2001-2020 has been updated using gridded rainfall data.

1.3 The East Peninsular India (EPI): It is portion of the country between 15ºN and 21ºN and east of 79ºE. This zone includes Telangana, part of Chhattisgarh, Orrisa and Andhra Pradesh. Earliest record for Puri is available from 1848; the data for all 22 stations of the selected network is available from 1871. The longest rainfall series could be developed for the period 1848-2000. The series has been updated from 2001-2020 using gridded data.

1.4 The North Central India (NCI): It is portion of the country north of the latitude 21ºN and between the meridians 80ºE and 88ºE. Bihar, Jharkhand, part of Uttar Pradesh, Orrisa, West Bengal, Madhya Pradesh and Chhattisgarh are included in this zone. Earliest record for Bankura is available from 1831; the data for all 65 raingauges of the selected network is available from 1871. The longest rainfall series could be developed for the period 1831-2000. The series has been updated from 2001-2020 using gridded data.

1.5 The North West India (NWI): This zone is portion of the country north of the latitude 21ºN parallel and west of the 80ºE meridian, excluding the Jammu & Kashmir, the Himachal Pradesh and the Uttaranchal states. Major states that included in this zone are Rajasthan, Gujarat, Delhi, Punjab, Haryana, part of Uttar Pradesh and Madya Pradesh. Earliest record for Nagpur is available from 1826; the data for all 116 raingauges of the selected network is available from 1871. The longest rainfall series could be developed for the period 1844-2000. The series has been updated from 2001-2020 using gridded data.

1.6 The North Mountainous India (NMI): The zone is consists of the Jammu & Kashmir, the Himachal Pradesh and the Uttaranchal states. Earliest rainfall record for the Dehradun station is available from 1844; the data for all 10 raingauges of the selected network is available from 1901. The areal representative series for the period 1901-2000 has been prepared from arithmetic mean of the 10 raingauges. For the period 1844-1900 the representative series has been constructed. Rainfall series from 2001-2020 has been updated using gridded rainfall data.

1.7 The North East India (NEI):. It is portion of the country north of 21ºN parallel and east of 88ºE meridian. All seven sister states of northeast India comes under this zone. Earliest rainfall record for Kolkata is available from 1829; the data for all 25 stations of the selected network is available from 1871. The longest rainfall series could be developed for the period 1829-2000. Rainfall series from 2001-2020 has been updated using gridded rainfall data.

2. Chief statistical features of annual and seasonal rainfall

Area-averaged monsoonal and annual rainfall series for all zones have been developed and analyzed. Climatological and fluctuation features have been calculated and documented. Table 2.2 and 2.3 shows the basic statistical parameters (e.g. mean, sd, median, cv, highest and lowest) calculated for the period 1901-2000 for annual and monsoon rainfall respectively. Normally the mean annual rainfall of all zones varies from 775.2mm over NWI to 2159.6mm over NEI. The coefficient of variation of the annual rainfall varies from 8.2% (NEI) to 18.2% (NWI). The year-wise highest annual rainfall varied between 367.8 mm (NWI) and 1725.1mm (NEI), while that of lowest from 367.8mm (NWI) to 1725.1mm (NEI). Normally the mean monsoon rainfall of all zones varies from 685.2mm over NWI to 1509.9mm over NEI. The coefficient of variation of the seasonal rainfall varies from 8.3% (NEI) to 19.2% (NMI). The year-wise highest monsoon rainfall varied between 950.9 mm (NWI) and 1930.8mm (NEI), while that of lowest from 327.3mm (NWI) to 1242.5mm (NEI).

Inter-annual variations in annual and seasonal rainfall are filtered with 9-point filtering technique in order to suppress the high frequency components and retain the variability in low frequency mode. The smoothed series display many aperiodic fluctuations. Epochs with persistently large-or smaller period under wet or dry condition (with respect to climatological normal) can be seen in the graphs. Seasonal and annual rainfall condition of a particular year are categorized as very dry, moderately dry, normal, moderately wet and very wet by using quintiles as a threshold calculated from the dataset of 1901-2000. Categorized rainfall time series for all major and minor basins have been prepared and analyzed. Fig 2.2-2.8 represent the inter-annual variation in the categorized monsoonal rainfall during available period of record for all subzones in order. Distinct epochs with persistently large-or smaller period under wet or dry condition (with respect to climatological normal) can be seen in the graphs. The epochal patterns in annual rainfall for all zones are documented in order.

1. SPI: 1813-1906 dry, 1907-1933 wet, 1934-1953 dry, 1954-1964 wet, 1965-1990 dry, 1991-2010 wet & 2011-2020 dry.
2. WPI: 1841-1877 dry, 1878-1894 wet, 1895-1952 dry, 1953-1964 wet, 1965-1986 dry & 1987-2020 wet.
3. EPI: 1848-1924 dry, 1925-1963 wet, 1964-1985 dry & 1986-2020 wet.
4. NCI: 1842-1908 dry, 1909-1950 wet, 1951-1969 dry, 1970-2003 wet & 2004-2020 dry.
5. NWI: 1861-1894 wet, 1895-1941 dry, 1942-1964 wet, 1965-1993 dry & 1994-2020 wet
6. NMI: 1852-1901 wet, 1902-1913 dry, 1914-1927 wet, 1928-1953 dry, 1954-1967 wet & 1968-2020 dry
7. NEI: 1829-1856 dry, 1857-1882 wet, 1883-1908 dry, 1909-1956 wet, 1957-1986 dry, 1987-2000 wet & 2001-2020 dry.

Figure 2.9 and 2.10 shows inter-annual variations in annual and monsoon rainfall of seven homogeneous zones respectively, while that of monthly rainfall (June, July, Aug and sept) in monsoon season are represented in figures 2.11-2.14 respectively. The smoothed series display many aperiodic fluctuations. Visual examination revels that the monthly, seasonal and annual rainfall is found to exhibit wide range of fluctuation characteristics across the country. But over a longer period of time, the time series of all zones is appear to be approximately homogenous and random.

3. Recent 20-year changes in annual and seasonal rainfall

Changes in annual and seasonal rainfall of seven zones during 2001-2020 have been tested in relation to more reliable instrumental monthly rainfall records of last 100 years (1901-2000). Table 2.4 documents the recent changes expressed in percentages. The significance of the changes have been tested by using students' t test for the difference between the two sub-period means. It has been seen that, in recent 20 years, the monsoon rainfall of NCI and NEI have been significantly (at 1% level) decreased by -9.7% and -7.3% respectively. While that of WPI, EPI and NWI are increases and NMI is decreases but not statistically significant. In case of annual rainfall, significant (1% level) decrease is noticed for NCI, NMI and NEI with -9.6%, -12.9% and -9.4% respectively. The SPI, WPI, EPI and NWI show increase in rainfall but not statistically significant. For the seasons other and monsoon , it has been seen that, the Jan-Feb (JF) rainfall shows significant decrease over EPI (-46.7%), NMI (-32.8%) and NEI (-56.5%). The Mar-April-May (MAM) rains shows significant decrease over NMI (-25.8%) while Oct-Nov-Dec (OND) rainfall shows significant decrease over NWI (-39.2%), NMI (-50.2%) and NEI (-22.9%).

4. Interannual variations in Precipitation concentration Index(PCI)

The Precipitation Concentration Index as defined by Oliver (1980) is an important and fruitful indicator of the temporal precipitation distribution over an area. Changes in seasonal precipitation can be quantitatively assessed using this index. PCI characterizes monthly precipitation on a scale that ranges from 8.3 to 100. The PCI less that 10 indicates mostly uniform distribution of monthly precipitation with many spells in a year while more than that is an indicator of concentrated occurrence of precipitation in few spells of various degrees. PCI calculation does not depends upon the total annual precipitation, it only replay upon the distribution of it across the 12 months in a year compare to its annual total. The annual and seasonal (JJAS) PCIs were calculated using following equations.

$$PCI_{annual} = \frac{\sum_{i=1}^{12} P_i^2}{\left(\sum_{i=1}^{12} p_i\right)^2} * 100; \qquad PCI_{monsoon} = \frac{\sum_{i=1}^{4} P_i^2}{\left(\sum_{i=1}^{4} p_i\right)^2} * 33$$

$where,\ \ P_i$=Monthly precipitation in ith month.

Computation of PCI are very useful for hydrological as well agricultural purposes. If rainfall is distributed over a longer period then that distribution is more useful for agricultural uses. But if rainfall is concentrated in a few intense spells, then that distribution will be producing more runoff and hence useful for hydrological purposes. Year-wise annual and seasonal PCI for each zone have been calculated using monthly rainfall data. Table 2.5 indicate mean (1901-2000 of annual and seasonal PCI for each zone. It has been seen that, the average annual PCI for an individual homogeneous zones varies form 14.1(±1.3) over SPI to 25.1(±3.3) over NWI. On annual scale the mean PCI of all zones indicate the marked seasonal distribution of annual rainfall. The rainfall is more uniformly distributed over SPI while more concentrated over NWI. The seasonal PCI of all zones ranges from 8.6(±0.3) over NEI to 10.4 (±1.1) over NWI and NMI. In order to understand temporal variations in the values of PCI, the annual PCI are plotted for each zone. Figure 2.15 shows interannual variations in values of annual PCI for seven homogeneous zones.

Visual examination revels that, the Interannual variations in PCI for all homogenous zones are homogeneous and random. No considerable significant long-term trend observed in time distribution of monthly rainfall across India. It indicates that, the annual and seasonal rainfall concentration has remain relatively stable in the country over long-period of time. However in recent years, positive/negative epochal can be observed in the PCI time-series. Table 2.5 documents the recent 20-years changes (2001-2020) in annual and seasonal PCI compare to last 100-years records (1901-2000). The significance has been tested using student t test. It has been seen that, the annual PCI shows significant increase over NMI (10.2%) and NEI (5.8%) both significant at 1% level (tested using student t-test) and 5.7% over EPI (5% level). However the seasonal PCI of NEI only shows significant increase (1% level) in recent 20 years compare to last 100-years. Rise in PCI values indicates that, the rainfall distribution over those regions are becoming more and more concentrated in recent years. The reason for increase in annual PCI over NMI and NEI may be due to the significant decrease in rainfall during non-monsoonal months and frequent occurrences of extremes during monsoon months.

5. The spectral Analysis:

We observe that, the longest instrumental rainfall series of homogeneous zones across the country does not show any significant long-term trend however inter-annual variations at different time-scales (annual, seasonal and monthly) does show a mixture of various periodic and random oscillations. Classical harmonic analysis has been used to understand the relative strength of periodic cycles in longest rainfall series.

The annual and seasonal mean is excluded from its respective individual time-series to reconstruct the power spectra for annual and monsoonal rainfall. The power spectra display the normalized spectral density (percentage of variance) against the wavelength of the waveform. The power spectra of annual and monsoon rainfall of all zones in order are shown in top panels of Fig 2.16-2.22. In order to easily identify the dominant peaks, the spectra are smoothed by 3-term running mean. The bottom panels of the figures shows the power spectra generated of 9-point filtered annual and monsoonal rainfall series. It has been seen that when high frequency components are removed from the series, prior to reconstruction of power spectra, sum total of variance of all the waveforms could explain only small percentage of variance of actual rainfall series. It has been seen that, the highest percentage of variance (27.9%).of annual rainfall series explained by filtered power spectra is for NEI followed by NMI (25.2%). While that of monsoon rainfall the highest percentage is observed for NEI (26.4%) followed by EPI (23.6%). This shows that the inter-annual variability of all rainfall series is highly dominated by the short term fluctuations contributed by high frequency components.

Visual examination of power spectra revels that, the significant peaks in the range of 1-10 years, 10-30 years and more than 30 years are consistently observed for all zones. In order to understand the detailed picture of the distribution of variance in these wavelength ranges, the waves are combined in three bands: (i) waves with a periodicity less than 10 years (short-term fluctuations); (ii) waves with a periodicity of 10–30 years (decadal variations); and (iii) waves with a periodicity of more than 30 years (long-term variability). The combined percentage of variance explained by these three wavelength bands for annual and monsoonal are given in Fig. 2.23. The combined variance of short-term variations in annual rainfall across the homogenous zones varies from 80.5% (SPI) to 65.5% (NEI). The decadal variability varies form 10.7% (EPI) to 16% (NWI). The long-term variability ranges from 5.3% (SPI) to 16.3% (NMI). For the monsoon rainfall, the combined variance across the country varies as follows: short-term variations from 66.9% (NEI) to 83.1% (SPI); decadal changes from 10.7% (NMI) to 22.2% (NEI); and long-term variability

from 4.8% (SPI) to 11.5% (NCI). It can be seen that, the largest contribution to the variance is from short-term variability followed by decadal and long-term variability in the annual and monsoonal rainfall of all homogenous zones.

The success of extrapolation of rainfall time series using harmonic analysis depends upon the degree of regularity present in that series. Ideally in any regular time series, the fewer number of waveforms represent larger portion of total variance. If variance contribution of many oscillations found through harmonic analysis show comparable values, the reliability of prediction by this method is observed to be weak. The results from the study revel that, the seasonal/annual rainfall extrapolation of rainfall time series is not possible using simple classical harmonic analysis. More sophisticated techniques like appropriate filtering of the dataset in order to retain predictable components and removal of noise by using singular spectrum analysis, variable/non-integer harmonic analysis in order to capture realistic periodicities etc. will be used and taken as a separate study.

Section –III

Fluctuation characteristics of 1- to 10-day Large-scale Extreme rain events over seven homogenous zones of India: 1951-2020

Based upon the similarity in the summer monsoon rainfall fluctuations, normal start and end of the monsoon rains, area-averaged monsoon rainfall etc. the country has been divided in to optimum (seven) number of homogenous zones (Sontakke and Singh 1996) (i) South Peninsular India (SPI); ii) West peninsular India (WPI); iii) East Peninsular India (EPI); iv) North west India; v) North Central India (NCI); vi) North East India (NEI); and North Mountainous India (NMI). The daily 0.5X0.5 degree gridded rainfall data for the period 1951-2020, from India Meteorological department is used to develop area averages daily rainfall series of seven homogenous zones of the county

The global daily reanalysis product of the atmospheric temperature, geopotential height, wind speed at(1000-100hPa), mean sea level pressure and precipitable water available at 2.5º grid resolution from 1979 to 2020 from 'The National Centers for Environmental Prediction (NCEP) Climate Forecast System Reanalysis (CFSR & CFSv2) are used.

1. Identification and climatological characteristics of 1- to 10-day large-scale EREs

The large-scale extreme rain events (EREs) of 1-to 10-days duration are intended to quantify severity of persisting intense rains over particular area. In order to understand the variability of EREs of different durations over seven homogeneous zones, 1- to 10- EREs concerning rainfall amount and rainfall intensity are identified for each year. 1- to 10-day extreme concerning rainfall amount (ERE-RA) refers to annual maximum cumulative rainfall for the duration 1- to 10-days. While 1- to 10-day extreme concerning rainfall intensity (ERE-RI) is the annual maximum daily mean rainfall calculated for the durations 1-day to 10-days respectively. The procedure has been applied for each year of the period 1951–2020 to get the sequences of ERE-RA and ERE-RI for 1–day to 10-days durations. The chief climatological features of the extreme events for seven zones are in following order.

1. South Peninsular India (SPI): Over the SPI, the mean cumulative rainfall amount of the ERE-RA increases from 30.2mm (±21.9) for 1-day to 143.2mm (±59.6) for 10-day duration. While the mean rainfall intensity of ERE-RI decreases from 30.2mm (±21.9) for 1-day to 14.3mm (±6.0) for 10-day duration. The most extreme

ERE-RI and ERE-RA (during 1951-2020) of 1-day duration occurred on 25 Jul2005 giving 199.0 mm rainfall over the region, while that of 10-day duration started on 27 Jul 2005, giving 589.0 mm rainfall with the intensity of 59mm per day.

2. West Peninsular India (WPI): Over the WPI, the mean cumulative rainfall amount of the ERE-RA increases from 32.1mm (±10.2) for 1-day to 175.3mm (±40.4) for 10-day duration. While the mean rainfall intensity of ERE-RI decreases from 32.1mm (±10.2) for 1-day to 17.5mm (±4.0) for 10-day duration. The most extreme ERE-RI and ERE-RA of 1-day duration occurred on 24 Jul 1989 giving 76.8.0 mm rainfall over the region, while that of 10-day duration started on 2Aug 2005, giving 377.1 mm rainfall with the intensity of 37.7mm per day.

3. East Peninsular India (EPI): Over the EPI, the mean cumulative rainfall amount of the ERE-RA increases from 41.2mm (±9.8) for 1-day to 182.5mm (±36.4) for 10-day duration. While the mean rainfall intensity of ERE-RI decreases from 41.2mm (±9.8) for 1-day to 18.3mm (±3.6) for 10-day duration. The most extreme ERE-RI and ERE-RA of 1-day duration occurred on 4 Aug 2006 giving 70.6 mm rainfall over the region, while that of 10-day duration started on 14 Aug 2005, giving 277.5.0 mm rainfall with the intensity of 27.7mm per day.

4. North West India (NWI): Over the NWI, the mean cumulative rainfall amount of the ERE-RA increases from 20.3mm (±3.3) for 1-day to 123.5mm (±17.9) for 10-day duration. While the mean rainfall intensity of ERE-RI decreases from 20.3mm (±3.3) for 1-day to 12.3mm (±1.8) for 10-day duration. The most extreme ERE-RI and ERE-RA of 1-day duration occurred on 28 Jul 2015 giving 29.5 mm rainfall over the region, while that of 10-day duration started on 29 Jul 2015, giving 174.4 mm rainfall with the intensity of 17.4mm per day.

5. North Central India (NCI): Over the NCI, the mean cumulative rainfall amount of the ERE-RA increases from 27.7mm (±4.1) for 1-day to 158.3mm (±16.4) for 10-day duration. While the mean rainfall intensity of ERE-RI decreases from 27.7mm (±4.1) for 1-day to 15.8mm (±1.6) for 10-day duration. The most extreme ERE-RI and ERE-RA of 1-day duration occurred on 29 Sep 2019 giving 40.8 mm rainfall over the region, while that of 10-day duration started on 22 Jul 1975 giving 193.3 mm rainfall with the intensity of 19.3 mm per day

6. North East India (NEI): Over the NEI, the mean cumulative rainfall amount of the ERE-RA increases from 45.2mm (±9.4) for 1-day to 245.1mm (±44.6) for 10-day duration. While the mean rainfall intensity of ERE-RI decreases from 45.2mm (±9.4) for 1-day to 24.5mm (±4.5) for 10-day duration. The most extreme ERE-RI and ERE-RA of 1-day duration occurred on 11 Aug 2017 giving 71.3 mm rainfall over the region, while that of 10-day duration started on 16 Jul 2019 giving 370.2 mm rainfall with the intensity of 37.0 mm per day

7. North Mountainous India (NMI): Over the NMI, the mean cumulative rainfall amount of the ERE-RA increases from 28.5mm (±11.6) for 1-day to 97.8mm (±33.8) for 10-day duration. While the mean rainfall intensity of ERE-RI decreases from 28.5mm (±11.6) for 1-day to 9.8mm (±3.4) for 10-day duration. The most extreme ERE-RI and ERE-RA of 1-day duration occurred on 26 Sep 1988 giving 60.5 mm rainfall over the region, while that of 10-day duration started on 25 Mar 1990 giving 197.3 mm rainfall with the intensity of 19.7 mm per day

It has seen that, the rainfall amount of ERE-RA increases with duration over all subzones (table3.2). The rate of increase of rainfall amount is lowest over NMI (7.7mm/day) and highest over NEI (22.2 mm/day). This indicates that, extreme rain events of highest rainfall amount are less persistent over NMI and well

persistent over NEI for longer duration. The rainfall intensity shows decrease in its value as the duration of extreme increases. The highest rate of decrease in RI with respect to duration is observed over EPI (-2.5mm/day) while lowest over NWI (-0.9mm/day). However, Table 3.1 shows that, the rainfall intensity does not shows large variation from 1-day to 10-day EREs for all subzones of the country. It indicates that, the duration is the most significant factor for the severity of large-scale EREs that the rainfall intensity.

2. Chief fluctuation features of 1 to 10-day large-scale EREs

Interannual variations in rainfall intensity of 1-to 10-day ERE-RI and rainfall amount of ERE-RA over seven zones during 1951-2020 have shown in figs 3.1-3.7. Visual examination of the series depict the epochal pattern as well short-term increasing and decreasing trends. Overall, the series appears stationary but in order to check any regular component, the series have been smoothen by 9-point Gaussian low pass filter, which eventually suppresses the higher frequency components. Some distinct wet/dry epochs that embedded in Inter-annual variations are observed in each series.

Mann-Kendall (MK) rank test of randomness against trend is applied to examine the long-term trend in rainfall amount and rainfall intensity of 1- to 10-day extremes. Table 3.3 and 3.4 shows Mann-Kendall test statistics (z-value and τ –value) for the 1-to 10-day ERE-RI and ERE-RA respectively. MK test is non-parametric test and is an excellent tool for detection of trend in any hydro-climatic time-series. The magnitude of the trend (mm/year) is calculated for those time series, which shows significant (5% level of significance; l.o.s.) increasing/decreasing trend using Sen's slope estimator method. Time series of RI and RA of 1-day ERE shows significant increasing trend over WPI, EPI and NMI. For 2-day EREs, the RA and RI shows significant increasing trend over WPI. The RA and RI of 3-to 6-day EREs does not show any significant trend over any subzones. The RA and RI of 7-to 10-day ERE shows significant decreasing trend over NCI only. It has seen that, the short term ERES are increasing over WPI, EPI and NMI while long-term EREs are decreasing over NCI.

Percentage change in rainfall intensity and rainfall amount of extremes in recent 20 years (2001-2020) have been calculated in reference to preceding 50 years (1051-2000). The results are shown in tables 3.5 and 6 respectively. The difference between to sub-period mean are tested using student's t-test. It has seen that, in recent years, the RI and RA of 1-day and 2-day EREs have increased by 16.9% and 18.3% (5% l.o.s) respectively over WPI. Over EPI, the increase is 15.7% , 13.1% and 12.2% for 1-day, 2-day and 5-day EREs respectively. The significant differences in RI and RA at 10% l.o.s. are documented in table 3.5 and 3.6 respectively.

2.1. The most extreme rain events of 1- to 10-days duration

The most extreme rain events concerning RI and RA of the duration 1- to 10-days during 1951-2020 have been identified and documented in detail. Table 7 to 13 gives the rainfall intensity and rainfall amount of most extreme cases during 1951-2020 for seven homogenous zones. The characteristics of most extremes for all zones are in order

1) *Southern Peninsular India:* Over SPI, the most extreme event of 1-to 10-days durations during the period 1951-2020 happened in the year 2005. On 25th July 199mm rainfall occurred in 1- day while from 27 July to 5th Aug, 589 mm rainfall occurred at the rate of 59mm/day.
2) *Western Peninsular India:* Over WPI, the 1-day most extreme occurred on 24th July 2005, when the area gets 76.8 mm rainfall in a day. The 2- to10-days, most extremes happened in the year 2005, whose starting date varies from 27th July to 2nd Aug, rainfall intensity varies from 65.8 mm/day to 37.7 mm/day and rainfall amount 131.6 mm to 377.1mm.

3) *East Peninsular India:* The EPI experienced 1-day to 4-day most extreme events starting on 4-5th Aug 2006. Highest RI was for 1-day ERE (70.6mm/day) and cumulative RA of 4-day ERE was 190.4mm. The 5- to 10-day highest EREs happened during year 1986. The RI varies form 41mm/day to 27.7 mm/day while the cumulative RA varies form 204.8 mm (5-day ERE) to 277.5 mm (10-day ERE).
4) *North west India:* Over NWI, the most extreme 1- to 10-day EREs occurred in year 2015. The area experiences 29.5mm/day rainfall for 1-day ERE and 17.4 mm/day for 10-day ERE with the accumulated rainfall of 174.4mm for 10-day ERE that started on 29th July.
5) *North Central India:* For NCI the most extreme 1- to 8-day EREs occurred in the year 2019. On 29th Sept the area received most extreme 1-day ERE with the RI of 40.8mm/day and reduced upto 21.5mm/day for 8-day ERE. The accumulated rainfall of 8-day ERE was 172.1 mm. The most extreme 9- and 10-days EREs occurred on 21st and 22nd July 1975 respectively when the area received accumulated rainfall of 193.3 mm for 10-day ERE at the rate of 19.3mm/day.
6) *North East India:* The NEI received most extreme 1- to 8-days EREs in the year 2017. On 11th Aug the area received most extreme 1-day ERE with the RI of 71.3mm/day and reduced upto 39.8mm/day for 8-day ERE. The accumulated rainfall of 8-day ERE was 318.4 mm. The most extreme 9- and 10-days EREs occurred on 15th and 16th July 2019 respectively when the area received accumulated rainfall of 370.2 mm for 10-day ERE at the rate of 37mm/day.
7) *North Mountainous India:* Over NMI, the most extreme 1- to 5-day ERE occurred starting from 26 Sept to 28 Sept 1988. On 26th Sept, the area received rainfall at the rate of 60.5 mm/day, which reduced to 32mm/day for 5-day most extreme with the accumulated rainfall of 159.9 mm. The 6- to 10-day most extreme EREs happened in the year 1990, with the starting date varies from 23rd march to 25th march. The RI varies from 28.9 mm/day to 19.7 mm/day and cumulative rainfall 173.7mm to 197.3 mm.

Section-IV

Global Climatic Changes in 3-D structure of Atmospheric temperature

Recent changes in global tropospheric thermal structure show that, global warming is not uniform throughout the globe. Such type of global temperature changes in last few decades are observed to make changes in rainfall pattern also. Few intense rain spells, consequently heavy flooding and disasters occur across the country even in dry monsoons. At such times sudden intensification of the monsoon circulation is seen associated with anomalous warming of the upper troposphere between Tibet and Turkey sector and development of strengthened ridge in upper tropospheric westerlies over there. Few case studies of extreme rain events carried out by us revels that, abrupt warming and cooling in the atmosphere drastically modulates the monsoon circulation and intensify the associated weather systems causing heavier rains over a region. Persistence in temperature and circulation anomalies across the globe are strongly linked to the occurrences of severe rain events over a wide-ranging scale from small-scale short-period heavy rain events to large-scale long-period extreme wet spells. Locations of warming and cooling across the globe are the determinant of the plausible locations for the origin of various type of weather systems. We are hereby investigating the 3D changes in global atmospheric thermal structure and its role in extreme phases of monsoon.

The global monthly reanalysis product of the atmospheric temperature at 37 vertical isobaric levels (1000-1hPa) available at 2.5º grid resolution from 1979 to 2018 from 'The National Centers for Environmental Prediction (NCEP) Climate Forecast System Reanalysis (CFSR & CFSv2) are used for global temperature changes studies. The column-area mean monthly temperature of the lower troposphere (LTT: 1000-600hPa), upper troposphere (UTT: 550-250hPa), tropopause (TPS: 200-100hPa) and stratosphere (STT: 70-1 hPa) have been area averaged at global, hemispheric, zonal and regional scale. Tropospheric mean temperature (TT: 1000-250hPa) are calculated by considering troposphere level at 250hPa. Observations show that temperature up to this height is always lower than that of the equator throughout the year.

1. Temperature Trends across the globe during 1979-2018

1.1. Division of globe in 11 subzones and 54 geo-domains:

We have analyzed the trend in the atmospheric temperature from 1000hPa to 1 hpa atmospheric levels at global, hemispheric, zonal and regional scale. Based upon geographical, astronomical and meteorological characteristics and climatic conditions (temperature, wind pattern, precipitation etc.), the whole globe (GLB) is divided into nine climatic zones: north polar (NP: 70°-90°N), north mid-latitudes (NMLAT: 45°-70°N), north subtropic (NSBT: 25°-45°N), north tropic (NTP: 2.5°-45°N), equator (EQ: 2.5°S-2.5°N), south tropic (STP: 2.5°-25°S), south subtropic (SSBT: 25°-45°S), south mid-latitudes (SMLAT: 45°-70°S), south polar (SP: 70°-90°S). Each climatic zone is further subdivided into 6 macro geodomains, so the whole globe is divided into 54 geodomains.

The calendar month-year temperature data of the period 1979-2018 has been homogenized (standardized with respective monthly mean and standard deviation and multiply with annual standard deviation) in order to make the monthly temperature variations comparable before plotting. Fig. 4.1 shows the homogenized month-year troposphere (1000−250-hPa) temperature (TT) variation during 1979-2018 over nine climatic zones, the two hemispheres and the globe. It also shows the 37-month (~3 year) running mean as well as the linear trend. The TT over the globe has been increased at the rate of 0.25° per decade. NH is warming at faster rate (0.30°/decade than SH (0.20°/decade). All climatic zones across the globe show consistent significant global warming trend for all zones except SP and SMLAT. The highest rate of increase is seen over NP (0.37°/decade) while lowest over SP (0.05°/decade).

The homogenized month-year temperature records averaged over the LTT, UTT, TPS and STT of the atmosphere are plotted (fig 4.2-4.5). The rate of rising/declining trend in temperature over different climatic zones are also calculated. Visual examination revel that, LTT of GLB, NH, SH and all climatic zones (except SP and SMLAT) shows significant rising trend during 1979-2018. In UTT the results are consistent with LTT except SMLAT. The LTT and UTT of the globe have been increased at the rate of 0.20°C/decade and 0.32°C/decade respectively. The warming trend of LTT is higher (0.27°C/decade) in NH than SH (0.12°C/decade) while they are comparable (0.32°C/decade and 0.30°C/decade respectively) in UTT. Across 9 climatic zones, the warming trend in LTT varies from 0.08°C/decade over SP to 0.47°C/decade over NP, that of UTT from 0.20°C/decade over SMLAT to 0.40°C/decade over EQ. The LTT of SMLAT and UTT of SP both have been cooled by -0.01°C /decade. At tropopause level, no change is seen in the tropopause temperature (TPS) of the GLB while TPS of NH is warming at the rate of 0.04°C/decade and SH is cooling at the rate of -0.03°C/decade. Stratosphere of the GLB shows cooling trend of -0.55°C/decade over GLB, -0.56°C/decadeover NH and -0.54°C/decade over SH. The cooling trend in STT continues in all climatic zones as well varies from -0.51°C/decade over SMLAT to -0.80°C/decade over NP. The stratospheric cooling throughout the globe may be driven by increase in well-mixed greenhouse gases and declining stratospheric ozone levels. In general, rate of warming trend increases from south polar towards

north polar throughout the troposphere, while beyond it, only EQ and tropics are warming, other climatic zones are cooling. Which could be the cause of occurrence of many unusual weather events across the globe.

2. Recent 10 year changes in atmospheric temperature records

Changes in LTT, UTT, TPS, STT and TT in recent 10 years (2009-2018) compare to earlier records (1979-2008) have been calculated and significance is tested using student t-test (fig 4.6). In recent years, the annual mean LTT, UTT, TT of the GLB, NH, SH and all climatic zones (except SP) have been increased significantly (significant at 1% level) While STT shows significant decrease. The TPS changes are significant only over NH, NTP and EQ. Over the GLB, the LTT has been increased significantly by 0.35°C, UTT 0.68°C, but not significant at TPS (0.16°C). Over NH the significant increase in LTT is 0.48°C, UTT 0.68°C and TPS 0.21°C. Over SH, the LTT and UTT shows significant increase by 0.22°C and 0.69°C respectively while not significant over TPS (0.12°C). Throughout the troposphere (TT), the NH is warming at faster rate (0.57°C) than SH (0.42°C). Across 9 climatic zones, the largest significant increase in LTT is seen over NP (0.97°C), UTT over EQ (0.82°C), TPS over EQ (0.50°C) and TT over NP (0.80°C). The rate of warming in NH climatic zones are higher compare to that of SH. For TT, the highest change is observed over NP (0.80°C) while lowest over SP (0.07°C). The significant cooling is observed in stratosphere across the globe. The STT of GLB has been significantly decreased by -0.96°C, NH -0.96 °C and SH -0.97°C. The largest (-1.11°C/decade) is observed over NTP followed by EQ (-1.11°C) and STP (-1.08°C) significant tat 1% level.

2.1. Recent 10 year changes over 54 geodomains

Recent 10 year changes have been analyzed for 54 geodomains and documented (fig 4.7-4.10). It has been seen that the LTT over most of the geodomains show positive anomaly but SP and some part of SMLAT shows negative anomaly. In NH, the highest positive anomaly is seen over geodomains of NP (+1.22°C) followed by eastern NSBT (+0.69°C) and eastern NMLAT (+0.62°C). In SH, the highest positive anomaly is seen over southern Indian Ocean (+0.59°C) followed by central Pacific both in STP (+0.4°C). Over the EQ, the anomaly does not show much variation especially over oceanic areas (~+0.50°C). The largest negative anomaly is observed over SP (-0.51°C). The UTT shows consistent positive anomaly throughout the globe. In the NH, the highest value is observed over western Asia-Africa (+0.81°C), followed by south west Indian subcontinent and Arabian Sea (+0.79°C) both in NTP. In SH, the highest anomaly is over South Africa (+0.96°C) followed by south Indian Ocean (+0.91°C) both in STP belt. Over the equatorial belt, the anomaly varies from +0.76°C to +0.94°C over equatorial Indian Ocean. It has been seen that the upper troposphere of Oceanic regions are warming at higher rate than that over land areas across the globe. The TPS temperature shows mixed anomalies throughout the atmosphere. The highest positive anomaly is observed over Southeast Asian region, Indian Ocean over the equator (+0.65°C). While the largest negative anomaly is observed over geodomains of eastern SMLAT. The tropopause of tropical and subtropical regions are warming while multitude regions are cooling. The NP is warming but SP shows cooling tendency. Stratospheric cooling throughout the globe is clearly observed in recent years. In NH, maximum cooling is depicted over Arabian Sea, tropical Indian subcontinent and north tropical Southeast Asia (-1.21°C). In SH, the maximum reduction in STT is over eastern geodomains of SMLAT.

Summarized changes in column mean TT across the globe are also calculated. The largest change in TT of NH is observed over eastern NP geodomains (+0.98°C). The geodomains of NH are showing significant changes in TT in recent years as compare to those in SH. Some geodomains in SP even show cooling as well. From the dynamical perspective of Indian summer monsoon occurrence and establishment,

eastern NSBT areas are of great importance. It has been seen that, In recent 10 years, the troposphere of Asia-India sector of NSBT belt was comparatively cooler (0.44°C) than the surrounded NW Asia in west (0.70°C) and Tibet-China in east (0.58°C). It leads to frequent formation of deep trough over western slopes of Himalaya. An incursion of cool-dry westerlies over Central Asia-India sector and its frequent interaction with warm-moist tropical easterlies, and its forced exit from western Himalaya itself caused the formation of cloudburst events over the NW Himalaya.

In general, rate of warming trend increases from south polar towards north polar throughout the troposphere, while beyond it, only EQ and tropics are warming, other climatic zones are cooling. This asymmetric changes in thermal structure reflected in the significant decrease in inter-hemispheric temperature contrast over most of the climatic zones and weakening of thermally directed Asia-Pacific Monsoon circulation and hence monsoon rainfall across the country and unpredictable weathers across the globe.

3. Global Atmospheric conditions associated with Wet/Dry monsoon months

An attempt has been made to understand the meteorological changes associated with the most extreme wet and dry monsoon months (June to September) in the recent 37 years (1979-2015) over India. Longest instrumental area-averaged monthly rainfall series of All India available from 1813-2000 constructed using 316 well-spread rain gauge stations has been updated by using 1-deg gridded daily rainfall data up to 2015. Composite anomalies in the temperature, geopotential height at 12 isobaric levels and mean sea level pressure across the globe during most extreme four wet and dry years for India have been constructed. Further the anomalies are averaged for 11 subzones and 54 geo-domains across the globe in order to comprehend the result.

3.1 Identification of most extreme wet and dry months

The years with greatest and least rainfall for each month during the 1979-2015 monsoon period (June to September) have been identified (table 4.1). Composites of percentage departure from normal in monthly rainfall for four extreme wet and dry months have been prepared. It has been seen that the most extreme June rainfall occurred during the years 2001, 2008, 2011 and 2013 when monthly rainfall was 36.8% above normal. While extreme July and Aug rainfall was 19.9% above normal and occurred during 1981, 1988, 1994, 2013 and 1988, 1993, 1994, 2011 respectively. The most extreme September rainfall was 36.3% above normal during 1983,1998,2007,2010. The most extreme dry years in monthly rainfall with their percentage departure are as below: June: 1987, 2009, 2012 & 2014 (-41.1%); July: 1982, 1987, 2002, 2004 (-30.8%); Aug: 1993, 2005, 2009, 2015 (-25.7%); September: 1982, 1986, 2001, 2015 (-33.2%).

3.2 Departure in atmospheric parameters over 11 subzones:

Composite values of monthly averaged tropospheric temperature and thickness for extreme wet and dry months over 11 climatic zones are calculated (fig 4.11). Results show that, during wettest months, the tropospheric of NH was warmer and thicker in June (0.2°C/7.62m) cooler and thinner in July (-0.04°C/-1.2m) and August (-0.05°C/-1.14m) and again warmer and thicker in Sept (0.2°C/8.4m). The SH troposphere was warmer and thicker in June (0.1°C/4.5m), cooler but thicker in July (-0.01°C/0.4m), cooler and thinner in Aug (-0.1°C/-2.6m), and again warmer and thicker in Sept (0.2°C/8.6m). This lead to positive interhemispheric (NH-SH) temperature contrast during June, Aug and negative during July and Sept. During driest months, the tropospheric of NH was warmer and thicker in June (0.13°C/6.6m) cooler and

thinner in July (-0.1°C/-5.4m), warmer and thicker in August (0.1°C/5.6m) and again cooler and thinner in Sept (-0.2°C/-7.5m). The SH troposphere was warmer and thicker in June (0.2°C/9.2m), cooler and thinner in July (-0.1°C/-3.9m), warmer and thicker in Aug (0.1°C/4.9m), and cooler and thinner in Sept (-0.1°C/-4.5m). This lead to negative interhemispheric contrast during June, July, and September and positive during August. Overall, during extreme wet years most of the subzones show positive departure in temperature and thickness field. However, there are variations from June through September.

Broad features of departure fields in tropospheric temperature and thickness during wet and dry monsoon months over 11 subzones are as follows: During wettest June, tropics, subtropics and mid-latitude regions of both hemispheres were warmer and thicker than normal. While SP is cooler and thinner. NP and NSBT are thick but no temperature change has been seen. In driest June month, the anomalies are more or less same, except NSBT, where no change is seen. During extreme wet July, NTP, STP, and SMLAT are cooler and thinner, while NSBT, NMLAT, SSBT, and SP are warmer and thicker than normal. Cooling of tropics may be due to the wide coverage and excessive rainfall in the month of July, while during driest month, NSBT, NMLAT, SMLAT, and SP are cooler and thinner, while NTROP and NP are warmer and thicker. Cooling of NSBT and NMLAT during July is an indicator of the weaker monsoon circulation and hence subdued rainfall. During extreme wet August, both tropics and SSBT are cooler and thinner while both poles and NMALT are warmer and thicker. During extreme driest month of August, both tropics and SSBT are warmer and thicker while both poles and mid-latitudes are cooler and thinner. In wettest September month, almost whole globe is warmer and thicker while during driest September, whole globe is cooler and thinner except SMLAT, which is warmer and thick than normal.

During extreme wet years, although significant changes in departure field have not noticed across the globe, NSBT and TBT show comparatively intense departure field than other subzones. Tibet is warmer by 1.1º and thicker by 43.9m than normal in June, 0.54°C/23.6m in July, 0.2°C/7.9m in Aug and 0.04°C/7.8m in Sept. NH-SH contrast also did not show much variation during extreme wet years. During extreme dry years, majority of the subzones show negative departure field compare to normal. Tibet is cooler by -0.22°C and thinner by 10m in June, -0.32°/-19.7m in July, -0.25°C/-7.3m in Aug and -0.54°C/-24.8m in Sept as compare to its normal values. It has been seen that even small changes on terrestrial scale may produce vigorous changes on local-scale.

3.3 Spatial distribution of Atmospheric anomalies:

Global distribution of composite anomalies for four extreme wet and dry months in atmospheric parameters (tropospheric temperature, thickness, and MSLP) is observed (fig 4.12-4.14). It has been seen that, during extreme wet June, prominent warm anomalies are observed across north and south tropics-subtropics with a hot core over Middle East and western Tibet and another over western Russia. North Pole and south multitude appear to be cooler than normal. During extreme dry June, although whole north tropics and south tropics are warm, the Middle East and western Tibet are showing cool anomaly

During extreme wet July, the whole north and south tropics are cool but the warm anomaly is extending from Middle East to eastern Tibet and China. North Pole is cool but South Pole is warmer than normal. During driest July, the Middle East, the whole Tibet and Indian Ocean are showing negative anomaly. North Pole is warmer while South Pole is cooler than normal.

In extreme August month, warm anomaly core is observed over Central and western Tibet. Another core is observed over Japan and North America. The whole Indian Ocean is warmer than normal, while Pacific and Atlantic are cooler than normal. During extreme Dry August, cool anomaly is observed starting

from Middle East to Japan, Magnolia extending northwards up to North Pole. Surprisingly whole tropics of north hemisphere and Southern hemisphere are warmer than normal and south pole cooler than normal.

During extreme wet September, most parts of the globe in both hemispheres are under warm anomaly with the core over Japan-Magnolia. Although central and eastern Pacific and North Pole are cooler than normal. During driest September, opposite picture can be seen. The most part of the globe is under cool anomaly. Middle East and Tibet-Himalaya are also anomalously cooler than normal. While eastern part of equatorial and north pacific and some parts of south mid-latitude are under positive anomaly conditions.

In short, during wet months of the season, subtropical Asia especially Tibet-Himalaya is warmer and thicker and entire equatorial-tropical Pacific and Asian landmass is under negative pressure anomaly extends up to north pole. During driest months, the subtropical Asia is cooler and thinner while entire Asia-Pacific region is under positive pressure anomaly.

Section V

Interannual and multidecadal variability in relation to global climatic indices

The spectral analysis reveals that a significant portion of the interannual variability is driven by shorter-term cycles often result from dynamic interactions between atmospheric systems and global climatic indices, making ISMR highly volatile. Drawing from past experiences and studies, we've chosen ten different climatic indices that cover the five areas surrounding Indian monsoon domain: The North and tropical Pacific; North and tropical Atlantic; Indian Ocean; Eurasian land; and Southern Hemisphere for our analysis. Figure 5.1 illustrates the geographical locations and the extent of these oscillations, which are distributed globally, encompassing equatorial, tropical, subtropical, and polar latitudes around the Asia-Pacific monsoon belt.

Figure 5.1 bottom panel illustrates the interannual fluctuations of ten climatic indices according to the existing records. Most of these indices do not exhibit a significant long-term trend over an extended period, except for Dipole Mode Index (DMI), AAO, TSA, and TNA, which display a statistically significant increasing long-term trend. The increasing trend in the DMI can be attributed to the warming of western Indian Ocean, change in frequency and intensity of ENSO events and ongoing changes in global circulation pattern due to warming (Cai *et al*. 2014). Warming of tropical Atlantic and North Atlantic could lead to increase in TSA and TNA indices (Watanbe *et al*. 2000; Knight *et al*. 2006).

1. Correlations with ISMR

In recent years, various oscillations have shown increasing or decreasing epochal patterns. The strength of the robust, enduring concurrent relationship/teleconnection between the longest monthly and monsoonal rainfall of All India with each of the 10 climatic indices is represented by Correlation Coefficients (CC) in table 5.1. Climatic indices like Niño 3.4, SOI, and AO consistently show significant correlations with rainfall across all months during the monsoon season. Niño 3.4 has the strongest negative correlation with ISMR (CC = -0.60). El Niño events (warmer sea surface temperatures in the central and eastern Pacific) are known to suppress monsoon rainfall due to weakened convection over India. This effect is especially

pronounced in September when monsoon withdrawal begins. The strongest monthly negative correlation in September (CC = -0.45) indicates that ENSO's effect intensifies toward the end of the monsoon season. SOI which atmospheric counterpart of Niño3.4 displays a significant positive correlation, also peaking in September (CC = 0.40), and has the second-highest correlation with ISMR (CC = 0.48). Positive SOI events, enhance the monsoon's strength by promoting favorable moisture transport and convection over the Indian subcontinent.

The AO impacts mid-latitude atmospheric circulation, including the monsoon. It has a significant negative correlation with rainfall, strongest in September (CC = -0.31). This could be due to changes in the subtropical jet stream and its interaction with the monsoon trough, which influences monsoon dynamics. The PDO influences long-term climate variability in the Pacific and can modulate ENSO effects. PDO shows negative correlations with rainfall only in June (CC = -0.30) and September (CC = -0.28) indicating that, negative phases of the PDO (cooler Pacific waters) suppress the early and late monsoon rains by altering the atmospheric circulation, reducing moisture inflow into the Indian subcontinent. NAO and DMI exhibit significant but weaker correlations with rainfall in June (NAO: CC = 0.27) and September (DMI: CC = -0.17). Their effects on the Indian monsoon may be more localized or secondary compared to other indices. AMO, TSA, and TNA do not display significant correlations with overall India-level rainfall but have notable correlations at the basin scale.

The analysis of ISMR and climatic indices shows that correlations between them are stronger in June and September, but weaker during July and August, which are critical months for monsoon rains. This suggests that the monsoon is becoming less predictable in its peak period, possibly may be due to the complex interactions between multiple indices leading to non-linear responses in monsoon rainfall.

2. Spatial variability across river basins

Figure 5.2 shows spatial distribution of significantly correlated climatic indices with monthly and seasonal rainfall across river basins. SOI has the highest correlation during the monsoon season, being strongly correlated with 11 river basins. It shows the strongest positive correlation with the Indus (CC= 0.44) and the Ganga (CC= 0.42). It reflects that La Niña conditions lead to enhanced monsoon activity, particularly in northern river basins. La Niña strengthens convection over India, increasing moisture influx from the Bay of Bengal and Arabian Sea into these basins. Niño 3.4 is highly negatively correlated with the Ganga (CC= -0.53) and the Indus (CC= -0.46) tends to suppress rainfall by weakening monsoon circulation and reducing moisture transport into northern India. AO has a significant positive correlation with the Indus and Ganga (CC= 0.30 each) followed by the Godavari and Narmada (CC= 0.28 each). A positive phase of the AO strengthens the westerly winds and shifts the jet stream, which can enhance the monsoon trough over northern India, promoting rainfall in these regions. PDO is negatively correlated with five basins, most strongly with the Indus (CC= -0.25) followed by the Ganga and Krishna (CC= -0.21 each). During the negative phase, the cooling conditions over the pacific, reduces large-scale moisture flux to northern basins. DMI has a weaker negative correlation with four basins, especially the Ganga (CC= -0.22) followed by the Cauvery (CC= -0.20) indicating its secondary role in influencing northern basins compared to ENSO. AAO, NAO, and AMO each negatively correlate with two basins, with the highest correlations for the Narmada, Brahmaputra, and Cauvery respectively. TSA and TNA show negative correlations with only one basin each: Brahmaputra (CC= -0.23) and the Cauvery (CC= -0.33) respectively.

Only a few indices show significant correlations consistently throughout the monsoon season. E.g. Niño 3.4 has a persistent significant negative correlation with rainfall of Indus and Ganga basins from June

through September. SOI is positively correlated with rainfall in the Brahmaputra basin throughout the monsoon season and with the Ganga basin, except in August. AO is positively correlated with Ganga basin's rainfall throughout the monsoon season. PDO shows a strong negative correlation with rainfall in the Indus basin, except in August. For most other basins, no single climatic index consistently correlates with monthly rainfall for more than two months in a season. Additionally, most indices show stronger correlations with basin rainfall in June and September, and comparatively weaker in July and August. The results are in line with those of All India. It suggest that, these relationships are influenced by multiple factors, including the phase, timing, and interactions between the indices as well as broader climatic trends like Arctic warming and complicate the traditional connections.

3. Temporal changes in climatic correlations

A 31-year running correlation analysis was conducted to assess the evolving relationship between various climatic indices and ISMR as shown in figure 5.3. This method smooths short-term variability and highlights decadal to multi-decadal shifts in correlations, while also detecting lagged effects of climatic changes on rainfall patterns. The analysis revealed that, throughout the study period, the AO and SOI maintained a strong in-phase correlation with ISMR, while Niño3.4 consistently showed an out-of-phase relationship. However, the association between AO and ISMR has weakened in recent years, and other indices did not show consistent relationships with ISMR. The weakening correlation between AO and ISMR in recent years suggests that other factors, like ENSO, IOD, or the MJO, are increasingly influencing Indian monsoon behavior, complicating the role of AO in driving monsoon variability (Hrudya et.al. 2024). The weakening effect potentially may be also related to the global climatic shifts, such as warming in the Arctic region, which alters atmospheric circulation patterns (Terray 2023). The Quasi-Biennial Oscillation (QBO) has also been found to influence the relationship between AO and ISMR (Bhatla, 2016).

Figure 5.3 illustrates the 31-term running correlation between monsoon rainfall across 11 major basins and selected climatic indices that have shown significant long-term correlations. For basin-level rainfall, the correlation analysis revealed that several climatic indices have recently lost their association with rainfall. Niño3.4 and SOI however, continue to exhibit significant correlations with the Indus, Ganga, Brahmaputra, Godavari, Krishna, Tapi, and Cauvery basins, while the Sabarmati, Mahi, Narmada, and WCDS basins have lost these connections. Additionally, AO has maintained significant correlations with the Godavari, Narmada, and Tapi basins, but its association with other major basins, including the Indus, Ganga, Krishna, and others, has diminished. Many climatic indices have recently lost their strong associations with rainfall. This weakening may reflect local and regional variations in how these basins respond to broader climatic signals, possibly influenced by land use changes, irrigation practices, or changes in atmospheric circulation patterns.

4. Interconnectedness of climatic indices

Niño3.4 and SOI, while traditionally linked to monsoon rainfall, are also affected by interactions with other indices such as the PDO, Medan-Julian Oscillation (MJO), and the IOD. The intensity and timing of ENSO events, along with their interaction with other indices, result in varying impacts on seasonal rainfall. Further analysis shows the interconnectivity between many climatic indices. For instance, the PDO negatively correlates with SOI and AO (CC = -0.31 and -0.35, respectively) and positively with Niño3.4 (CC = +0.48). Similarly, Niño3.4 has a strong positive correlation with the DMI (CC = +0.50) and a negative correlation with AO (CC = -0.33). DMI also exhibits positive correlations with AO and AAO (CC = +0.23 and +0.24, respectively). TSA and TNA are strongly positively correlated with the AMO (CC = +0.31 and +0.86, respectively) and AAO (CC = +0.29 and +0.34, respectively). TSA and TNA also share a positive correlation with each other (CC = +0.36). The interrelationships between various climatic indices

shows that the global atmospheric and oceanic phenomena do not operate in isolation, further complicating their individual relationships with monsoon rainfall. The timing, intensity, and phase of one index can alter the behavior of others, impacting the seasonal distribution of rainfall in complex ways.

6. Relationship with global tropospheric temperature distribution

We found that, global climatic indices are the weak representative of monsoon rainfall performance especially during July and August. This study highlights the rainfall peak during July-August is primarily driven by the location, size, intensity, and reach of the well-established Asia-Pacific monsoon circulation. Its location, form, size, and intensity are primarily impacted by the tropospheric temperature/thickness contrast between the Tibetan anticyclone and eight deep highs worldwide.

To quantify the thermal state of the atmosphere, the 'Tropospheric Thickness Index' (TZI) has been formulated using temperature and thickness values between 1000hPa and 250hPa. The TZI was computed monthly for the monsoon period (JJAS) from 1949 to 2020.

$TZI_{mon} = ½ *[(TT_{mon} – TT_{mean})/ TT_{std}] + [(THK_{mon} – THK_{mean})/ THK_{std}]$ Where,

TT_{mon} & THK_{mon} are the monthly mean of tropospheric temperature and thickness of a grid

TT_{mean} & THK_{mean} are mean values calculated for the study period

TT_{std} & THK_{std} are standard deviation for the study period

Figure 5.4 illustrates the spatial distribution of correlation coefficients between TZI and monthly rainfall of All India during the monsoon season. For June, the warmest and thickest troposphere over western and central Tibet showed the highest correlation (CC = 0.6) with rainfall across India. In July and August, a division of the Tibetan high into two hot cores (east and west) was linked to rainfall patterns, with correlations ranging between 0.4 and 0.5. The performance of September rainfall was tied to the well-developed, single-cell hot-thick core of deep anticyclone over the Tibetan area extending from the Middle East to the Mongolia region (CC =0.4 to 0.6).

The study extended this analysis to 11 major river basins in India, depicting the spatial distribution of correlation coefficient in figure 5.5. The results illustrated that the monsoon rainfall of northern and eastern basins (Indus, Ganga, Brahmaputra, and Mahanadi) is significantly correlated to the extreme east and central subtropical Afro-Asian highland's hot and thick cores (CC varies between 0.4 to 0.6). Central India's river basins (e.g., Godavari, Krishna, Sabarmati, mahi, tapi etc.) showed significant correlations with warm and thick troposphere of northern tropics and that of southern tropical and subtropical regions. This indicates the involvement of all subtropical high-pressure cells from both hemispheres leading to a well-established monsoon circulation.The southern peninsular rivers displayed different behaviors: for instance, the Cauvery basin showed a negative correlation with global warming patterns, indicating that its monsoon dynamics might be more closely linked to the equatorial climate and strength of southwesterly monsoon flow rather than the large-scale monsoon circulatory systems over the Tibetan plateau.

Section VI: Major Results

Results (Section I):

Time series analysis and modelling of 'updated longest instrumental area averaged basin-scale monthly rainfall series for 11 major basins, 9 independent minor basins, west coast drainage system and for the whole country earliest available from 1813-2015 revel some important facts. Climatological and fluctuation features of annual and monsoonal rainfall of each river basin have been analyzed to understand short term tendencies as well long-term trend. Relative strengths of the periodic cycles of longest rainfall series have also been analyzed. The results from the study are summarized as follows.

1. Normal (1901-2000) annual rainfall of the river basins across the country varies from 487.7mm (Luni) to 2519.5mm (Surma). Normal annual rainfall of the country is 1165.9mm, highest rainfall of 1435.3mm occurred during year 1917 and lowest of 895.7mm during year 1918.
2. Normal (1901-2000) monsoon rainfall of the river basins across the country varies from 445.4mm (Luni) to 1706.6mm (Surma). For the country as a whole, the normal monsoon rainfall is 906.5mm, highest rainfall of 1088.8mm occurred during year 1961 and 661.3mm during year 1918.
3. Significant increasing trend is noticed in recent 101 years in monsoon rainfall over Krishna major (2.9%), Tapi (4.2%), WCDS (2.9%), Surma (2.1%), Pennar (2.8%) and the whole country (1.3%) compare to preceding instrumental period. While significant decreasing trend is noticed in Brahmaputra (-1.8%) and Brahmani (-1.4%).
4. During recent 15 years (2006-2020) compare to entire record, monsoon rainfall over Brahmaputra is decreased significantly by -7.1%, Cauvery -15.2%, Brahmani -11.4% and pallar& Ponniyar -15.3% relative to entire available instrumental records. While significant increase is noticed over Krishna Major (10.1%), Tapi(13.5%), WCDS(10.6%), Surma(9.0%) and Pennar(15.0%).
5. During recent 20 years (2001-2020) compare to last century (1901-2000), the significant decrease is noticed in monsoon rainfall of Ganga major (-6.6%), Brahmaputra major (-7.6%), Cauvery (18.7%), Brahmani (-12.9%) and Pallar and Ponniyar (-19.7%). While significant increase is seen over Surma basin (7.9%)
6. Compare to 20th century (1901-2000) monsoon rainfall over basins in northeast India, central northeast India and parts of south-east peninsular India has been lesser while that over central northwest India, north peninsular India and north India higher in recent 20 years.
7. The inter-annual variability of the All India and other major basins rainfall series are highly dominated by the short term fluctuations followed by decadal and long-term variability

Results (Section II):

Time series analysis and modeling of the 'updated longest instrumental area averaged monthly rainfall series' of seven homogeneous zones across the country earliest available from 1813-2020 revels some important facts. Climatological and fluctuation features of annual and monsoonal rainfall of each zone have been analyzed. Temporal distribution of rainfall in a year and in a season has been studied using PCI analysis. Recent year changes in annual and monsoon rainfall and PCI values are studied and documented. Relative strengths of the periodic cycles of longest rainfall series have also been analyzed. The results from the study are summarized as follows.

1. Normal (1901-2000) annual rainfall of seven homogeneous zones varies from 775.2mm over NWI to 2159.6mm over NEI. The year-wise highest rainfall varies between 1181.9 mm (NWI) and 2490.8mm (NEI), while that of lowest from 367.8mm (NWI) to 1725.1mm (NEI).
1. Normal (1901-2000) monsoon rainfall of seven homogeneous zones varies from 685.2mm over NWI to 1509.9mm over NEI. The year-wise highest rainfall varies between 950.9mm (NWI) and 1930.8mm (NEI), while that of lowest from 327.3mm (NWI) to 1242.5mm (NEI).
2. In recent 20 years, the monsoon rainfall of NCI and NEI have been significantly decreased by -9.7% and -7.3% respectively, while that of WPI and NWI increased significantly by 7.5% and 4.5 % respectively
3. The annual rainfall of NCI, NMI and NEI are decreased significantly by -9.6%, -12.9% and -9.4% respectively and SPI and WPI ae increased significantly by 1.1% and 5.5% respectively.
4. The average annual PCI for an individual homogeneous zones varies form 14.1 over SPI to 25.1 over NWI. It Indicates that, the rainfall is more uniformly distributed over SPI while more concentrated over NWI. The monsoonal PCI varies from 8.6 over NEI to 10.4 over NWI, indicating uniformly distributed rainfall during monsoon season
5. No considerable significant long-term trend is observed in annual and seasonal rainfall time distribution across India. However in recent 20 years, annual rainfall of NMI, NEI and EPI and monsoonal rainfall of NEI are more concentrated in few spells.
6. The Spectral analysis revels that, when high frequency components are removed from the series, prior to reconstruction of power spectra, sum total of variance of all the waveforms could explain only small percentage of variance of actual rainfall series.
7. The Interannual variability of rainfall series of all zones are highly dominated by short-term fluctuations (~75%), followed by decadal changes (15%) and long-term variability (~10%). Simple classical harmonic analysis doesn't serve the purpose of extrapolation of rainfall time series

Results (Section III):

1. The mean (1951-2020) RI of 1-day ERE-RI varies from 20.3mm over Northwest India (NWI) to 45.2mm over Northeast India (NEI) while that of 10-day ERE-RI varies form 9.8 mm over North mountainous India (NMI) to 24.5mm over NEI. The mean cumulative rainfall of 10-day ERE-RA varies form 97.8 mm over NMI to 245.1mm over NEI.
2. The rainfall amount of ERE-RA increases with duration over all subzones. The rate of increase of rainfall amount is lowest over NMI (7.7mm/day) and highest over NEI (22.2 mm/day). The rainfall intensity shows decrease in its value as the duration of extreme increases. The highest rate of decrease in RI with respect to duration is observed over EPI (-2.5mm/day) while lowest over NWI (-0.9mm/day).
3. Significant increasing trend is noticed in rainfall of 1-day EREs over WPI, EPI and NMI, while significant decreasing trend is noticed in RI and RA of 7- to 10-day EREs over NCI during 1951-2020.
4. In recent 20 years (2001-2020) the WPI experiences, significant increase in rainfall of 1- 2-day EREs (16.9% and 18.3% respectively). The EPI experiences significant increase for 1-. 2- and 5-day EREs (15.7%, 13.1% and 12.2% respectively).

Results (Section IV):

1. The tropospheric temperature across the globe has been increased significantly, since 1979-2018 at the rate of 0.25°C/decade. NH is warming at a faster rate (0.30°C/decade) than SH (0.20°C/decade). The rate of warming in LTT is higher (0.27°C/decade) over NH than SH (0.12°C/decade) while they are comparable in UTT (~ 0.31°C/decade). At tropopause level, no change is seen in the tropopause

temperature (TPS) of the GLB. Stratosphere of the GLB, NH and SH shows cooling trend (approx. -0.55°C/decade). All climatic zones across the globe show consistent significant global warming trend throughout the troposphere except SMLAT and SP.

2. During 2009-2018, compare to base period of 30 years (1979-2008), the annual mean LTT, UTT, TT of the GLB, NH, SH and all climatic zones (except SP) have been increased significantly. The TT of the globe has been increased by 0.50°C, NH (0.57°C) and SH (0.42°C). The highest change is observed over NP (0.80°C) while lowest over SP (0.07°C).
3. Across 54 geodomains, in recent 10 years, the highest positive anomaly in LTT is seen over eastern NP (+1.22°C), followed by eastern NSBT (+0.69°C) in NH and southern and equatorial Indian Ocean (+0.59°C & 0.55°C respectively). The upper troposphere of oceanic regions are warming at higher rate than that over land areas across the globe. The tropopause of tropical and subtropical regions are warming while midlatitude regions are cooling.
4. In recent 10 years, over Asia-pacific region, the troposphere of Asia-India sector of NSBT belt has been comparatively cooler (+0.44°C) than the surrounded NW Asia in west (+0.70°C) and Tibet-China in east (+0.58°C). This temperature structure is favorable for the frequent formation of deep troughs over western slopes of Himalaya that casing frequent formation of extreme events over the area.
5. During wet months of the season, subtropical Asia especially Tibet-Himalaya is warmer and thicker and entire equatorial-tropical Pacific and Asian landmass is under negative pressure anomaly extends up to north pole. During driest months, the subtropical Asia is cooler and thinner while entire Asia-Pacific region is under positive pressure anomaly.

Results (Section V):

The study explores the relationship of year-to-year as well multi-decadal variability of ISMR with global climatic indices, revealing complex and evolving interconnections.

1. The Niño3.4 index has a strong negative correlation (-0.60) with ISMR, while other indices such as SOI, AO, PDO, and DMI also influence rainfall patterns with varying degrees of correlation.
2. Spatial analysis shows that SOI, Niño3.4 and AO are the most influential indices across all river basins, with significant monthly correlations during the monsoon season. Notably, Niño3.4 is consistently linked to rainfall in the Indus and Ganga basins, while SOI has a strong positive correlation with the Brahmaputra and Ganga basins, AO has correlation with the Ganga basin and PDO to the Indus basin.
3. Interestingly, many climatic indices exhibit strong correlations with rainfall in June and September, but weaker correlations during July and August, the peak of the monsoon season. It could be due to the overlapping influences of various phenomena such as Niño3.4, AO, PDO and DMI, that disturbs the linear relationship. The indices directly influence the transition and intensity of monsoon winds, so the correlations may be more pronounced at the onset and retreat phases of the monsoon.
4. The study also emphasize the dynamic nature of correlation with ISMR over time. For instance, the AO has shown a weakening relationship with ISMR since the 1980s, preferably due to Arctic warming affecting key basins like the Indus, Ganga, Krishna, Cauvery and WCDS while correlations with basins like Godavari and Narmada have strengthened.
5. While Niño3.4 and SOI remain key predictors of monsoon rainfall variability, the influence of other indices like PDO and AO is less consistent, and their correlations have shifted over time. These evolving relationships have significant implications for hydrological modeling and infrastructure

planning. As historical correlations are often used to predict annual and seasonal peak flows and water availability in river basins,

6. The study emphasizes the importance of revisiting these predictive models in light of shifting climatic influences to reduce uncertainties in future projections and ensure sustainable management of water resources. This also highlights the need for adaptive and region-specific approaches in water resource management and climate risk planning, as climatic indices can have differential impacts across basins and time scales.
7. The research also highlights the connection between monsoon rainfall patterns and global tropospheric warming, particularly in relation to the Tibetan anticyclone and the Afro-Asian highlands. Northern and eastern basins, such as Indus and Brahmaputra, exhibit strong correlations with the warm, thick troposphere over eastern and central subtropical Afro-Asian highlands. Central Indian basins, like the Godavari and Krishna, show significant relationships with warming patterns over northern hemisphere and southern tropical and subtropical regions, reflecting the global nature of monsoon circulation.
8. In contrast, southern basins, such as the Cauvery, are primarily influenced by equatorial climate dynamics and the strength of the southwesterly monsoon flow play a larger role than large-scale monsoon circulations. These findings underscore the intricate relationship between global tropospheric warming and regional rainfall patterns, highlighting the need for a nuanced understanding of monsoon dynamics in the context of global climate variability. As global temperatures continue to rise, understanding these interactions will be crucial for predicting monsoon performance and managing water resources effectively.

Important Conclusion:

The considerable rising or falling tendency in monsoon rainfall across India has some rationale. However, neither of them can conclusively claim that they are uniform and random. This study demonstrates the importance of understanding both the short- and long-term variability of monsoon rainfall across across 20 river basins of India. The research findings indicate that short-term fluctuations are the primary drivers of rainfall variability in India, overshadowing decadal and long-term trends. This makes predicting future rainfall patterns based on long-term cycles alone unreliable. The study highlights significant declines in monsoonal rainfall in key basins such as the Ganga, Brahmaputra, and Cauvery, alongside modest increases in others. The basin-specific trends emphasize the need for localized water management strategies to address the diverse impacts of changing rainfall patterns.

The intricate web of interactions between climatic indices collectively influences monsoon rainfall patterns reflecting regional differences as well evolving nature. The shifting correlations over time underscore the dynamic nature of these relationships, driven by a multitude of factors. It suggested the predictive models to account these shifting correlations to ensure accurate water management projections. Additionally, the study underlines the influence of global tropospheric warming on rainfall patterns, highlighting the critical need to consider the broader implications of climate change on India's monsoon dynamics. The monsoon circulation, though vigorous, exhibits a distorted 3D structure and variable interaction with global climatic indices and uneven global warming. This leads to heterogeneous rainfall distribution over space and time, with unpredictable and inconsistent extreme rain events. As India continues to face the challenges of global temperature rise and climate change, these findings underscore the urgency of developing adaptive, region-specific strategies for managing river basins, assessing groundwater recharge potential, and aiding local agricultural planning for sustainable development and ensuring water security for future generations.

Acknowledgements: The author is grateful to Director, National Institute of Hydrology, Roorkee for the necessary facilities to pursue the study, and to the India Meteorological Department for providing the necessary station as well as gridded rainfall datasets.

References:

Blanford, H. F., 1886: Rainfall of India. India Meteorological Memoirs, Vol. 81, Vol. III, 658 pp.

Elliot J. 1902: Monthly and annual rainfall of 457 stations in India to the end of 1900. India Meteorological Department Memoirs, Vol. XIV, 709 pp.

Goswami BN, Venugopal V, Sengupta D, Madhusoodanan MS, Xavier PK (2006) Increasing trend of extreme rain events over India in a warming environment. Science 314:1442–1445

Guhathakurta P, Sreejith OP, Menon PA (2011) Impact of climate change on extreme rainfall events and flood risk in India. J Earth Syst Sci 120(3):359–373

IPCC (2007) Climate change 2007. The physical science basis. The contribution of working group I to the fourth assessment report of the intergovernmental panel on climate change. Cambridge University Press, Cambridge, pp 504–511

IPCC (2021) Climate Change (2021) The physical science basis. Working Group I contribution to the Sixth Assessment Report of the Intergovernmental Panel on Climate Change, Cambridge University Press, Cambridge, In Press.

Mooley, D. A. and Parthasarathy, B., 1984: Fluctuations in all-India summer monsoon rainfall during 1871-1978, *Climatic Change*, 6: 287-301.

Rajeevan M, Bhate Jyoti, Jaswal AK (2008) Analysis of variability and trends of extreme rainfall events over India using 104 years of gridded daily rainfall data. Geophys Res Lett 35:L18707

Ranade A, Singh N (2014) Large-scale and spatio-temporal extreme rain events over India: a hydrometeorological study. Theor Appl Climatol 115:375–390

Ranade, Ashwini., N. Singh, H. N. Singh, and N. A. Sontakke, 2008: On variability of hydrological wet season, seasonal rainfall and rainwater potential of the river basins of India (1813-2006). J. Hydrol. Res. Dev., 23, 79–108.

Ranade, Ashwini., Nityanand Singh 2019: Equatorially/Globally conditioned meteorological analysis of heaviest rains over India during 23-28 July 2005, *Meteorology and Atmospheric Physics*, 131:919-944.

Ranade, Ashwini., Nityanand Singh 2021: Evaluation of 3D Structural Changes in General Atmospheric and Monsoon Circulations during Kedarnath Disaster (India, 16-17 June 2013. *Meteorology and Atmospheric Physics*, 133(3),857-878

Rainbird, A.F. (1967) Methods of Estimating Areal Average Precipitation. WMO/IHD Report No. 3, World Meteorological Organization, Geneva, 42 pp.

Senior CA, Jones RG, Lowe JA, Durman CF, Hudson D (2002) Predictions of extreme precipitation and sea-level rise under climate change. Phil Trans R Soc Lond A 360:1301–1311

Sontakke, N. A. and Singh, N., 1996: Longest instrumental regional and all-India summer monsoon rainfall series using optimum observations: reconstruction and update, The Holocene, 6, 315-331.

Sontakke, N. A. ,N. Singh, and H. N. Singh, 2008: Instrumental period rainfall series of the Indian region (1813-2005): Revised reconstruction, update and analysis. Holocene, 17, 1055–1066.

Singh N, S. K. Baek and W. T. Kwon (2002): Seasonal/Subseasonal rainfall prediction through time series modelling and extrapolation using Harmonic analysis. Korean Jr. of Atmos. Sci., 5, 131-145

Singh N, Ranade A (2010) The wet and dry spells across India during 1951–2007. J Hydrometeorol 11:26–45

Wigley, T.M.L., Briffa, K. R. and Jones, P. D., 1984: On the average value of correlated time series, with application in dendroclimatology and hydrometeorology, J. Climat Appl. Meteorol. 23:202-213.

W.M.O., 1966: Climaric Change, *World Meteorological Organization Technical Note No. 79,*

****

Table 1.1: Physical properties, number of available rain gauges, annual and monsoonal rainfall during 1901-2000 and water resources status of All India, 11 major basins and west coast drainage system till 2014

Sr. no.	Major river basins	Drainage area (km^2)	Length of the river (km)	No. of major tributaries	Highest Elevation (m)	No. of rain-guages since 1901	Surface water potential (bcm)	Ground water potential (bcm)	Utilizable surface water (bcm)	Live storage capacity (bcm)	No. of dams	No. of other water assets
1.	**Indus major**	2,91,749	1,114 (in India)	5	8,566	19	73.31	26.49	46	16.57	39	76
2.	**Ganga major**	8,60,884	2,525	33	7,512	131	525.02	170.99	250	60.66	784	204
3.	**Brahmaputra major**	1,86,773	720	18	8,401	11	537.24	26.55	24	11.68	16	26
4.	**Godavari major**	3,30,628	1,465	8	1,664	22	110.54	40.65	76.3	31.33	921	109
5.	**Krishna major**	2,95,650	1,400	11	1,903	25	78.12	26.41	58	49.55	660	195
6.	**Sabarmati major**	36,688	300	5	1,173	4	3.81		1.9	1.37	50	12
7.	**Mahi major**	41,179	533	5	1011	8	11.02		3.1	4.98	134	7
8.	**Narmada major**	94,562	1,312	41	1317	8	45.64	10.83	34.5	23.60	277	8
9.	**Tapi major**	65,041	724	14	1556	7	14.88	8.27	14.5	10.26	356	32
10.	**Mahanadi major**	1,45,040	587	7	1321	11	66.88	16.46	50.0	14.21	253	28
11.	**Cauvery major**	91,691	800	13	2629	13	21.36	12.3	19	8.87	96	35
12.	**The WCDS**	1,17,962	-	98	2674	21	200.71	17.69	36.2	26.28	288	20
13.	**All India**	31,88,111	-		8611	316	1869.45	431.43	1123	304.35	4728	837

Table 1.2: Land use land cover statistics of All India, 11 major basins and west coast drainage system.

Sr. no.	Major river basins	Percentage of area under (%)						
		Built up land	**Agricultural land**	**Forest**	**Grassland**	**Wasteland**	**Waterbodies**	**Snow/ Glaciers**
1.	**Indus major**	2.09	35.80	15.09	4.19	28.53	1.85	12.46
2.	**Ganga major**	4.28	65.57	16.0	0.85	8.89	3.47	0.94
3.	**Brahmaputra major**	1.63	25.91	55.48	4.39	5.20	5.79	1.6
4.	**Godavari major**	1.66	59.57	29.78	0.03	5.36	3.6	-
5.	**Krishna major**	2.29	75.86	10.04	0.11	7.64	4.07	-
6.	**Sabarmati major**	1.95	74.68	11.98	0.05	7.15	4.19	-
7.	**Mahi major**	1.25	63.63	19.29	0.23	11.26	4.34	-
8.	**Narmada major**	1.13	56.90	32.88	0.01	6.13	2.95	-
9.	**Tapi major**	1.24	66.19	24.41	0.01	5.16	2.99	-
10.	**Mahanadi major**	3.30	54.27	32.74	-	5.24	4.45	-
11.	**Cauvery major**	4.01	66.21	20.50	1.33	3.86	4.09	
12.	**The WCDS**	4.51	48.39	34.94	0.49	8.50	3.88	-
13.	**All India**	2.72	55.07	21.48	1.03	9.95	3.74	1.45

Table 1.3. Basic statistical parameters of Annual rainfall during 1901-2000 over 11 major and 9 independent minor river basins

Sr. No.	Basin Name	Mean (mm)	Median (mm)	SD (±mm)	CV (%)	Highest (mm)	Lowest (mm_
Major Basins							
1.	Indus major	860.4	825.1	172.0	20.0	1399.5	508.4
2.	Ganga major	1083.5	1090.7	125.8	11.6	1405.5	807.5
3.	Brahmaputra major	2478.3	2483.3	237.1	9.6	3161.6	1979.2
4.	Godavari Major	1068.3	1059.0	167.5	15.7	1433.4	604.0
5.	Krishna major	825.7	821.1	122.5	14.8	1116.4	555.7
6.	Sabarmati	742.8	725.0	269.1	36.2	1622.9	248.9
7.	Mahi	825.4	831.6	225.4	27.3	1433.3	383.7
8.	Narmada	1107.3	1081.9	199.1	18.0	1588.7	727.0
9	Tapi	894.4	881.1	183.3	20.5	1323.9	457.0
10.	Mahanadi	1410.4	1397.1	202.2	14.3	1915.8	942.3
11.	Cauvery	1265.5	1268.6	152.1	12.0	1739.7	926.4
12.	West Coast Drainage system	2528.5	2527.5	284.4	11.2	3340.6	1857.7
13.	All India	1165.9	1177.1	106.2	9.1	1435.3	895.7
Independent minor basins							
14.	Luni	487.7	464.7	182.2	37.4	1097.7	167.5
15.	Surma	2519.5	2498.5	306.1	12.1	3352.5	1835.2
16.	Kasai	1442.6	1427.7	242.7	16.8	2046.6	963.2
17.	Damodar	1473.4	1448.8	222.5	15.1	2080.8	978.1
18.	Suvarnarekha	1509.5	1483.1	214.7	14.2	2083.0	1080.2
19.	Brahmani	1434.3	1439.7	205.6	14.3	1930.7	1008.5
20.	Pennar	870.2	839.7	170.8	19.6	1328.5	469.8
21.	Pallar & Ponniyar	1194.4	1179.4	266.7	22.3	1916.5	650.5
22.	Vaigai	904.2	903.4	144.3	16.0	1245.4	590.9

Table 1.4. Basic statistical parameters of Monsoon rainfall during 1901-2000 over 11 major and 9 independent minor river basins

Sr. No.	Basin Name	Mean (mm)	Median (mm)	SD (±mm)	CV (%)	Highest (mm)	Lowest (mm_
Major Basins							
1.	Indus major	619.5	606.5	164.7	26.6	1091.9	248.7
2.	Ganga major	919.1	941.6	110.7	12.0	1165.0	602.4
3.	Brahmaputra major	1706.6	1684.9	181.1	10.6	2291.4	1359.3
4.	Godavari Major	901.7	870.8	146.3	16.2	1208.1	541.6
5.	Krishna major	581.4	575.3	101.9	17.5	831.3	311.2
6.	Sabarmati	708.3	698.2	264.1	37.3	1579.8	194.9
7.	Mahi	772.4	794.1	218.4	28.3	1254.4	333.6
8.	Narmada	997.2	985.0	182.7	18.3	1530.9	587.4
9	Tapi	781.8	782.1	172.3	22.0	1197.5	353.4
10.	Mahanadi	1185.4	1190.9	175.9	14.8	1642.3	754.1
11.	Cauvery	767.0	761.9	114.7	15.0	1139.0	399.9
12.	West Coast Drainage system	1957.0	1940.7	273.3	14.0	2645.0	994.9
13.	All India	906.5	919.4	88.3	9.7	1088.8	661.3
Independent minor basins							
14.	Luni	445.4	434.8	170.8	38.3	871.0	123.3
15.	Surma	1586.7	1571.3	222.3	14.0	2188.1	1149.3
16.	Kasai	1114.2	1130.2	189.4	17.0	1584.8	758.0
17.	Damodar	1123.3	1087.6	176.0	15.7	1596.3	724.2
18.	Suvarnarekha	1146.7	1123.7	163.4	14.3	1578.0	842.7
19.	Brahmani	1140.2	1129.6	183.1	16.1	1597.1	646.3
20.	Pennar	368.2	347.4	94.5	25.7	675.2	187.5
21.	Pallar & Ponniyar	434.3	408.4	108.5	25.0	752.1	237.0
22.	Vaigai	255.3	252.0	65.9	25.8	453.9	96.8

Table 1.5. Recent 15-, 31-, 51- and 101-year changes in summer monsoon rainfall of 11 major basins, 9 independent minor basins, west coast drainage system and All India relative to entire records (superscript indicates level of significance)

Sr. No.	Basin Name	Recent 15-year change (%age)	Recent 31-year change (%age)	Recent 51-year change (%age)	Recent 101-year change (%age)
1.	Indus major	-0.1	0.0	-0.1	0.5
2.	Ganga major	-5.9	-3.1	-1.6	0.1
3.	Brahmaputra major	-7.1[1]	-5.2[1]	-4.0[1]	-1.8[1]
4.	Godavari Major	-0.8	-1.9	-1.8	0.2
5.	Krishna major	10.1[5]	4.5	3.8	2.9[5]
6.	Sabarmati	13.2	2.4	-0.4	1.3
7.	Mahi	5.3	-2.8	-3.0	-0.4
8.	Narmada	-1.0	-1.1	-2.0	0.5
9	Tapi	13.5[5]	6.4	5.0	4.2[1]
10.	Mahanadi	-4.0	-3.7	-5.2[1]	-0.5
11.	Cauvery	-15.2[1]	-8.1[1]	-2.4	0.3
12.	WCDS	10.6[1]	4.3	3.6[5]	2.9[1]
13.	All India	0.3	-0.4	0.1	1.3[5]
Independent minor basins					
14.	Luni	11.6	5.9	2.8	1.2
15.	Surma	9.0[1]	0.9	1.2	2.1[1]
16.	Kasai	-2.3	0.9	2.0	0.5
17.	Damodar	-3.6	1.8	0.5	0.5
18.	Suvarnarekha	0.6	0.9	1.1	1.6
19.	Brahmani	-11.4[1]	-9.2[1]	-7.8[1]	-1.4[5]
20.	Pennar	15.0[1]	11.8[1]	8.4[1]	2.8[5]
21.	Pallar & Ponniyar	-15.3[5]	-14.2[1]	-5.9	-2.2
22.	Vaigai	8.2	-6.0	-2.0	-2.0

Table 1.6. Recent 20 Year Changes in annual and monsoonal rainfall of All India, 11 major basins and west coast drainage system relative to last 100 years (1901-2000) monthly record (superscript indicates level of significance)

Sr. No.	Basin Name	Annual (%age)	JJAS (%age)
Major Basins			
1.	Indus major	5.0	0.8
2.	Ganga major	-6.3[5]	-6.6[5]
3.	Brahmaputra major	-8.4[1]	-7.6[1]
4.	Godavari Major	-3.4	-1.3
5.	Krishna major	5.4	7.8
6.	Sabarmati	12.2	15.3
7.	Mahi	3.6	7.9
8.	Narmada	-4.5	-0.8
9	Tapi	5.9	12.1
10.	Mahanadi	-4.3	-4.2
11.	Cauvery	-13.6[1]	-18.7[1]
12.	West Coast Drainage system	6.3	9.3
13.	All India	-1.1	-1.1
Independent Minor Basins			
14.	Luni	9.6	12.6
15.	Surma	3.9[1]	7.9[1]
16.	Kasai	-3.9	-3.7
17.	Damodar	-4.7	-4.8
18.	Suvarnarekha	3.4	-0.4
19.	Brahmani	-13.6[1]	-12.9[1]
20.	Pennar	5.3	13.7
21.	Pallar & Ponniyar	-16.0[1]	-19.7[1]
22.	Vaigai	-2.7	7.7

Table 2.1: Physical properties, raingauges and rainy season details of seven homogeneous zones across the country

Sr. no.	Homogeneous zones	Area (km^2)	No. of rain-gauges	Earliest rainfall observation: Year {station(s)}	Rainy season (Start-end)	Annual rainy days
1.	The South Peninsular India (SPI)	3,42,020	41	1813 (Chennai)	20 Apr-2 Dec	76
2.	The West Peninsular India (WPI)	4,23,863	37	1817 (Mumbai)	8 Jun-11Oct	55
3.	The East Peninsular India (EPI)	3,26,629	22	1848 (Puri)	11 Jun-3 Nov	61
4.	The North Central India (NCI)	5,99,860	65	1831 (Bankura)	11 Jun-6 Oct	61
5.	The North West India (NWI)	10,20,792	116	1826 (Nagpur)	19 Jun-18 Sept	38
6.	The North Mountainous India (NMI)	3,31,475	10	1844 (Dehradun)	21Jan-22 Sept	76
7.	The North East India (NEI)	2,34,343	25	1829 (Kolkata)	29 Mar-28 Oct	103

Table 2.2. Basic statistical parameters of Annual rainfall for the period 1901-2000 over 7 homogeneous zones

Sr. No.	Homogeneous zones	Mean (mm)	Median (mm)	SD (±mm)	CV (%)	Highest (mm)	Lowest (mm_
1.	The South Peninsular India (SPI)	1555.3	1543.7	164.4	10.6	1995.8	1242.7
2.	The West Peninsular India (WPI)	1103.0	1086.5	177.1	16.1	1472.1	664.3
3.	The East Peninsular India (EPI)	1161.6	1133.7	154.4	13.3	1595.5	861.4
4.	The North Central India (NCI)	1211.5	1214.7	144.6	11.9	1615.1	835.2
5.	The North West India (NWI)	775.2	769.4	141.1	18.2	1181.9	367.8
6.	The North Mountainous India (NMI)	1562.1	1540.0	225.5	14.4	2182.0	1159.5
7.	The North East India (NEI)	2159.6	2171.2	176.9	8.2	2490.8	1725.1

Table 2.3. Basic statistical parameters of monsoon rainfall for the period 1901-2000 over 7 homogeneous zones

Sr. No.	Homogeneous zones	Mean (mm)	Median (mm)	SD (±mm)	CV (%)	Highest (mm)	Lowest (mm_
1.	The South Peninsular India (SPI)	925.5	926.1	132.6	14.3	1355.2	509.8
2.	The West Peninsular India (WPI)	932.3	936.5	156.5	16.8	1338.6	454.8
3.	The East Peninsular India (EPI)	852.2	837.8	107.8	12.7	1113.5	593.5
4.	The North Central India (NCI)	1028.3	1020.6	123.4	12.0	1369.8	668.0
5.	The North West India (NWI)	685.2	690.7	128.9	18.8	950.9	327.3
6.	The North Mountainous India (NMI)	1118.8	1116.1	220.8	19.7	1772.6	655.4
7.	The North East India (NEI)	1509.9	1517.4	124.7	8.3	1930.8	1242.5

Table 2.4: Recent 20 Year Changes (2001-2020) in annual and seasonal rainfall relative to last 100 years (1901-2000) monthly record over seven homogeneous zones (Significance is tested using student t-test)

Sr. No.	Homogeneous zones	JF (%age)	MAM (%age)	OND (%age)	JJAS (%age)	Annual (%age)
1.	The South Peninsular India (SPI)	-32.2	10.8	-9.7	4.6	1.1
2.	The West Peninsular India (WPI)	-27.2	4.3	-8.6	7.5	5.5
3.	The East Peninsular India (EPI)	-46.7[5]	-11.7	-3.5	4.3	0.7
4.	The North Central India (NCI)	-23.5	8.8	-17.0	-9.7[1]	-9.6[1]
5.	The North West India (NWI)	-13.2	14.6	-39.2[5]	4.2	1.8
6.	The North Mountainous India (NMI)	-32.8[1]	-25.8[1]	-50.2[1]	-4.9	-12.9[1]
7.	The North East India (NEI)	-56.5[1]	-6.6	-22.9[5]	-7.3[1]	-9.4[1]

Table 2.5. Mean and standard deviation of annual and seasonal (monsoon) PCI during 1901-2000 and recent 20-year changes during (2001-2020) over 7 homogenous zones

Sr. No.	Regions	Annual PCI		Seasonal PCI	
		Mean(±sd) (1901-2000)	%age change during (2001-2020)	Mean(±sd) (1901-2000)	%age change during (2001-2020)
1.	The South Peninsular India (SPI)	14.1 (±1.5)	1.5	9.1 (±0.6)	-1.4
2.	The West Peninsular India (WPI)	20.9 (±2.3)	-0.2	9.2 (±0.6)	-2.5
3.	The East Peninsular India (EPI)	17.2 (±1.8)	5.7[5]	9.0 (±0.5)	1.3
4.	The North Central India (NCI)	20.9 (±2.1)	-1.9	9.3 (±0.6)	-1.6
5.	The North West India (NWI)	25.1 (±3.1)	2.0	10.4 (±1.1)	-1.2
6.	The North Mountainous India (NMI)	18.0 (±2.7)	10.2[1]	10.4 (±0.9)	-2.3
7.	The North East India (NEI)	15.2 (±1.1)	5.8[1]	8.6 (±0.3)	2.1[1]

Table 3.1 Climatological characteristics (mean and std dev) of 1- to 10-day EREs concerning rainfall intensity over 7 homogeneous zones

Zones	Mean rainfall intensity of Extreme rain events (±SD) in mm									
	1-day	2-day	3-day	4-day	5-day	6-day	7-day	8-day	9-day	10-day
SPI	30.2 (±21.9)	25.9 (±17.8)	22.7 (±13.9)	20.5 (±11.9)	18.8 (±9.9)	17.5 (±8.6)	16.5 (±7.5)	15.7 (±6.7)	15.0 (±6.4)	14.3 (±6.0)
WPI	32.1 (±10.2)	28.6 (±8.6)	25.5 (±7.5)	23.2 (±6.6)	21.6 (±5.8)	20.4 (±5.0)	19.5 (±4.6)	18.8 (±4.3)	18.1 (±4.2)	17.5 (±4.0)
EPI	41.2 (±9.8)	36.0 (±8.4)	31.0 (±7.4)	27.1 (±6.5)	24.1 (±5.7)	22.0 (±4.9)	20.6 (±4.3)	19.7 (±3.9)	18.9 (±3.8)	18.3 (±3.6)
NWI	20.3 (±3.3)	18.5 (±2.8)	17.0 (±2.7)	15.7 (±2.5)	14.7 (±2.3)	13.9 (±2.0)	13.3 (±1.9)	13.0 (±1.9)	12.7 (±1.8)	12.4 (±1.8)
NCI	27.7 (±4.1)	24.7 (±3.2)	22.5 (±2.8)	20.9 (±2.4)	19.5 (±2.2)	18.5 (±2.1)	17.7 (±1.9)	17.0 (±1.8)	16.3 (±1.7)	15.8 (±1.6)
NEI	45.2 (±9.4)	40.6 (±9.2)	36.8 (±8.4)	34.2 (±7.5)	31.7 (±6.7)	29.7 (±6.1)	28.0 (±5.5)	26.6 (±5.1)	25.5 (±4.8)	24.5 (±4.5)
NMI	28.5 (±11.6)	23.7 (±10.0)	19.6 (±8.2)	16.5 (±6.7)	14.5 (±5.8)	12.9 (±5.0)	11.8 (±4.5)	11.0 (±4.0)	10.3 (±3.7)	9.8 (±3.4)

Table 3.2 Climatological characteristics (mean and std dev) of 1- to 10-day EREs concerning cumulative rainfall amount over 7 homogeneous zones

Zones	Mean Cumulative rainfall amount of Extreme rain events (±SD) in mm									
	1-day	**2-day**	**3-day**	**4-day**	**5-day**	**6-day**	**7-day**	**8-day**	**9-day**	**10-day**
SPI	30.2 (±21.9)	51.9 (±35.7)	68.2 (±41.8)	81.8 (±47.6)	93.8 (±49.7)	104.8 (±51.5)	115.6 (±52.7)	125.6 (±53.7)	134.6 (±57.9)	143.2 (±59.6)
WPI	32.1 (±10.2)	57.1 (±17.2)	76.5 (±22.6)	92.9 (±26.6)	108.0 (±28.8)	122.3 (±30.1)	136.3 (±31.9)	150.4 (±34.7)	163.3 (±38.2)	175.3 (±40.4)
EPI	41.2 (±9.8)	72.1 (±16.9)	92.9 (±22.1)	108.5 (±26.0)	120.7 (±28.4)	132.1 (±29.4)	144.4 (±29.8)	157.5 (±31.6)	170.5 (±33.9)	182.5 (±36.4)
NWI	20.3 (±3.3)	36.9 (±5.7)	50.9 (±8.2)	63.0 (±10.0)	73.5 (±11.3)	83.3 (±11.9)	93.4 (±13.1)	103.9 (±15.0)	113.9 (±16.6)	123.5 (±17.9)
NCI	27.7 (±4.1)	49.4 (±6.4)	67.4 (±8.3)	83.6 (±9.7)	97.6 (±11.1)	110.8 (±12.6)	123.8 (±13.5)	136.0 (±14.7)	147.0 (±15.5)	158.3 (±16.4)
NEI	45.2 (±9.4)	81.2 (±18.4)	110.5 (±25.1)	136.8 (±29.9)	158.7 (±33.6)	178.2 (±36.6)	196.0 (±38.7)	213.2 (±41.0)	229.6 (±42.8)	245.1 (±44.6)
NMI	28.5 (±11.6)	47.3 (±20.0)	58.8 (±24.5)	66.2 (±26.9)	72.3 (±29.0)	77.5 (±30.1)	82.7 (±31.2)	88.0 (±32.3)	92.7 (±33.0)	97.8 (±33.8)

Table 3.3. Trend analysis of rainfall intensity of 1- to 10-day large-scale EREs over seven homogenous zones using Mann Kendall rank test. (Bold figures indicate significant trend at 5% level)

Subzones		**SPI**	**WPI**	**EPI**	**NWI**	**NCI**	**NEI**	**NMI**
1-day ERE	z-value	1.18	**2.30**	**2.72**	-0.92	-0.06	-0.16	**2.12**
	τ-value	0.09	**0.18**	**0.22**	-0.07	-0.01	-0.01	**0.17**
2-day ERE	z-value	0.06	**2.09**	1.80	-0.91	-0.11	-0.50	1.44
	τ-value	0.01	**0.17**	0.14	-0.07	-0.01	-0.04	0.11
3-day ERE	z-value	-0.10	0.89	1.49	-0.35	-0.53	-0.39	1.31
	τ-value	-0.01	0.07	0.12	-0.02	-0.04	0.03	0.10
4-day ERE	z-value	-0.56	0.56	1.10	-0.28	-1.03	-0.38	1.44
	τ-value	-0.04	0.04	0.09	-0.02	-0.08	-0.03	0.11
5-day ERE	z-value	-0.79	0.71	1.26	0.22	-1.51	-0.329	1.24
	τ-value	-0.06	0.05	0.10	0.01	-0.12	-0.02	0.10
6-day ERE	z-value	-0.88	0.33	0.78	0.09	-1.78	-0.45	1.28
	τ-value	-0.07	0.02	0.06	0.01	-0.14	-0.03	0.10
7-day ERE	z-value	-0.97	0.18	0.59	0.38	**-2.34**	-0.37	1.12
	τ-value	-0.07	0.01	0.04	0.03	**-0.17**	-0.03	0.09
8-day ERE	z-value	-1.13	0.02	0.52	0.82	**-2.77**	-0.44	0.90
	τ-value	-0.09	0.00	0.04	0.06	**-0.23**	-0.03	0.07
9-day ERE	z-value	-1.06	-0.23	0.71	1.37	**-2.67**	-0.45	0.94
	τ-value	-0.08	-0.02	0.05	0.11	**-0.21**	-0.03	0.07
10-day ERE	z-value	-0.94	-0.30	0.55	1.75	**-2.60**	-0.91	0.82
	τ-value	-0.07	-0.02	0.04	0.14	**-0.21**	-0.07	0.06

Table 3.4. Trend analysis of rainfall amount of 1- to 10-day large-scale EREs over seven homogenous zones using Mann Kendall rank test. (Bold figures indicate significant trend at 5% level)

Subzones		**SPI**	**WPI**	**EPI**	**NWI**	**NCI**	**NEI**	**NMI**
1-day ERE	z-value	1.19	**2.30**	**2.72**	-0.92	-0.06	-0.16	**2.12**
	τ-value	0.09	**0.19**	**0.22**	-0.07	-0.01	-0.01	**0.17**
2-day ERE	z-value	0.06	**2.09**	1.80	-0.91	-0.11	-0.52	1.44
	τ-value	0.01	**0.17**	0.14	-0.07	-0.01	-0.04	0.11
3-day ERE	z-value	-0.10	0.89	1.49	-0.35	-0.53	-0.39	131
	τ-value	-0.01	0.07	0.12	-0.02	-0.04	0.03	0.10
4-day ERE	z-value	-0.56	0.56	1.10	-0.28	-1.03	-0.38	1.44
	τ-value	-0.04	0.04	0.09	-0.02	-0.08	-0.03	0.11
5-day ERE	z-value	-0.79	0.71	1.26	0.22	-1.51	-0.29	1.24
	τ-value	-0.06	0.05	0.10	0.01	-0.12	-0.02	0.10
6-day ERE	z-value	-0.88	0.33	0.78	0.09	-1.78	-0.45	1.28
	τ-value	-0.07	0.02	0.06	0.01	-0.14	-0.03	0.10
7-day ERE	z-value	-0.97	0.18	0.59	0.38	**-2.34**	-0.37	1.12
	τ-value	-0.07	0.01	0.04	0.03	**-0.17**	-0.03	0.09
8-day ERE	z-value	-1.13	0.02	0.52	0.82	**-2.77**	-0.04	0.90
	τ-value	-0.09	0.00	0.04	0.06	**-0.23**	-0.03	0.07
9-day ERE	z-value	-1.06	-0.23	0.711	1.37	**-2.67**	-0.41	0.94
	τ-value	-0.87	-0.01	0.05	0.11	**-0.21**	-0.03	0.07
10-day ERE	z-value	-0.94	-0.31	0.55	1.75	**-2.60**	-0.91	0.82
	τ-value	-0.07	-0.02	0.04	0.14	**-0.21**	-0.07	0.06

Table 3.5. Recent 20 years (2001-2020) percentage change in rainfall intensity of 1- to 10-day extremes (ERE-RI) over seven subzones compare to 1951-2000. (significance is tested using student's t-test)

Zones	%age change in RI of ERE-RI									
	1-day	**2-day**	**3-day**	**4-day**	**5-day**	**6-day**	**7-day**	**8-day**	**9-day**	**10-day**
SPI	38.6^{10}	29.2	22.4	19.3	15.6	13.3	11.7	10.4	11.1	10.8
WPI	16.9^{5}	18.3^{5}	13.2^{10}	12.0	11.5	8.6	7.5	7.6	8.3	8.3
EPI	15.7^{5}	13.1^{5}	11.7^{10}	11.8^{10}	12.2^{5}	9.5	7.7	7.9	9.0	8.0
NWI	-3.7	-1.4	-0.4	0.7	1.1	0.7	0.6	1.8	2.4	3.4
NCI	2.9	1.7	1.1	1.1	0.7	0.1	-1.3	-2.4	-2.9	-4.0
NEI	2.1	-0.3	1.1	1.2	2.1	2.2	2.0	1.8	0.9	0.2
NMI	0.0	-8.2	-9.5	-8.3	-9.4	-9.2	-8.6	-8.4	-8.7	-7.0

Table 3.6. Recent 20 years (2001-2020) percentage change in cumulative rainfall amount of 1- to 10-day extremes (ERE-RA) over seven subzones 1951-2000. (significance is tested using student's t-test)

Zones	%age change in RA of ERE-RA									
	1-day	**2-day**	**3-day**	**4-day**	**5-day**	**6-day**	**7-day**	**8-day**	**9-day**	**10-day**
SPI	38.6[10]	29.2	22.4	19.3	15.6	13.3	11.7	10.4	11.1	10.8
WPI	16.9[5]	18.3[5]	13.2[10]	12.0	11.5	8.6	7.5	7.6	8.3	8.3
EPI	15.7[5]	13.1[5]	11.7[10]	11.8[10]	12.2[5]	9.5	7.7	7.9	9.0	8.0
NWI	-3.7	-1.4	-0.4	0.7	1.1	0.7	0.6	1.8	2.4	3.4
NCI	2.9	1.7	1.1	1.1	0.7	0.1	-1.3	-2.4	-2.9	-4.0
NEI	2.1	-0.3	1.1	1.2	2.1	2.2	2.0	1.8	0.9	0.2
NMI	0.0	-8.2	-9.5	-8.3	-9.4	-9.2	-8.6	-8.4	-8.7	-7.0

Table 3.7. : Most extreme 1- to 10-day rain events during 1951-2020 over South Peninsular India (SPI).

Sr. No.	**Duration of ERE**	**ERE concerning rainfall Intensity**		**ERE concerning Rainfall Amount**	
		Rainfall Intensity(mm/day)	**period**	**Rainfall Amount (mm)**	**period**
1.	**1-day**	199.0	25 Jul-2005	199.0	25 Jul-2005
2.	**2-day**	161.6	24-25 Jul-2005	323.3	24-25 Jul-2005
3.	**3-day**	128.1	24-26 Jul-2005	384.2	24-26 Jul-2005
4.	**4-day**	110.2	23-26 Jul-2005	440.8	23-26 Jul-2005
5.	**5-day**	93.0	22-26 Jul-2005	464.9	22-26 Jul-2005
6.	**6-day**	81.0	22-27 Jul-2005	486.1	22-27 Jul-2005
7.	**7-day**	72.3	22-28 Jul-2005	505.9	22-28 Jul-2005
8.	**8-day**	65.4	22-29 Jul-2005	522.8	22-29 Jul-2005
9.	**9-day**	63.0	18-26 Jul-2005	567.9	18-26 Jul-2005
10	**10-day**	59.0	18-27 Jul-2005	589.2	18-27 Jul-2005

Table 3.8. : Most extreme 1- to 10-day rain events during 1951-2020 over West Peninsular India (WPI).

Sr. No.	Duration of ERE	ERE concerning rainfall Intensity		ERE concerning Rainfall Amount	
		Rainfall Intensity(mm/day)	period	Rainfall Amount (mm)	period
1.	**1-day**	76.8	24-Jul-1989	76.8	24-Jul-1989
2.	**2-day**	65.8	26-27 Jul -2005	131.6	26-27 Jul -2005
3.	**3-day**	60.2	25-27 Jul-2005	180.5	25-27 Jul-2005
4.	**4-day**	54.5	25-28 Jul-2005	217.9	25-28 Jul-2005
5.	**5-day**	48.5	24-28 Jul-2005	242.4	24-28 Jul-2005
6.	**6-day**	43.5	23-28 Jul-2005	261.0	23-28 Jul-2005
7.	**7-day**	40.3	22-28 Jul-2005	282.3	22-28 Jul-2005
8.	**8-day**	39.5	25 Jul-1 Aug-2005	316.2	25 Jul-1 Aug-2005
9.	**9-day**	39.2	25 Jul- 2 Aug-2005	352.5	25 Jul- 2 Aug-2005
10	**10-day**	37.7	24 Jul- 2 Aug-2005	377.1	24 Jul- 2 Aug-2005

Table 3.9 : Most extreme 1- to 10-day rain events during 1951-2020 over East Peninsular India (EPI).

Sr. No.	Duration of ERE	ERE concerning rainfall Intensity		ERE concerning Rainfall Amount	
		Rainfall Intensity(mm/day)	period	Rainfall Amount (mm)	period
1.	**1-day**	70.6	4 Aug-2006	70.6	4 Aug-2006
2.	**2-day**	65.9	3-4 Aug-2006	131.9	3-4 Aug-2006
3.	**3-day**	55.2	3-5 Aug 2006	165.5	3-5 Aug 2006
4.	**4-day**	47.6	2-5 Aug-2006	190.4	2-5 Aug-2006
5.	**5-day**	41.0	10-14 Aug-1986	204.8	10-14 Aug-1986
6.	**6-day**	36.4	9-14 Aug-1986	218.7	9-14 Aug-1986
7.	**7-day**	32.7	8-14 Aug-1986	229.2	8-14 Aug-1986
8.	**8-day**	30.2	7-14 Aug-1986	241.2	7-14 Aug-1986
9.	**9-day**	28.5	6-14 Aug-1986	256.8	6-14 Aug-1986
10	**10-day**	27.7	5-14 Aug-1986	277.5	5-14 Aug-1986

Table 3.10: Most extreme 1- to 10-day rain events during 1951-2020 over North West India (NWI).

Sr. No.	Duration of ERE	ERE concerning rainfall Intensity		ERE concerning Rainfall Amount	
		Rainfall Intensity(mm/day)	period	Rainfall Amount (mm)	period
1.	**1-day**	29.5	28 Jul-2015	29.5	28 Jul-2015
2.	**2-day**	26.7	27-28 Jul-2015	53.4	27-28 Jul-2015
3.	**3-day**	26.9	26-28 Jul-2015	80.6	26-28 Jul-2015
4.	**4-day**	25.7	26-29 Jul-2015	103.0	26-29 Jul-2015
5.	**5-day**	23.8	25-29 Jul-2015	119.1	25-29 Jul-2015
6.	**6-day**	22.1	24-29 Jul-2015	132.6	24-29 Jul-2015
7.	**7-day**	20.4	24-30 Jul-2015	143.1	24-30 Jul-2015
8.	**8-day**	18.8	23-30 Jul-2015	150.5	23-30 Jul-2015
9.	**9-day**	17.7	22-30 Jul-2015	159.4	22-30 Jul-2015
10	**10-day**	17.4	20-29 Jul-2015	174.4	20-29 Jul-2015

Table 3.11: Most extreme 1- to 10-day rain events during 1951-2020 over North Central India (NCI).

Sr. No.	Duration of ERE	ERE concerning rainfall Intensity		ERE concerning Rainfall Amount	
		Rainfall Intensity(mm/day)	period	Rainfall Amount (mm)	period
1.	**1-day**	40.8	29 Sep-2019	40.8	29 Sep-2019
2.	**2-day**	36.2	28-29 Sep-2019	72.5	28-29 Sep-2019
3.	**3-day**	33.8	27-30 Sep-2019	101.5	27-30 Sep-2019
4.	**4-day**	31.4	26-30 Sep-2019	125.7	26-30 Sep-2019
5.	**5-day**	28.7	25-30 Sep-2019	143.6	25-30 Sep-2019
6.	**6-day**	26.3	24-30 Sep-2019	157.6	24-30 Sep-2019
7.	**7-day**	23.7	23-30 Sep-2019	166.2	23-30 Sep-2019
8.	**8-day**	21.5	22-30 Sep-2019	172.1	22-30 Sep-2019
9.	**9-day**	20.2	13-21 Jul-1975	181.9	13-21 Jul-1975
10	**10-day**	19.3	13-22 Jul-1975	193.3	13-22 Jul-1975

Table 3.12: Most extreme 1- to 10-day rain events during 1951-2020 over North-East India (NEI).

Sr. No.	Duration of ERE	ERE concerning rainfall Intensity		ERE concerning Rainfall Amount	
		Rainfall Intensity(mm/day)	period	Rainfall Amount (mm)	period
1.	**1-day**	71.3	11 Aug-2017	71.3	11 Aug-2017
2.	**2-day**	70.7	11-12 Aug-2017	141.5	11-12 Aug-2017
3.	**3-day**	63.7	10-12 Aug-2017	191.2	10-12 Aug-2017
4.	**4-day**	55.7	9-12 Aug-2017	223.0	9-12 Aug-2017
5.	**5-day**	50.7	9-13 Aug-2017	253.3	9-13 Aug-2017
6.	**6-day**	47.1	8-13 Aug-2017	282.8	8-13 Aug-2017
7.	**7-day**	43.0	8-14 Aug-2017	301.1	8-14 Aug-2017
8.	**8-day**	39.8	7-14 Aug-2017	318.4	7-14 Aug-2017
9.	**9-day**	38.3	7-15 Jul-2019	344.9	7-15 Jul-2019
10	**10-day**	37.0	7-16 Jul-2019	370.2	7-16 Jul-2019

Table 3.13: Most extreme 1- to 10-day rain events during 1951-2020 over North Mountainous India (NMI).

Sr. No.	Duration of ERE	ERE concerning rainfall Intensity		ERE concerning Rainfall Amount	
		Rainfall Intensity(mm/day)	period	Rainfall Amount (mm)	period
1.	**1-day**	60.5	26 Sep-1988	60.5	26 Sep-1988
2.	**2-day**	50.0	25-26 Sep-1988	100.0	25-26 Sep-1988
3.	**3-day**	42.3	25-27 Dec-1988	126.9	25-27 Dec-1988
4.	**4-day**	36.6	24-27 Sep-1988	146.5	24-27 Sep-1988
5.	**5-day**	32.0	24-28 Sep-1988	159.9	24-28 Sep-1988
6.	**6-day**	28.9	18-23 Mar-1990	173.7	18-23 Mar-1990
7.	**7-day**	27.0	17-23 Mar-1990	188.9	17-23 Mar-1990
8.	**8-day**	24.4	17-24 Mar-1990	195.3	17-24 Mar-1990
9.	**9-day**	21.9	16-24 Mar-1990	197.0	16-24 Mar-1990
10	**10-day**	19.7	16-25 Mar-1990	197.3	16-25 Mar-1990

Table 4.1 : Composite of percentage Departure from normal in rainfall during four extreme wet and extreme dry months over All India

Months	Extreme wet years	%age departure from normal	Extreme dry years	%age departure from normal
Jan	1995, 1996, 2005, 2012	84.1	1988, 2006, 2007, 2011	-75.9
Feb	1990, 2003, 2007, 2013	118.9	1997, 2004, 2006, 2009	-79.5
March	1982, 2006, 2008, 2015	108.9	1992, 1999, 2004, 2012	-70.7
April	1983, 1997, 2001, 2015	57.1	1989, 1992, 1999, 2009	-45.8
May	1990, 1999, 2000, 2006	60.8	1984, 1996, 2003, 2012	-42.8
June	2001, 2008, 2011, 2013	36.8	1987, 2009, 2012, 2014	-41.1
July	1981, 1988, 1994, 2013	19.9	1982, 1987, 2002, 2004	-30.8
Aug	1993, 1988, 1994, 2011	19.8	1993, 2005, 2009, 2015	-25.7
Sept	1983, 1998, 2007, 2010	36.3	1982, 1986, 2001, 2015	-33.2
Oct	1985, 1998, 1999, 2013	70.6	1982, 2000, 2011, 2015	-46.4
Nov	1979, 1997, 2009, 2010	110.8	1983, 1984, 2003, 2007	-60.2
Dec	1980, 1983, 1987, 1997	139.3	1999, 2002, 2004, 2007	-73.0
JJAS	1983, 1988, 1994, 2007	15.3	1979, 1987, 2009, 2015	-17.9
ANN	1983, 1990, 1998, 2013	13.4	1979, 1987, 2002, 2009	-13.5

Table 5.1 Correlation coefficients between All India monsoon monthly rainfall and 10 climatic indices (* and ** indicates 5% and 1% level of significance respectively)

	PDO (167yr)	SOI (155yr)	NAO (197yr)	AMO (165yr)	AO (164yr)	Niño3.4 (151yr)	AAO (142yr)	DMI (151yr)	TSA (73yr)	TNA (73yr)
June	-0.30**	0.16*	0.27**	-0.05	0.30**	-0.43**	0.01	-0.13	0.07	-0.05
July	-0.10	0.18*	0.04	0.00	0.22**	-0.32**	-0.05	-0.08	-0.20	-0.09
August	-0.10	0.16*	-0.02	-0.05	0.24**	-0.23**	-0.03	0.00	-0.18	-0.11
September	-0.28**	0.40**	0.06	-0.01	0.31**	-0.45**	0.05	-0.17*	-0.05	-0.02
JJAS	-0.23**	0.48**	0.06	-0.01	0.37**	-0.60**	-0.09	-0.17*	-0.04	-0.05

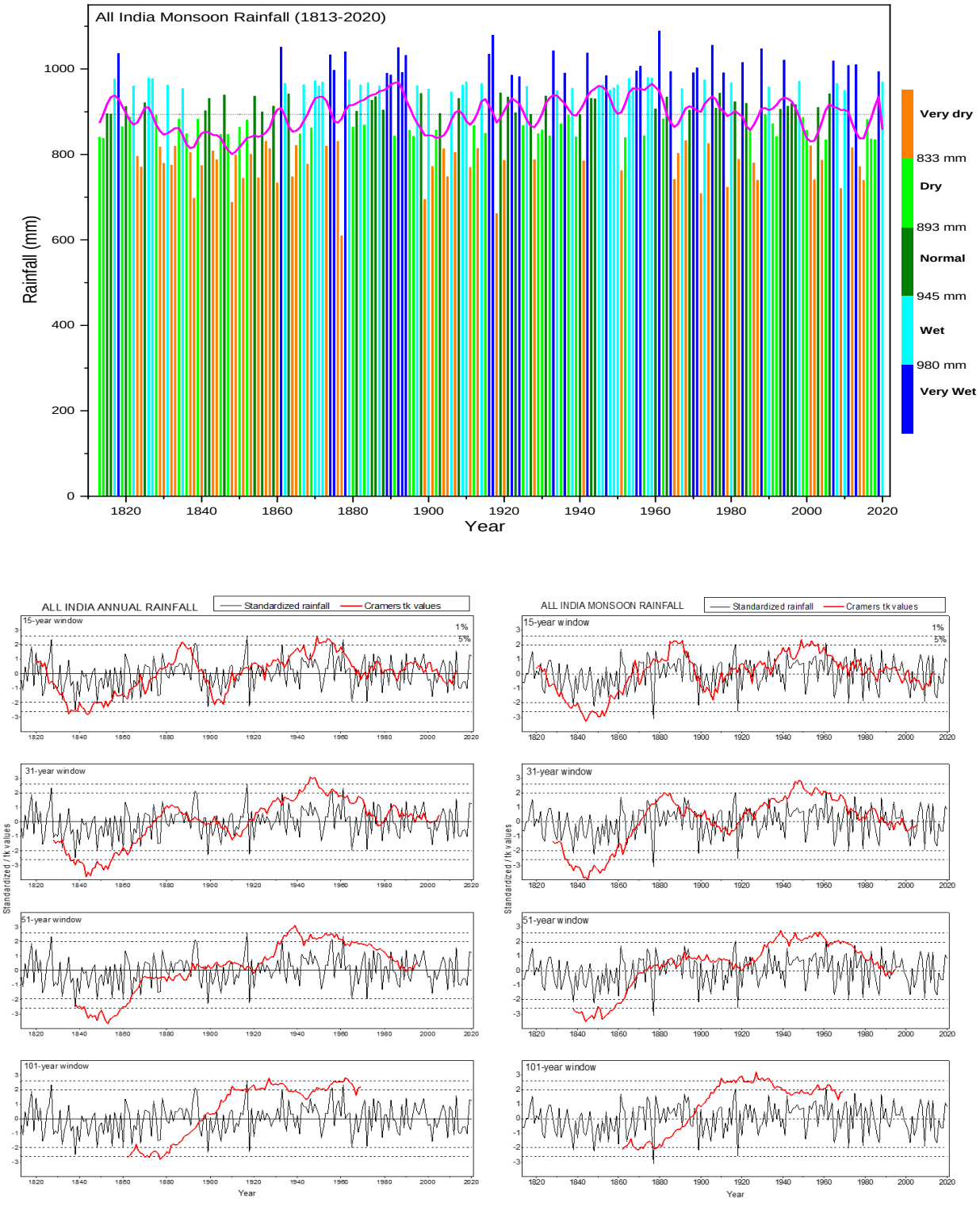

Fig.1 a) Interannual variations in categorized rainfall distribution and b) Cramers t_k statistics for 15-, 31-, 51- and 101-year moving averages of All India rainfall

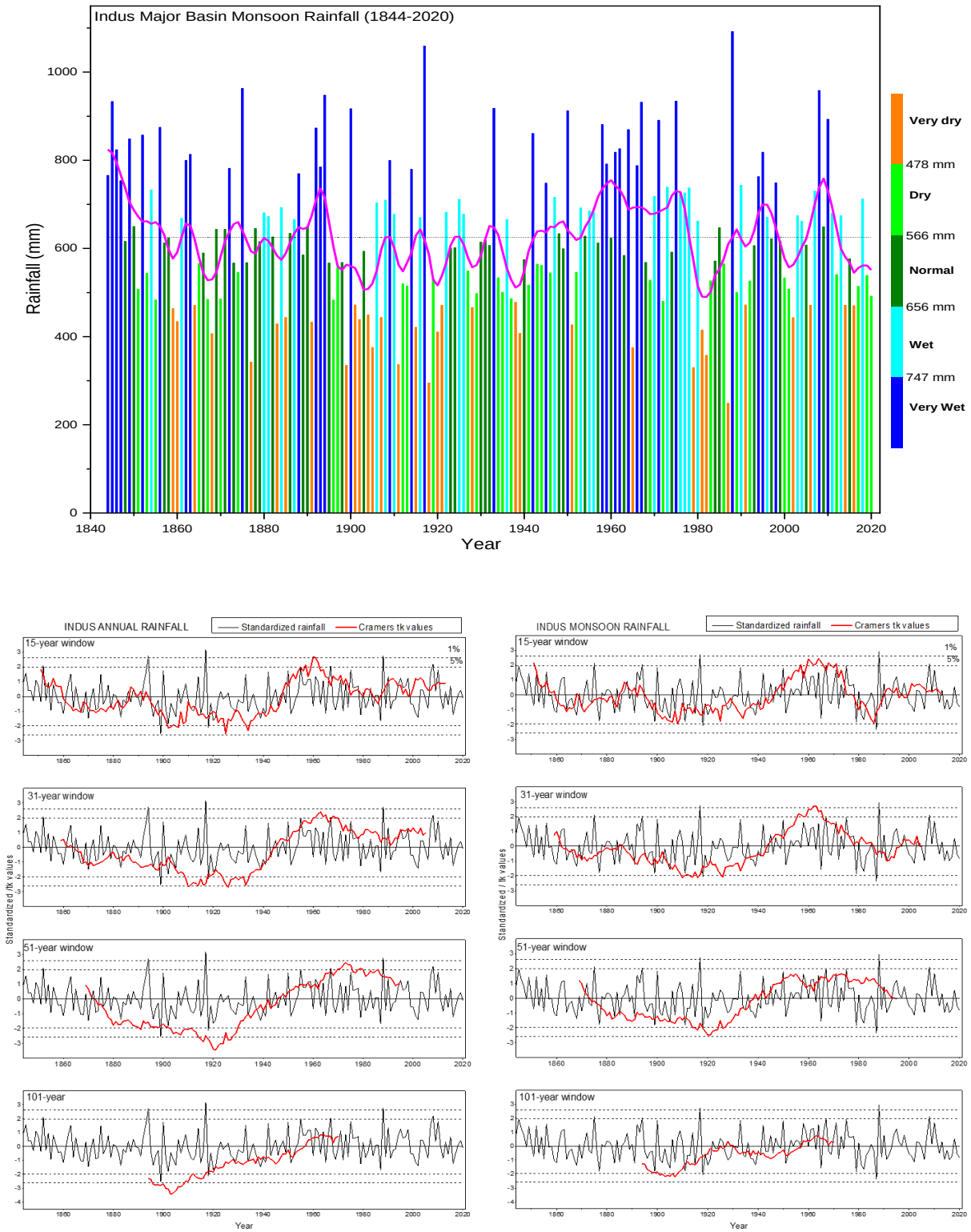

Fig.1.2 a) Interannual variations in categorized rainfall distribution and b) Cramers t_k statistics for 15-, 31-, 51- and 101-year moving averages of Indus major river basin rainfall

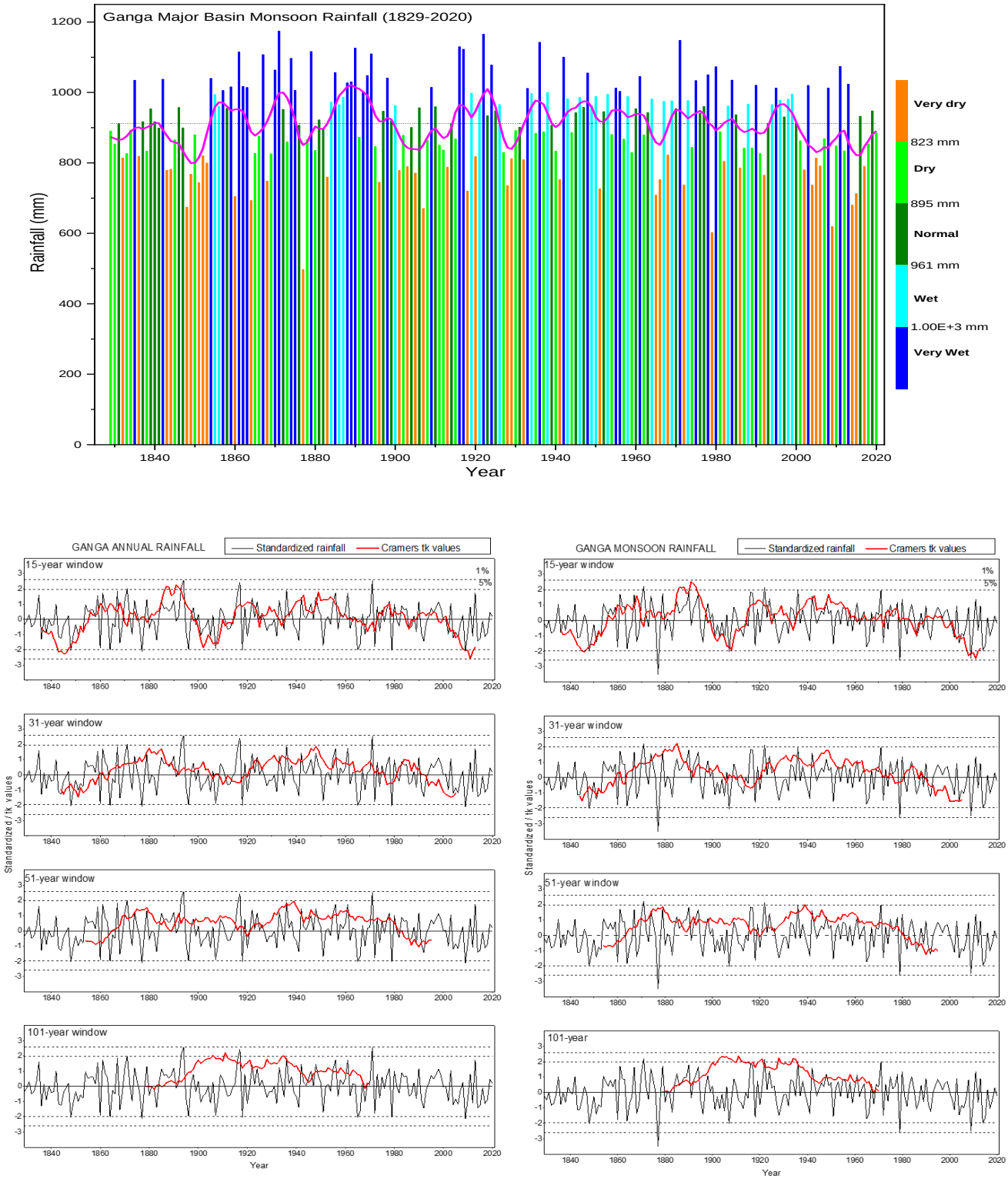

Fig.1.3 a) Interannual variations in categorized rainfall distribution and b) Cramers t_k statistics for 15-, 31-, 51- and 101-year moving averages of Ganga major river basin rainfall

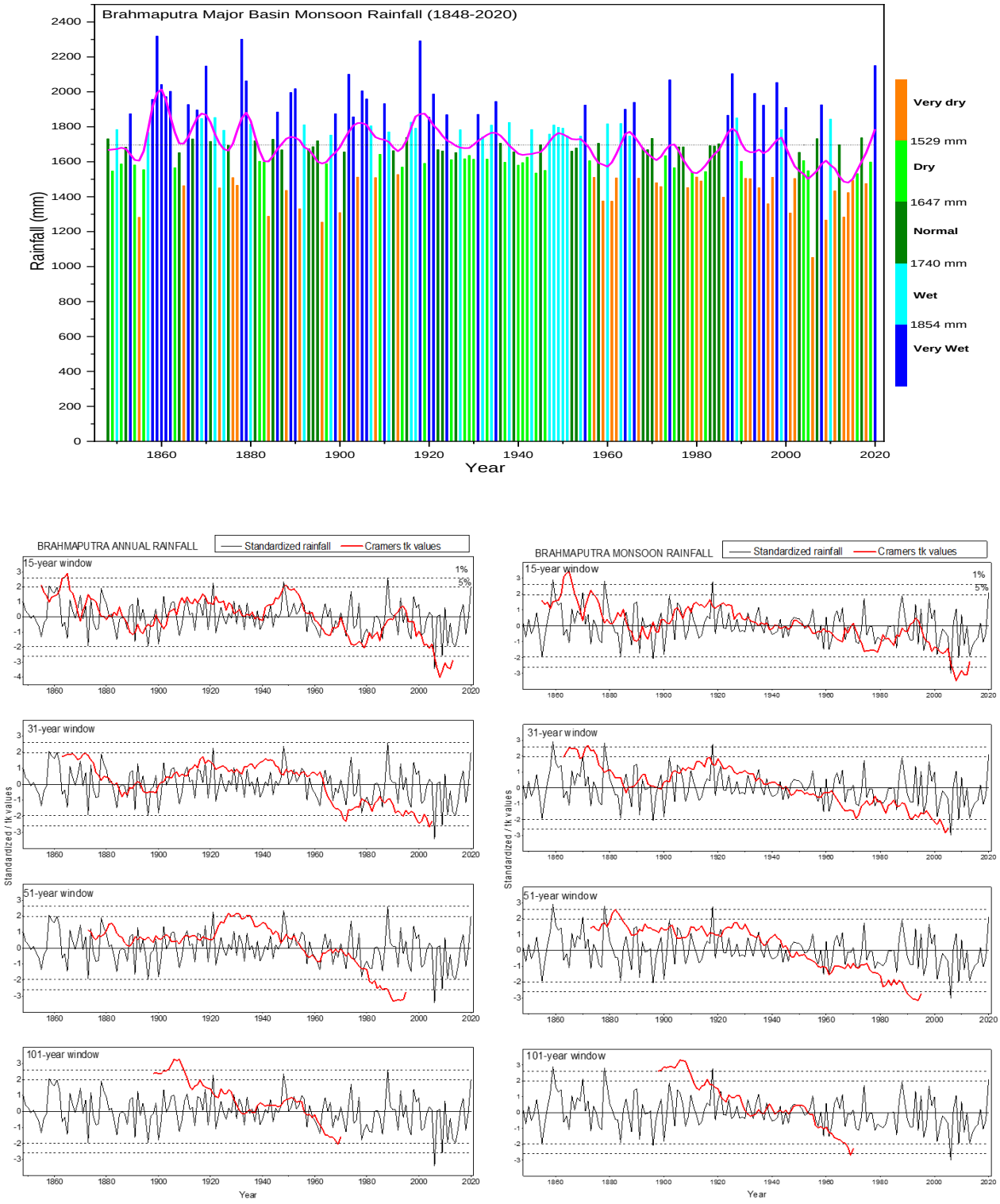

Fig.1.4 a) Interannual variations in categorized rainfall distribution and b) Cramers t_k statistics for 15-, 31-, 51- and 101-year moving averages of Brahmaputra major river basin rainfall

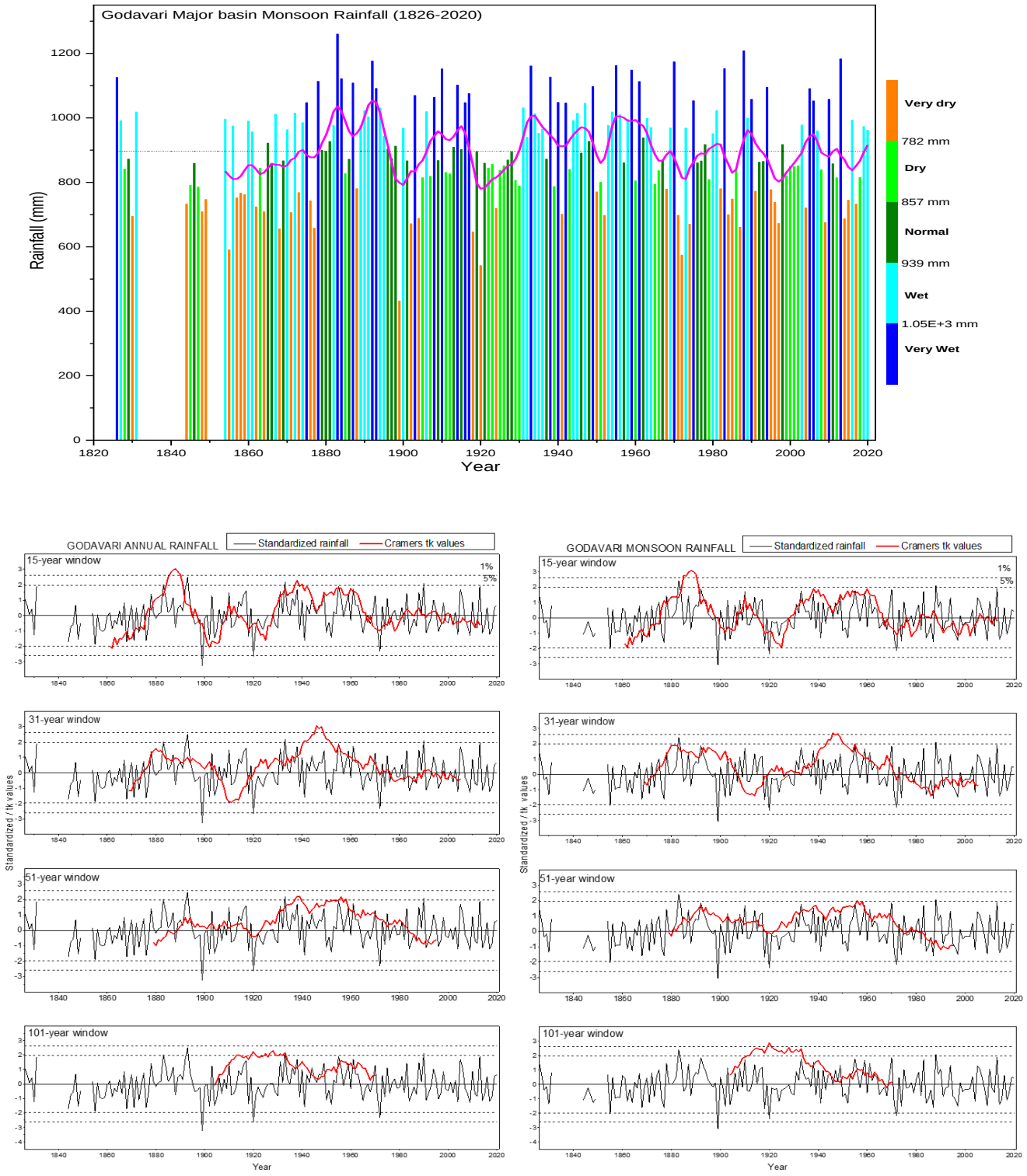

Fig.1.5 a) Interannual variations in categorized rainfall distribution and b) Cramers t_k statistics for 15-, 31-, 51- and 101-year moving averages of Godavari major river basin rainfall

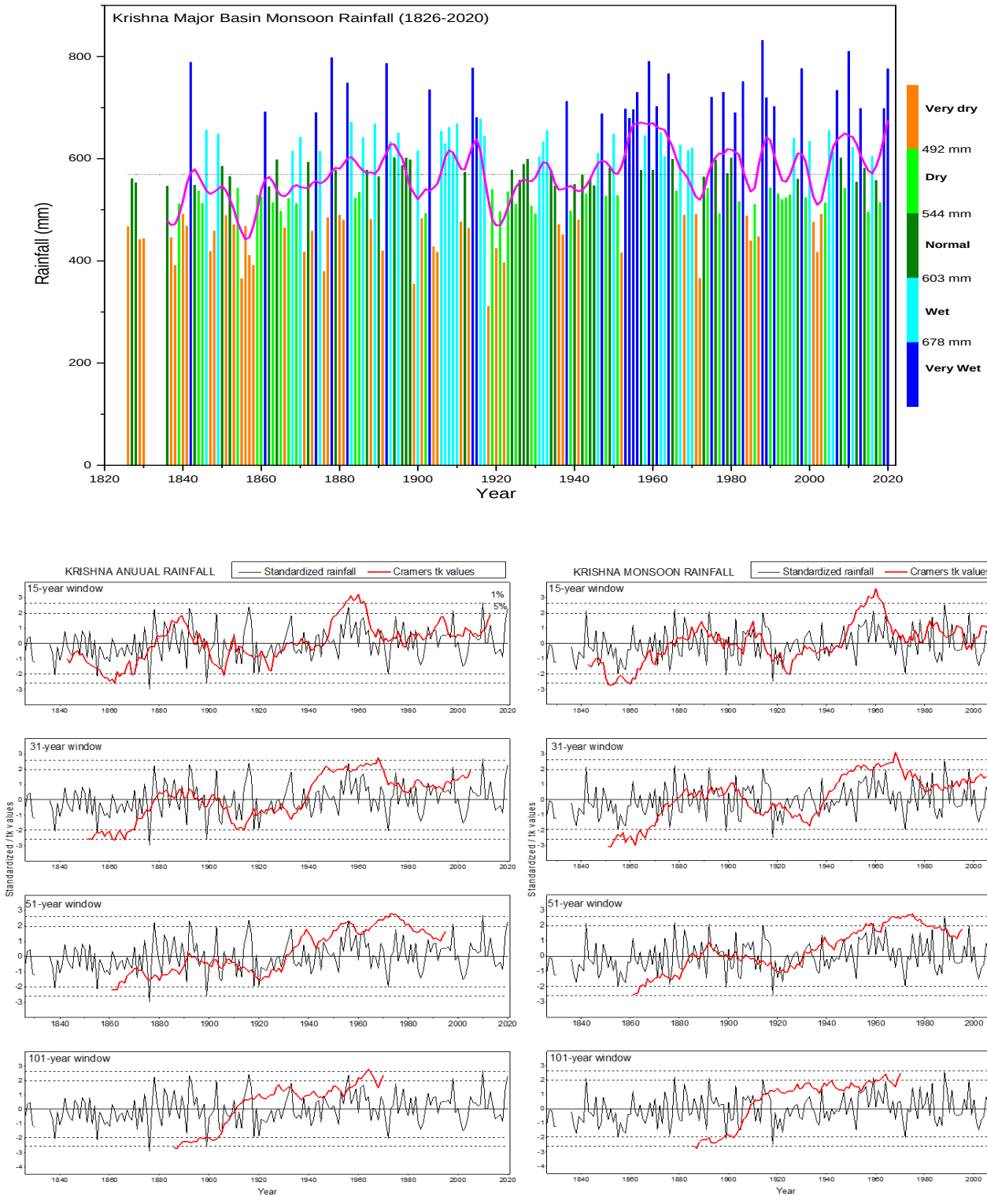

Fig.1.6 a) Interannual variations in categorized rainfall distribution and b) Cramers t_k statistics for 15-, 31-, 51- and 101-year moving averages of Krishna major river basin rainfall

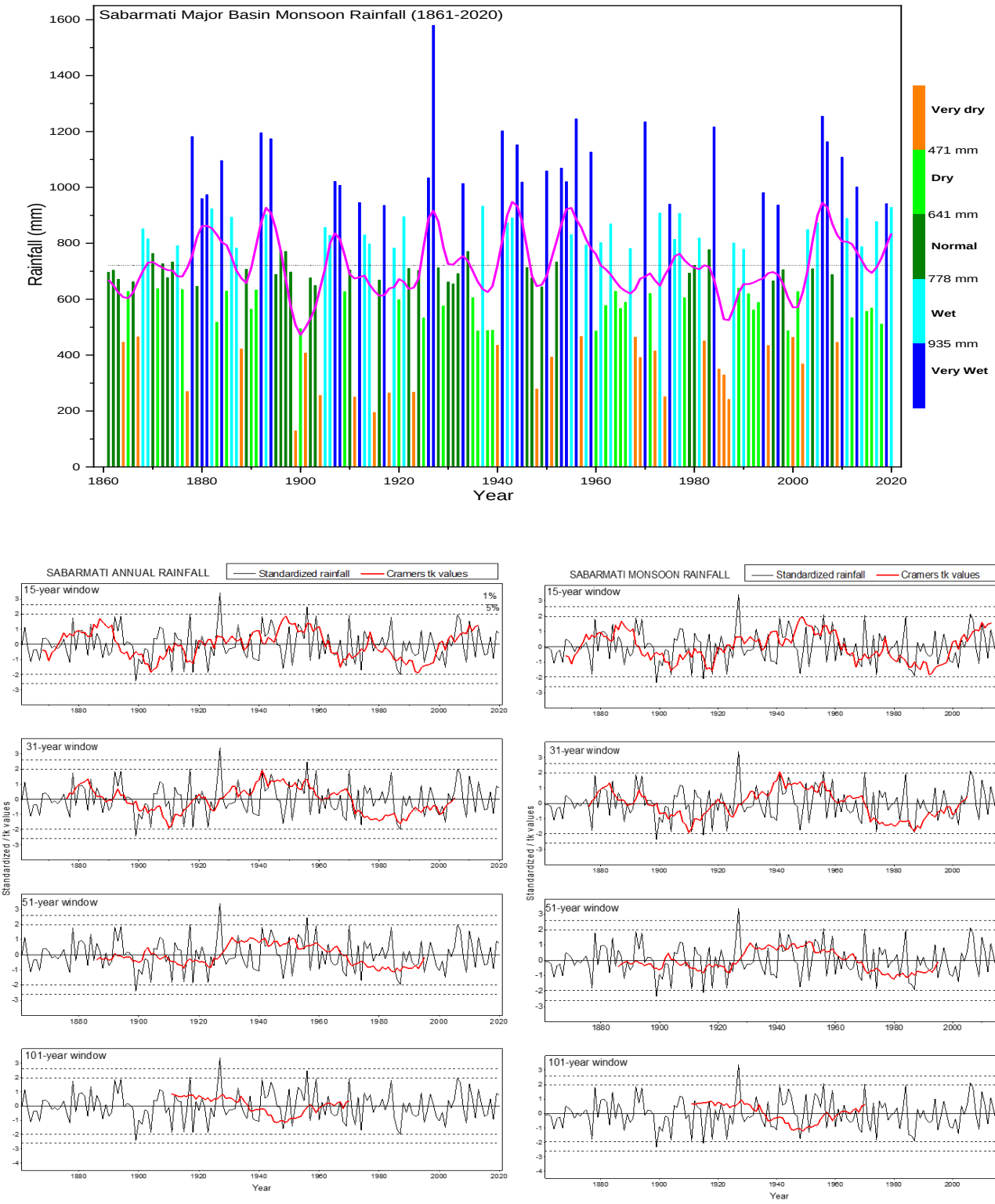

Fig.1.7 a) Interannual variations in categorized rainfall distribution and b) Cramers t_k statistics for 15-, 31-, 51- and 101-year moving averages of Sabarmati major river basin rainfall

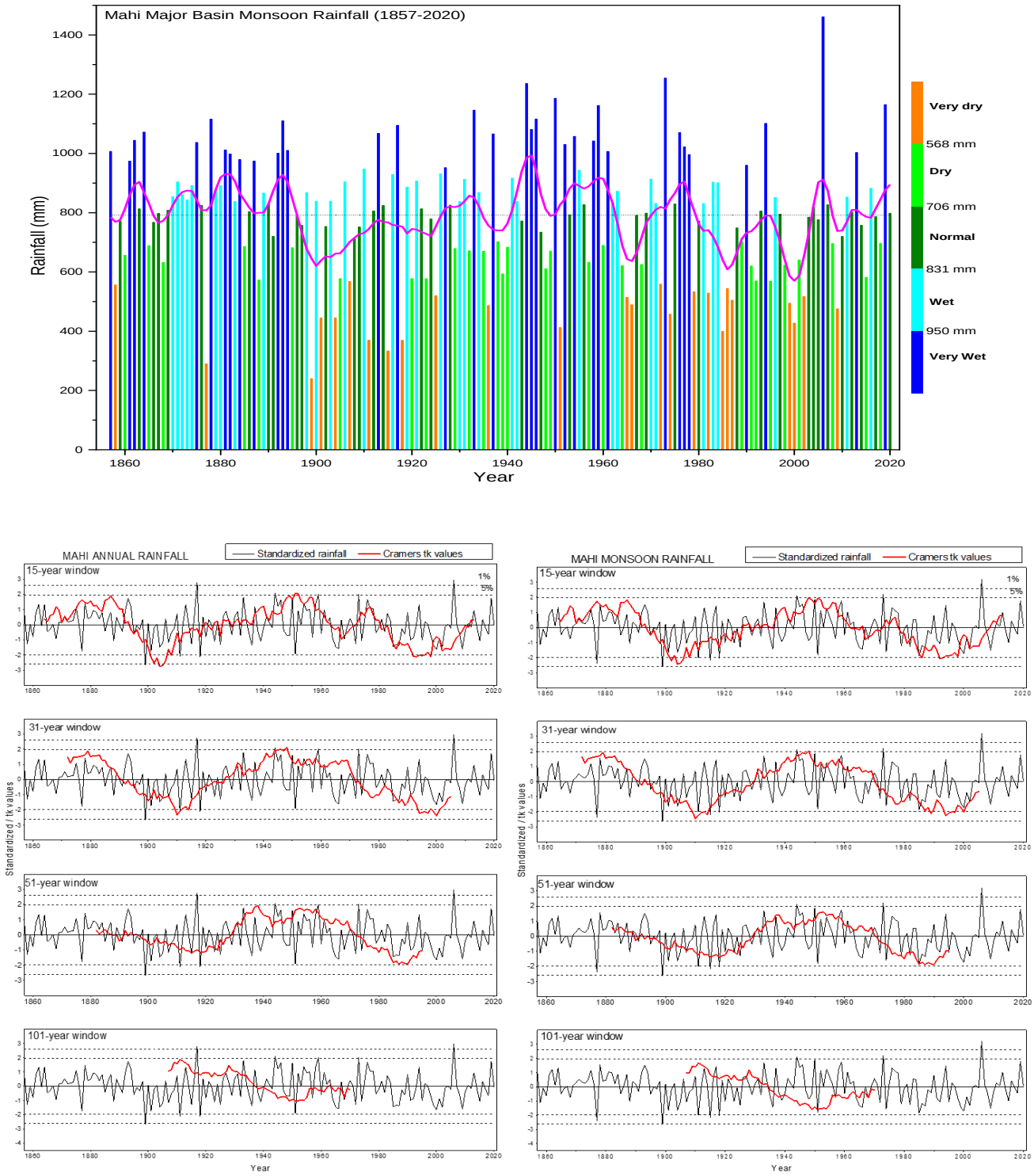

Fig.1.8 a) Interannual variations in categorized rainfall distribution and b) Cramers t_k statistics for 15-, 31-, 51- and 101-year moving averages of Mahi major river basin rainfall

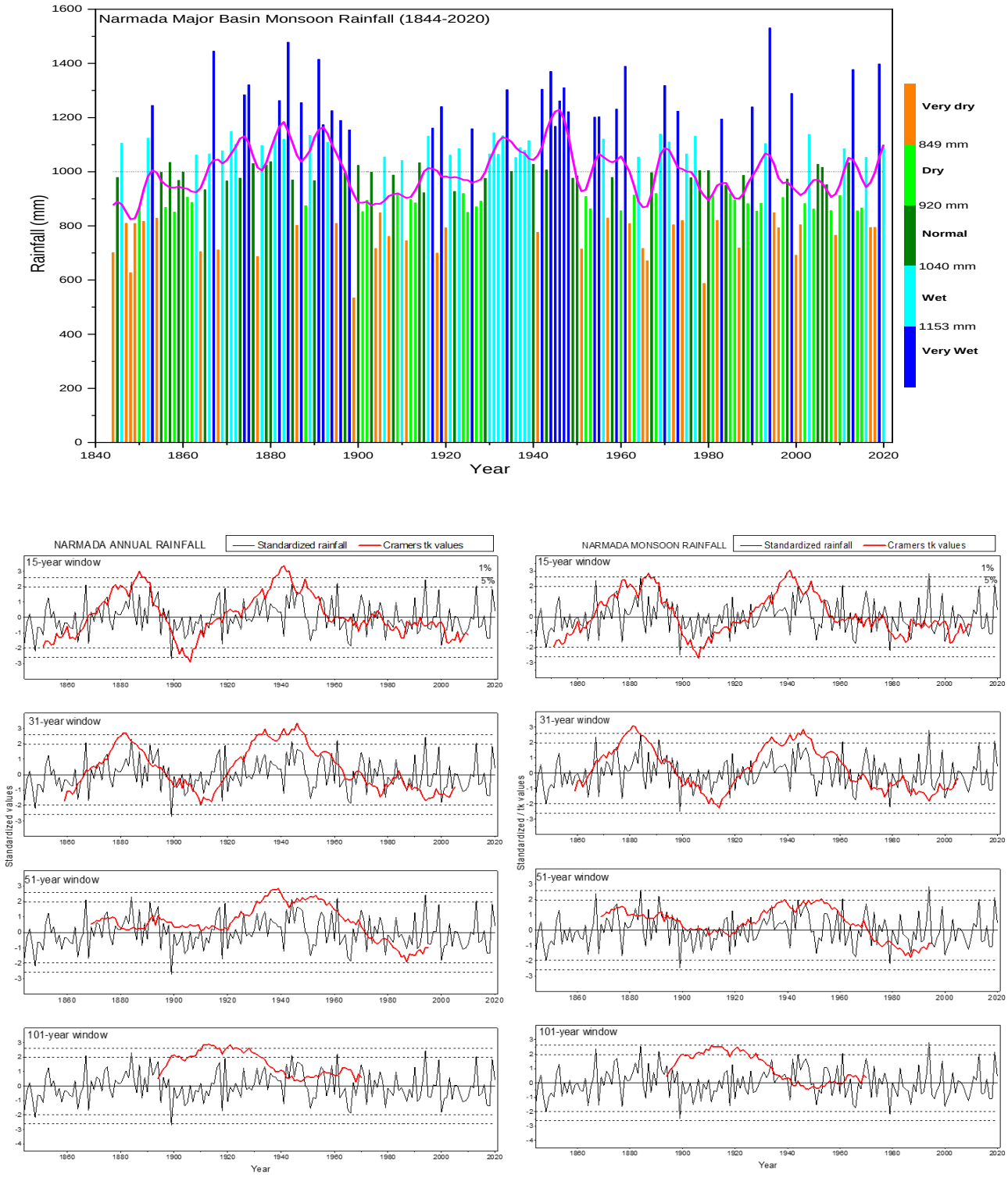

Fig.1.9 a) Interannual variations in categorized rainfall distribution and b) Cramers t_k statistics for 15-, 31-, 51- and 101-year moving averages of Narmada major river basin rainfall

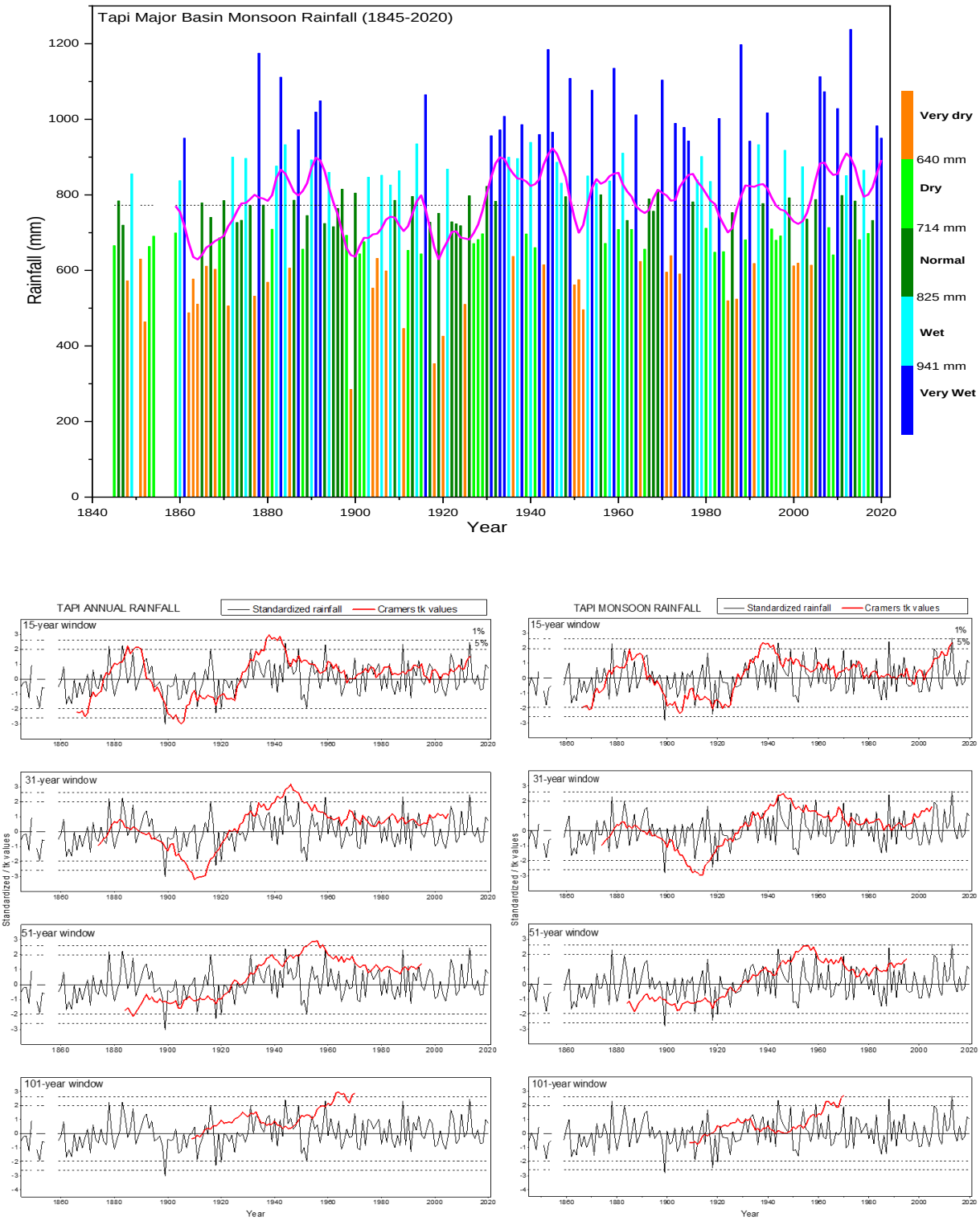

Fig.1.10 a) Interannual variations in categorized rainfall distribution and b) Cramers t_k statistics for 15-, 31-, 51- and 101-year moving averages of Tapi major river basin rainfall

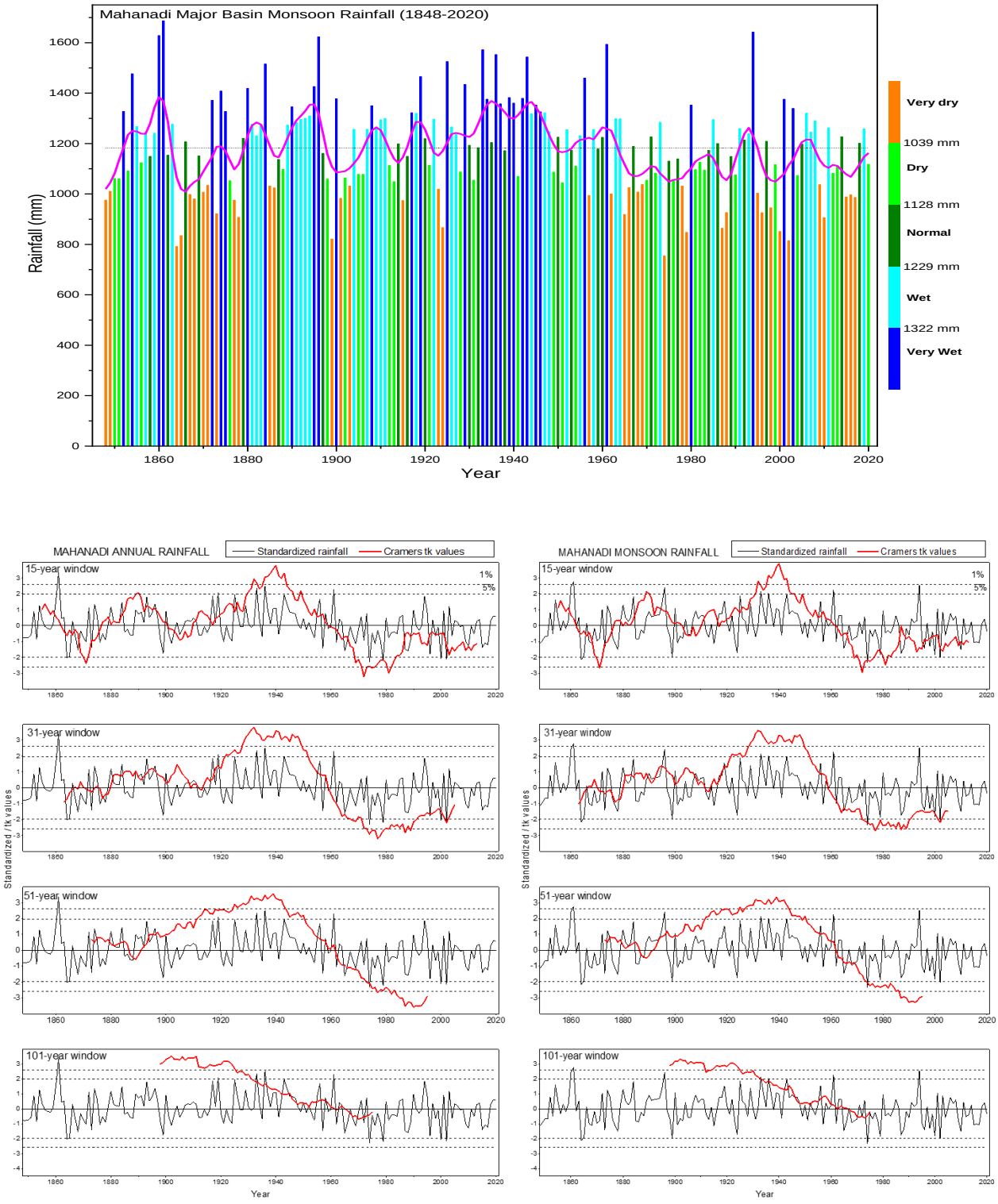

Fig.1.11 a) Interannual variations in categorized rainfall distribution and b) Cramers t_k statistics for 15-, 31-, 51- and 101-year moving averages of Mahanadi major river basin rainfall

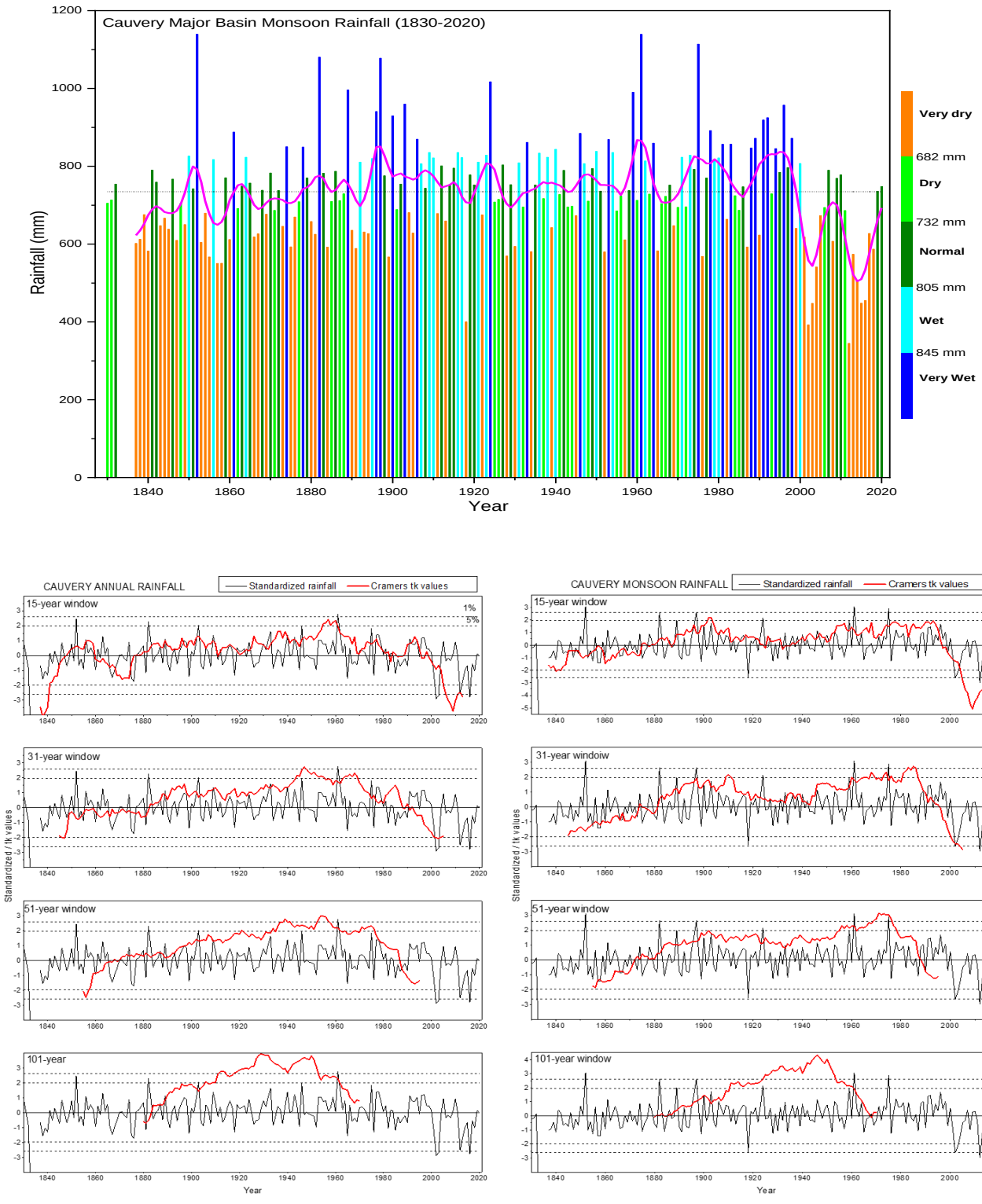

Fig.1.12 a) Interannual variations in categorized rainfall distribution and b) Cramers t_k statistics for 15-, 31-, 51- and 101-year moving averages of Cauvery major river basin rainfall

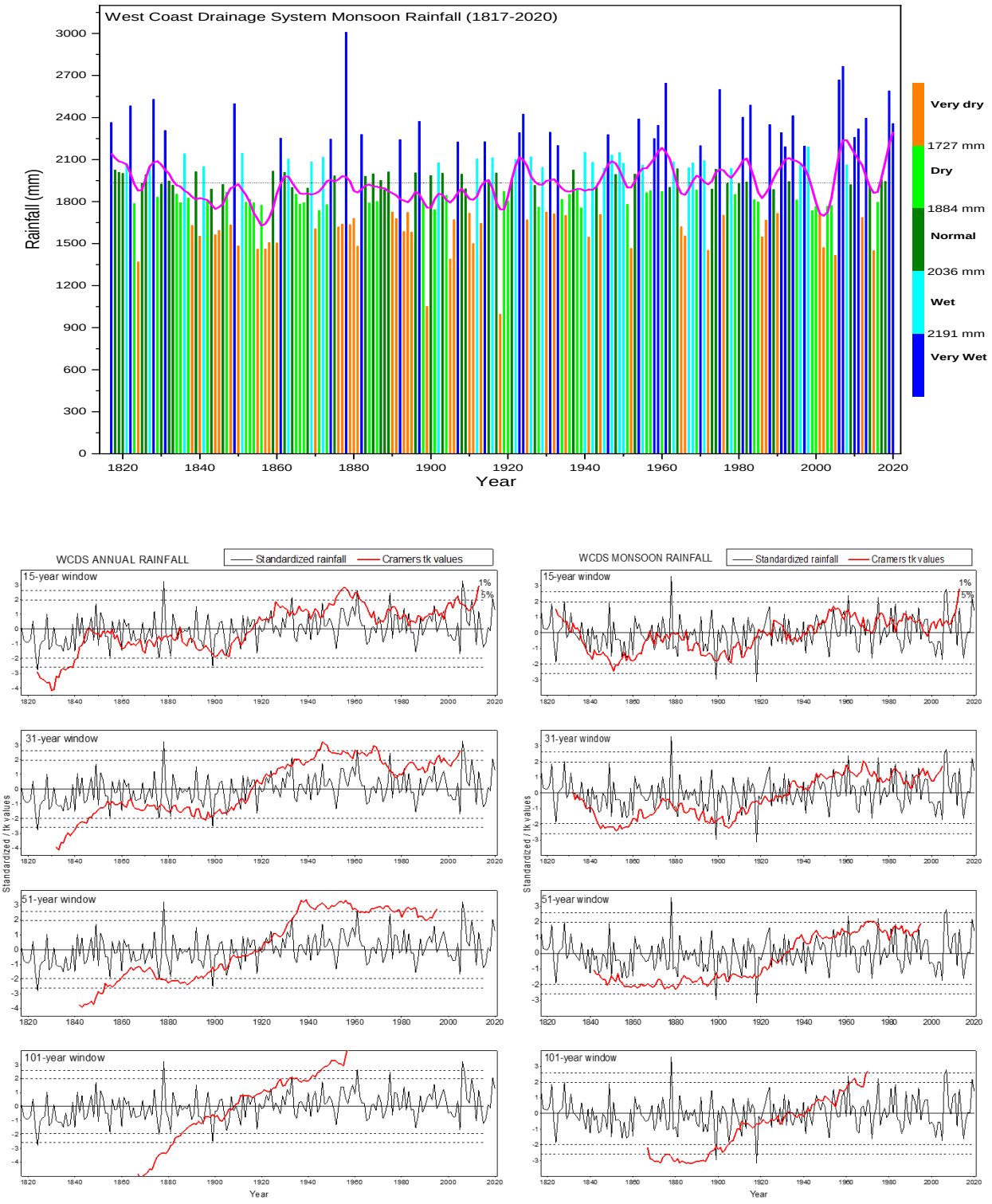

Fig.1.13 a) Interannual variations in categorized rainfall distribution and b) Cramers t_k statistics for 15-, 31-, 51- and 101-year moving averages of West Coast Drainage System rainfall

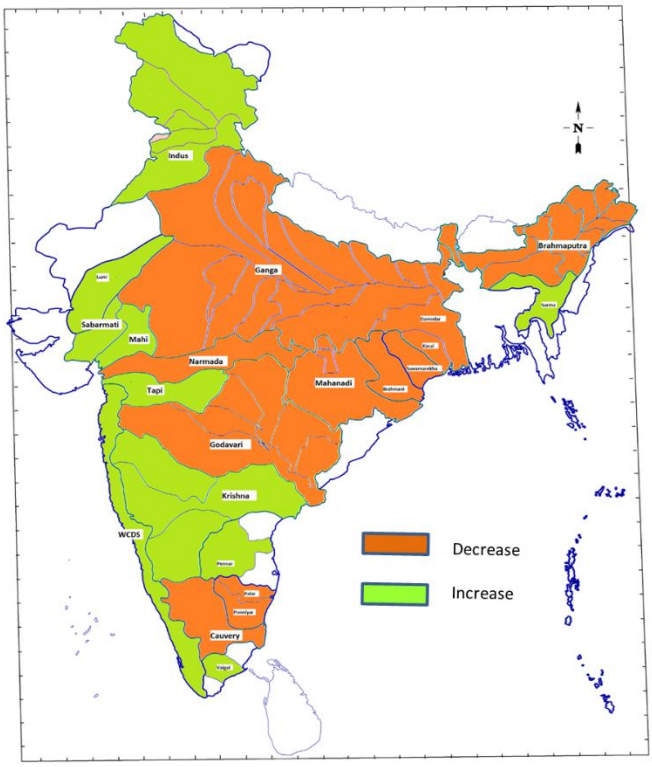

Fig. 1.14. Recent 20 year changes in seasonal (JJAS) rainfall compare to last century (1901-2000)

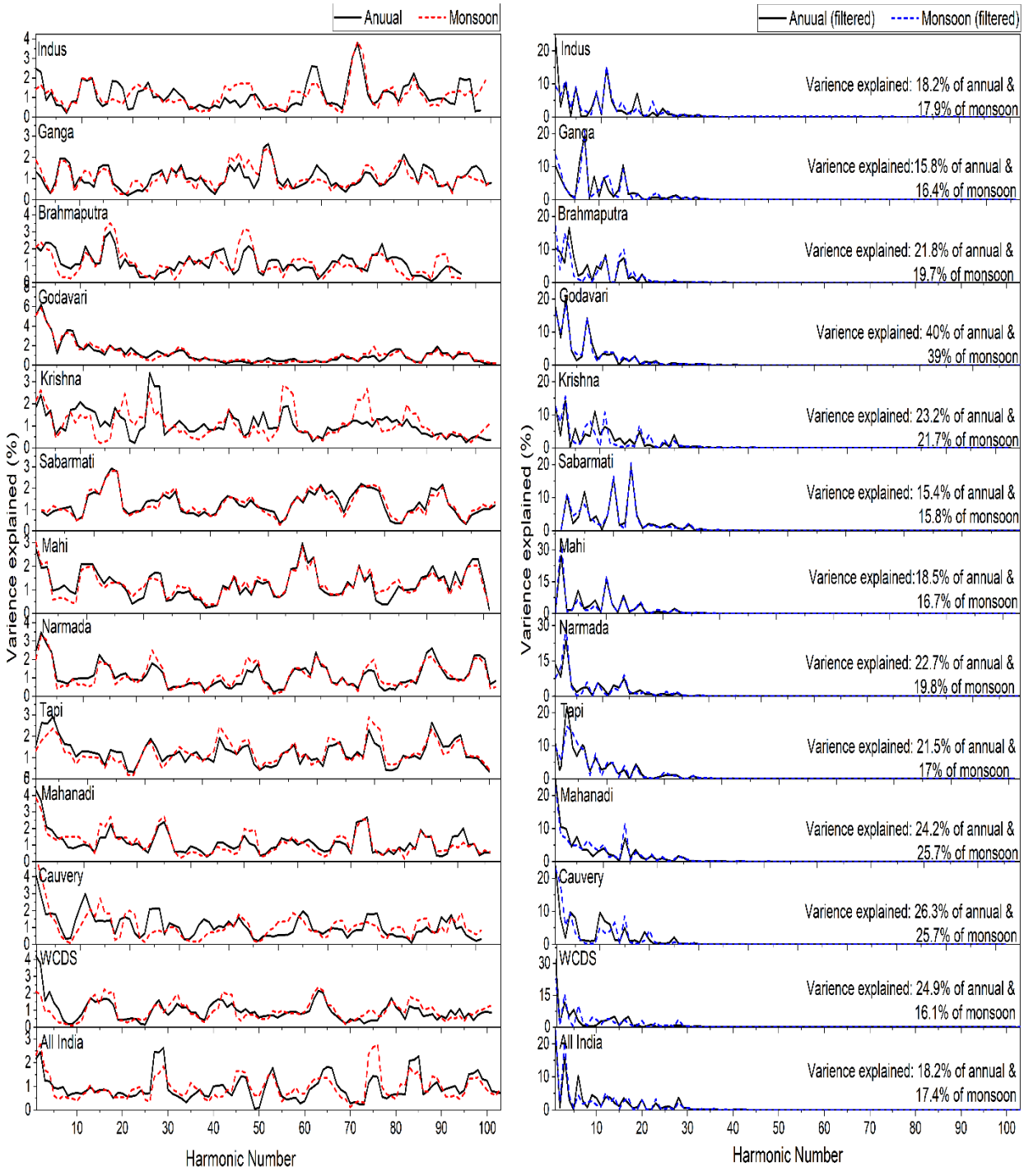

Fig 1.15 Power spectra of annual and monsoonal rainfall of All India, 11 major basins and WCDS with 3-term running mean (left panel) and calculated on 9-point filtered series (right panel)

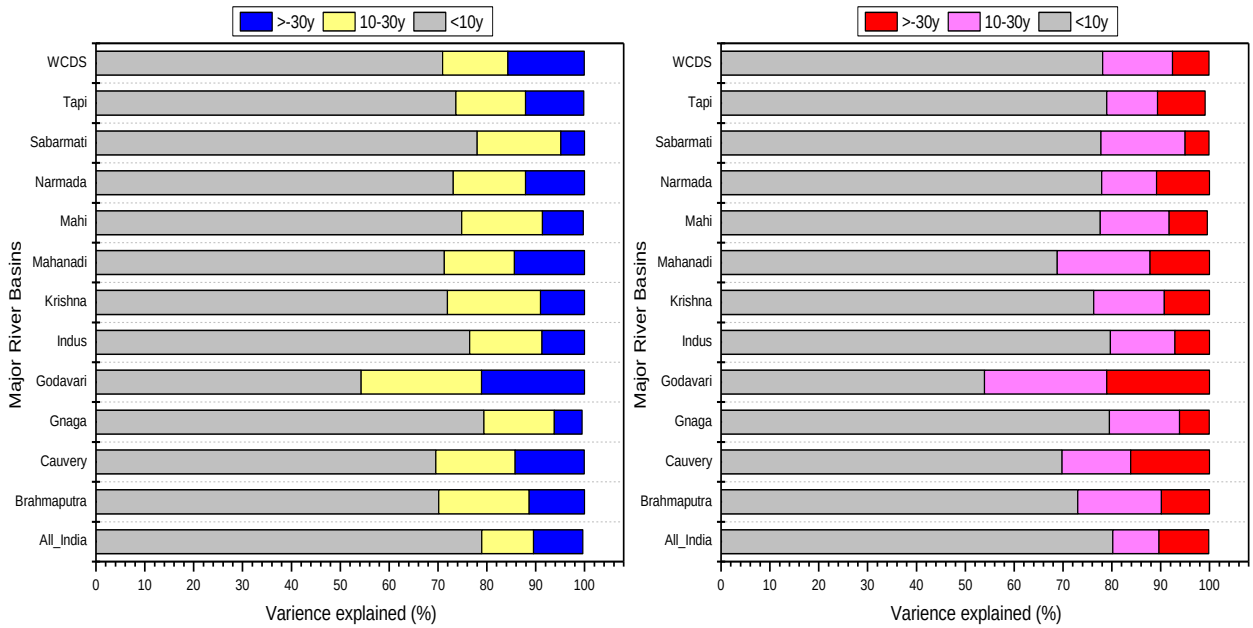

Fig. 1.16 Distribution of percentage of variance in short-term, decadal, and long-term variability of annual and monsoon rainfall of All India and Major River basins

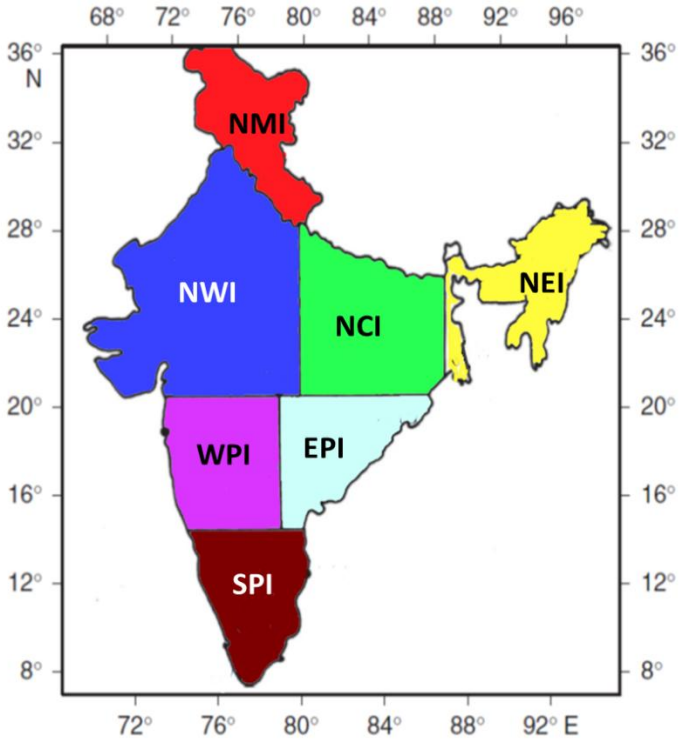

Fig 2.1. Location and geographical boundaries of seven homogeneous rainfall zones

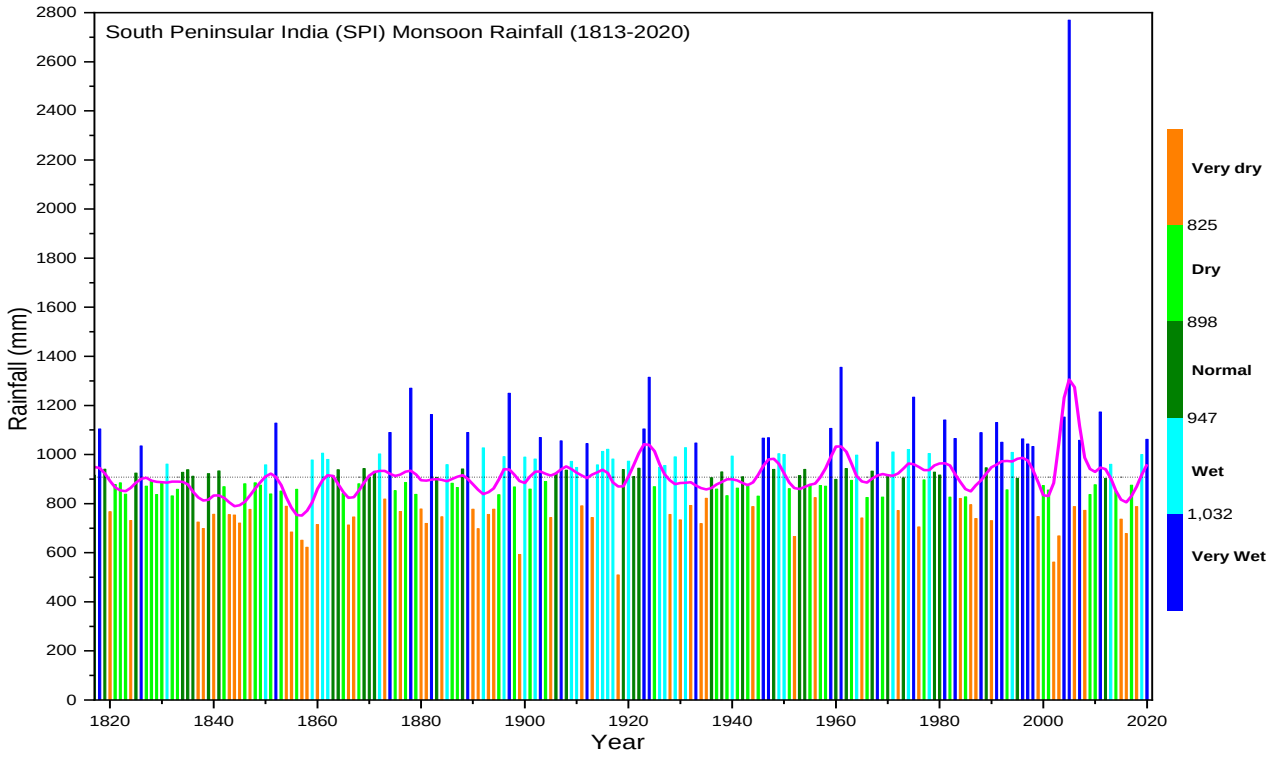

Fig 2.2. Interannual variations in categorized rainfall of South Peninsular India (SPI)

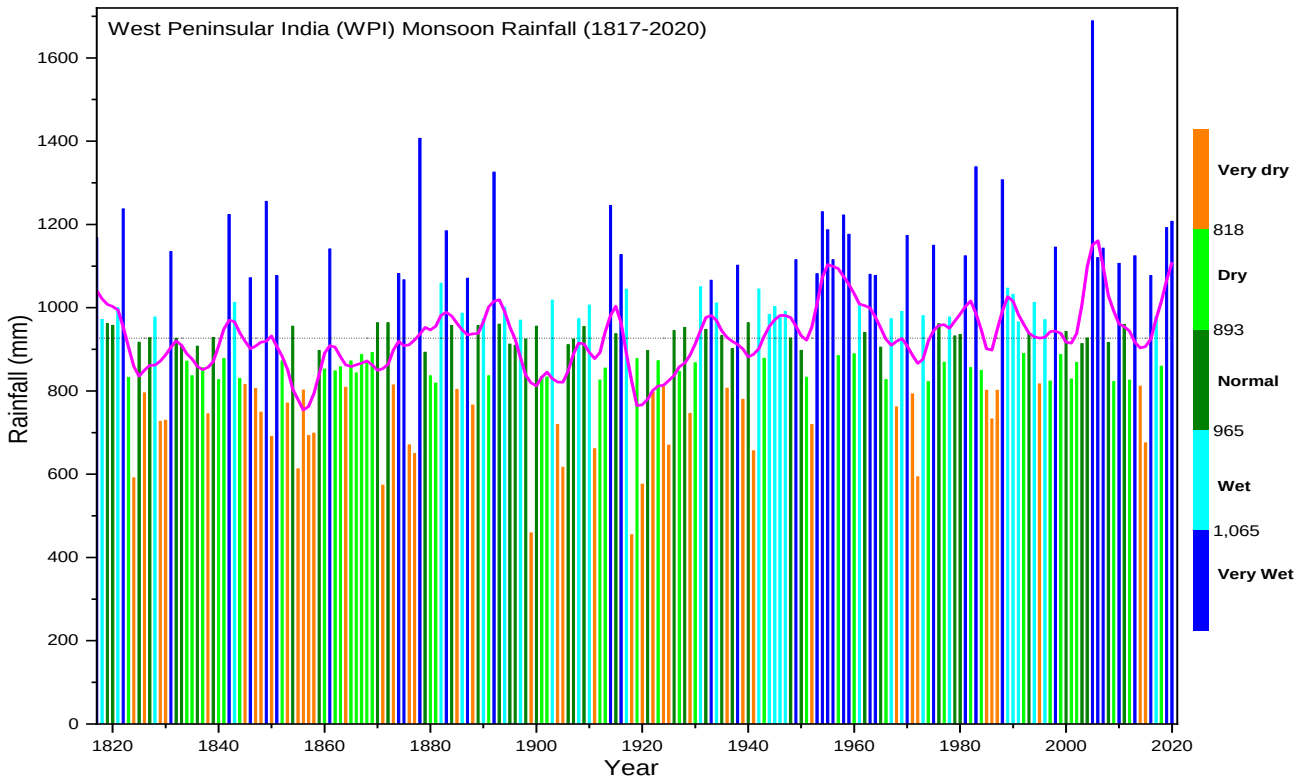

Fig 2.3. Interannual variations in categorized rainfall of West Peninsular India (WPI)

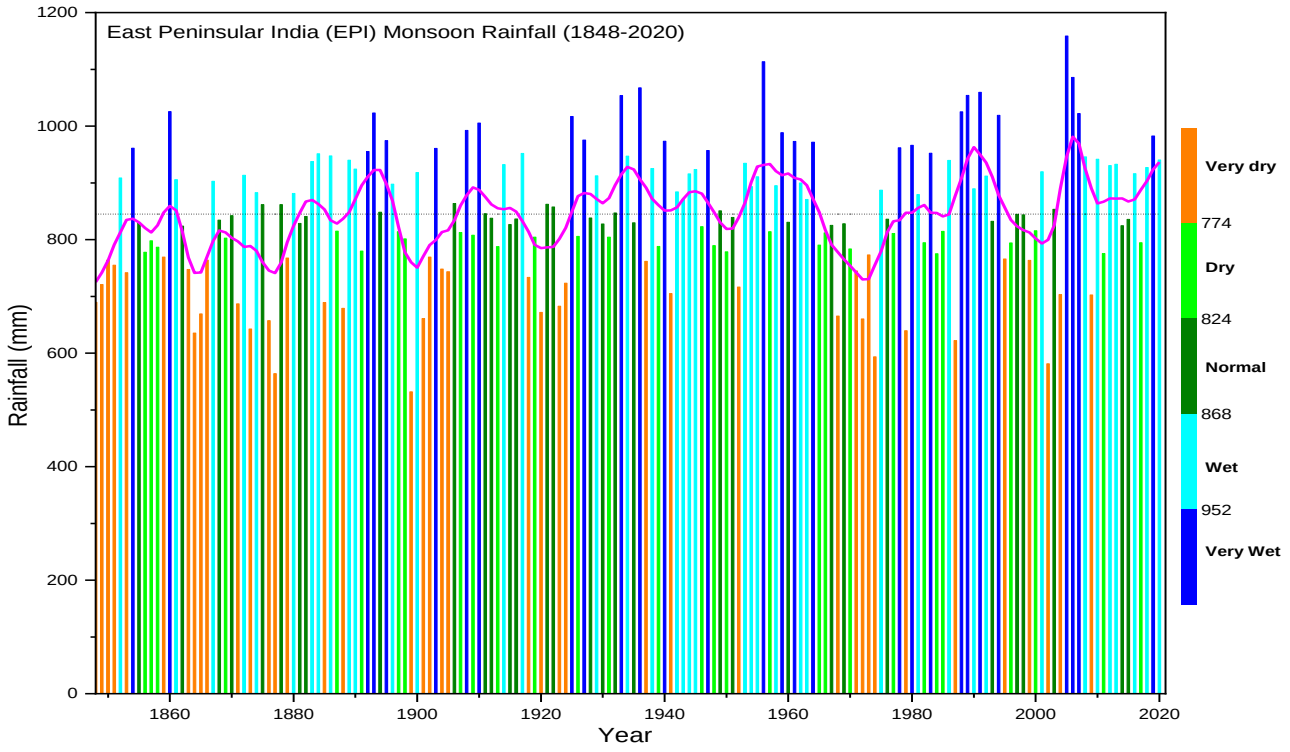

Fig 2.4. Interannual variations in categorized rainfall of East Peninsular India (EPI)

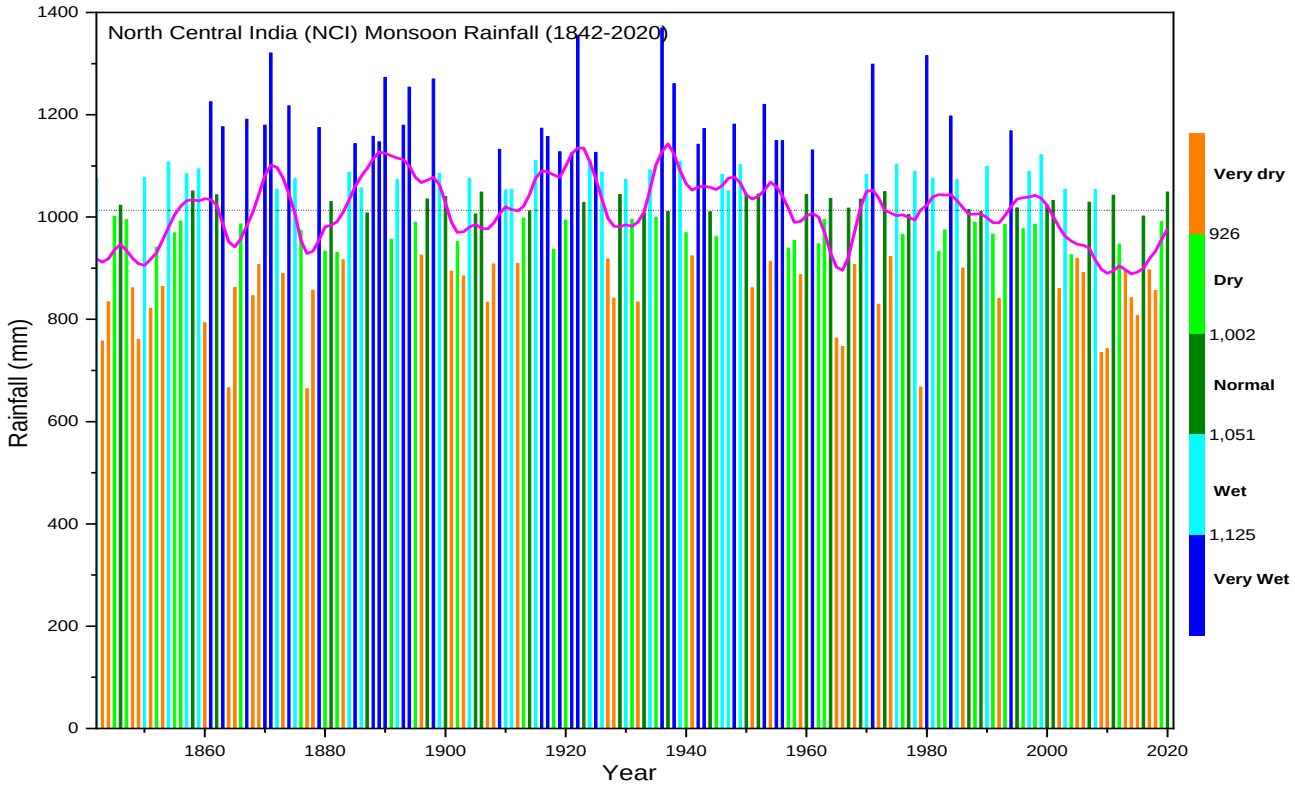

Fig 2.5. Interannual variations in categorized rainfall of North Central India (NCI)

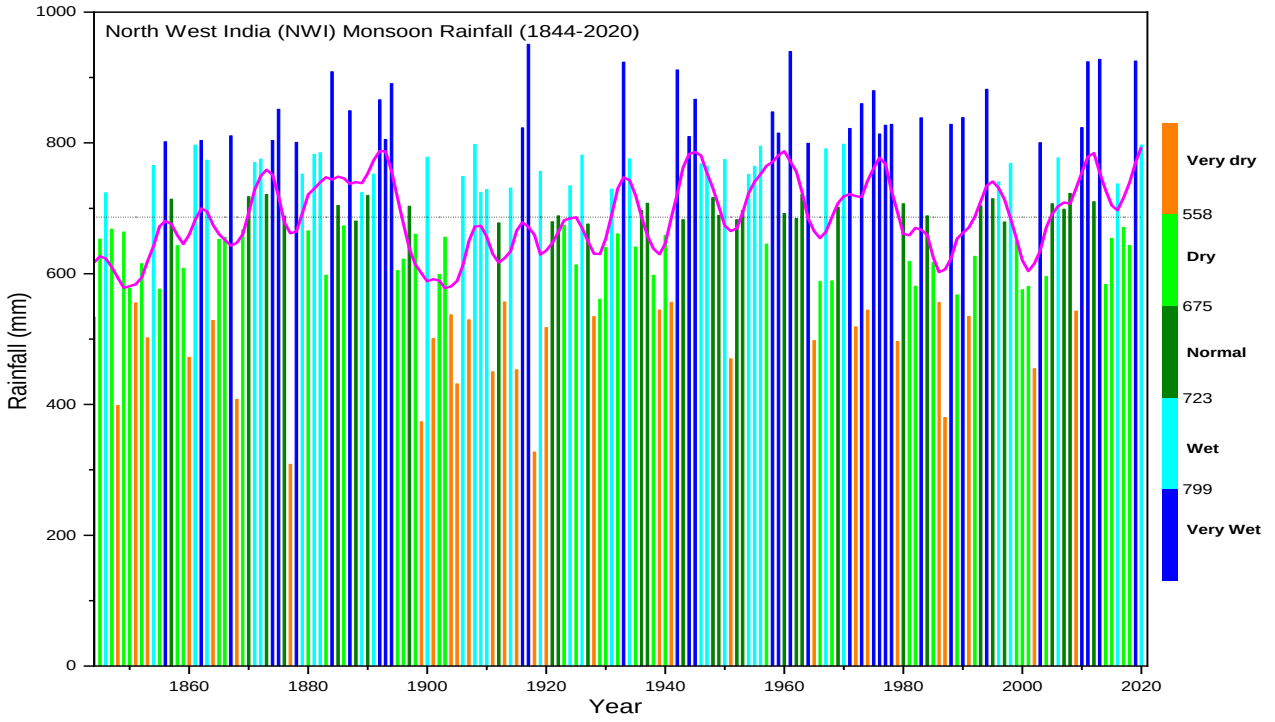

Fig 2.6. Interannual variations in categorized rainfall of North West India (NWI)

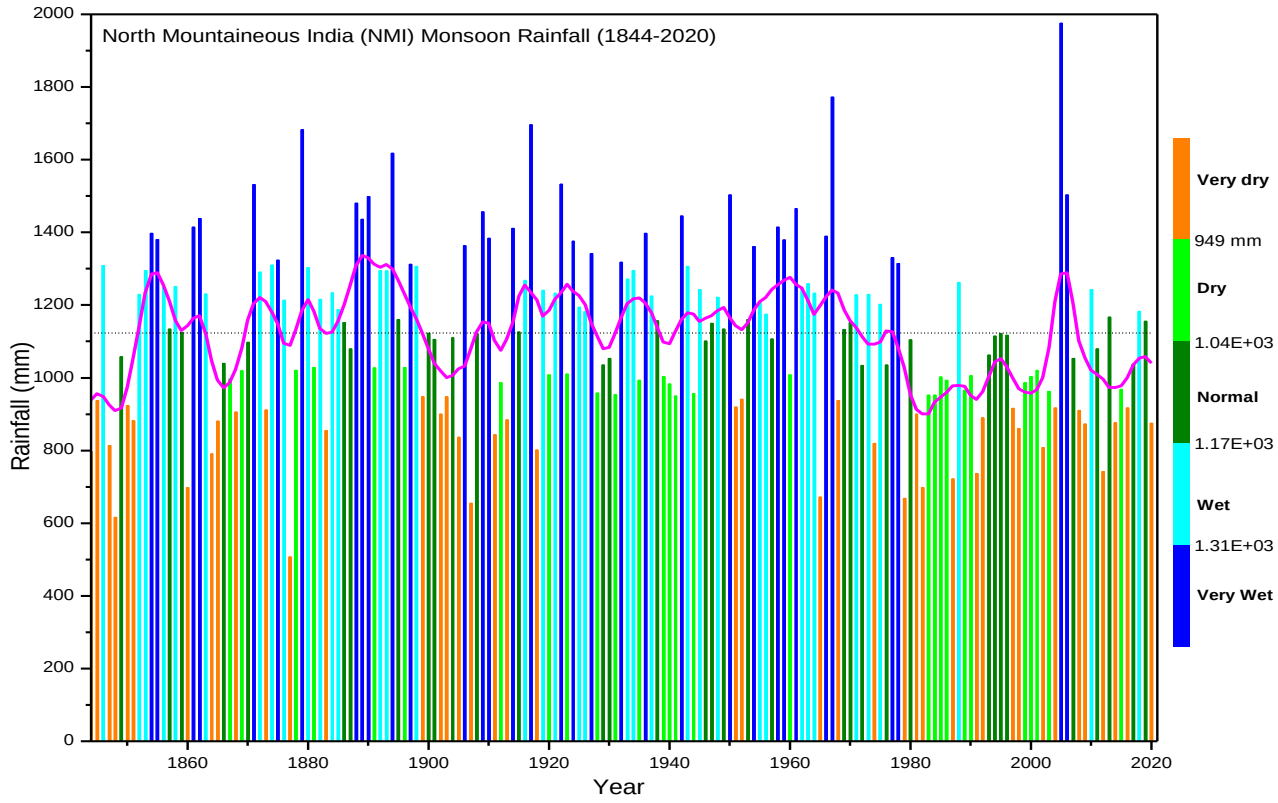

Fig 2.7. Interannual variations in categorized rainfall of North Mountainous India (NMI)

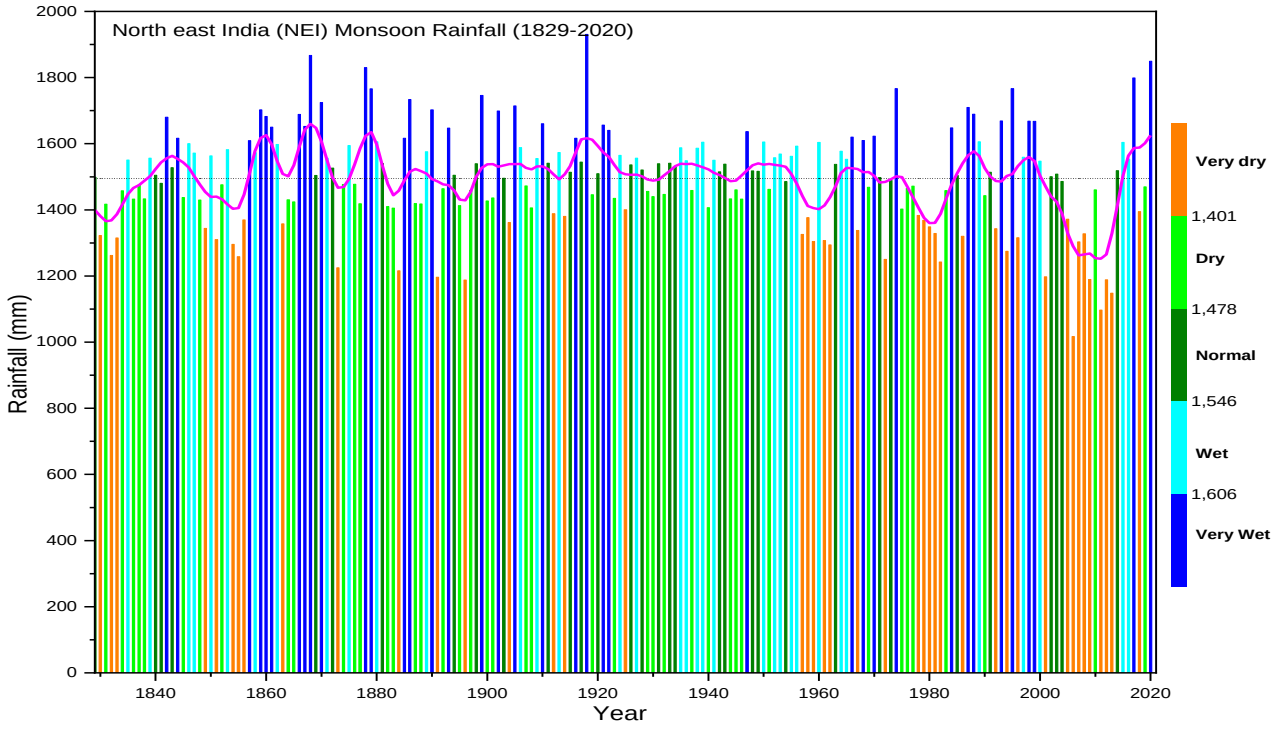

Fig 2.8. Interannual variations in categorized rainfall of North east India (NEI)

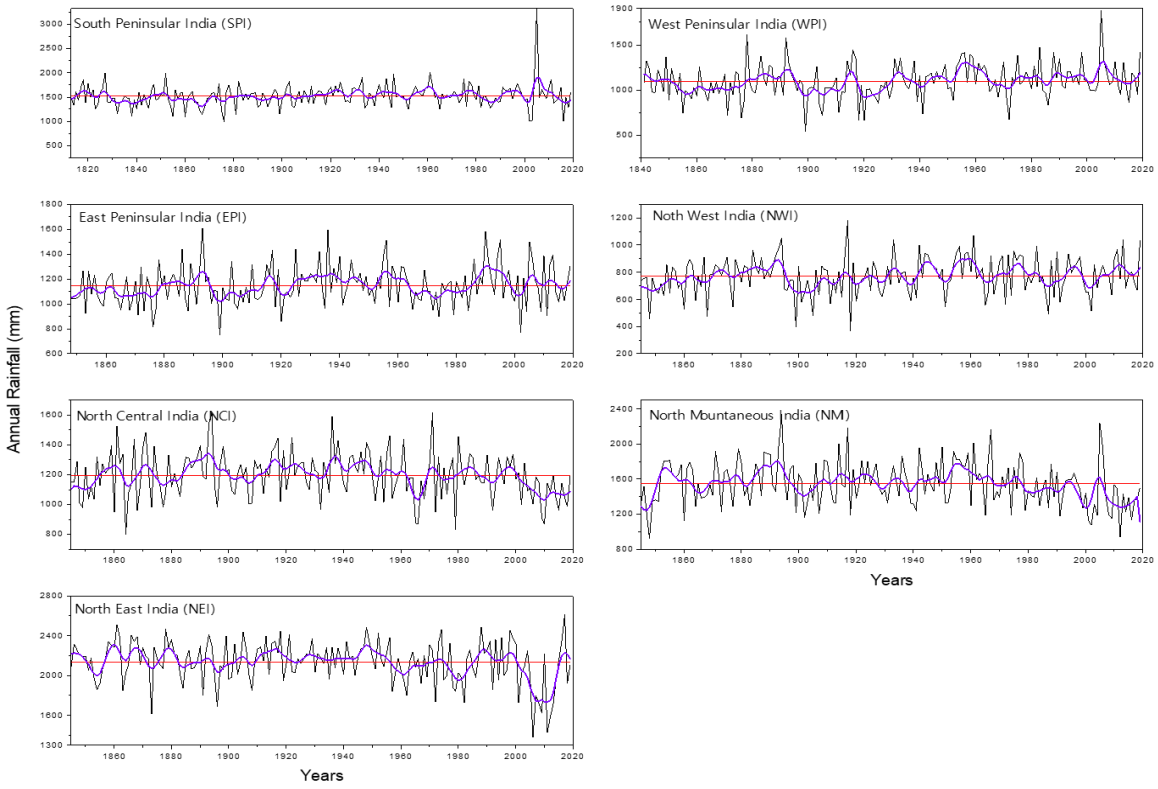

Fig 2.9. Inter-annual variations in annual rainfall of seven homogeneous rainfall zones

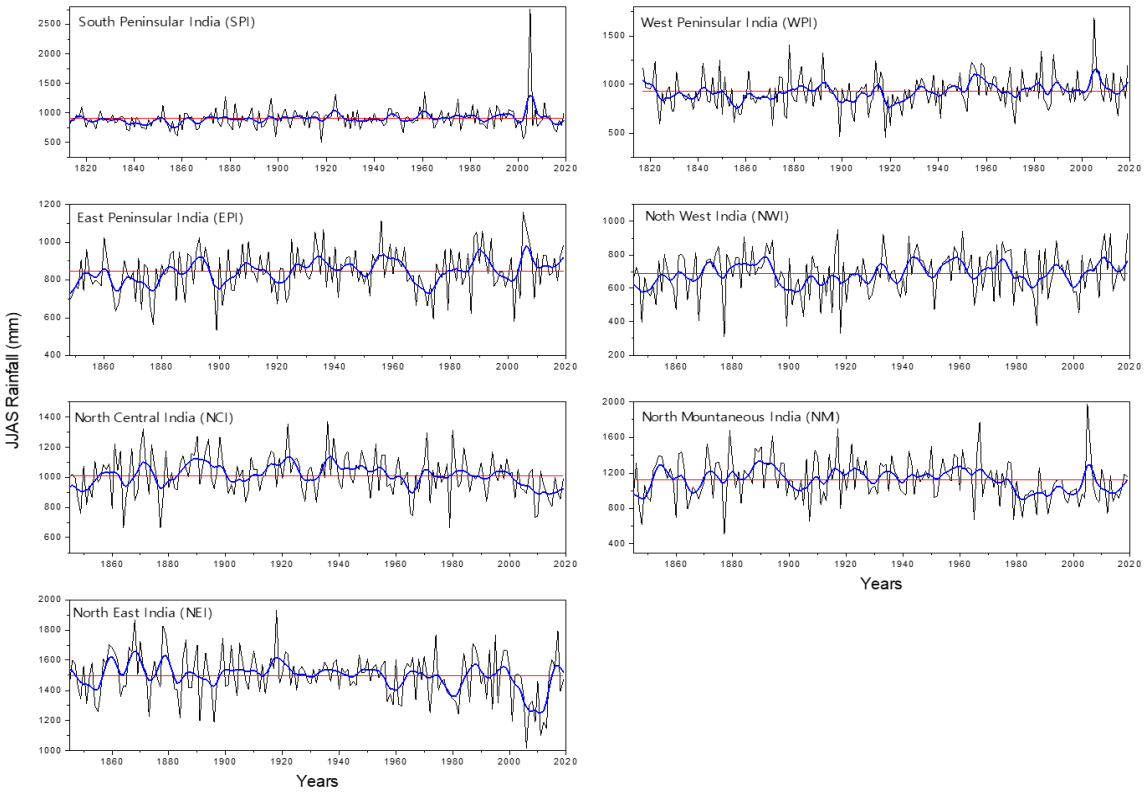

Fig 2.10. Inter-annual variations in monsoon rainfall of seven homogeneous rainfall zones

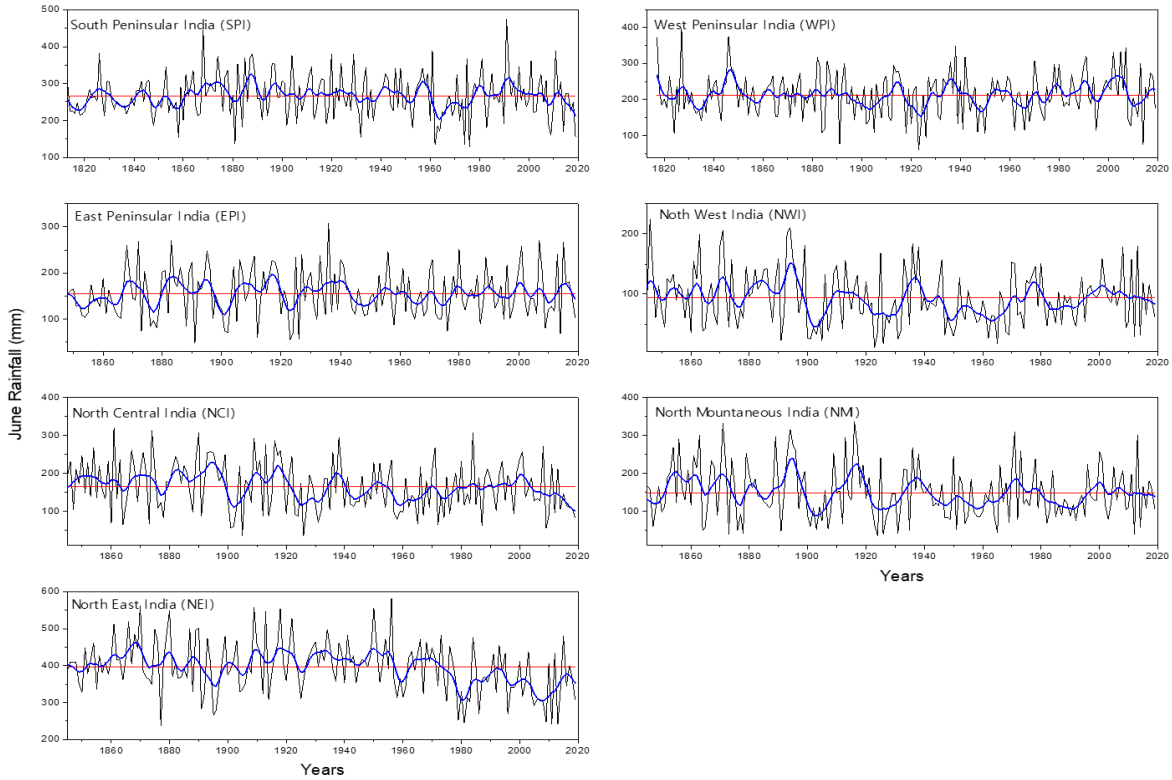

Fig 2.11. Inter-annual variations in June rainfall of seven homogeneous rainfall zones

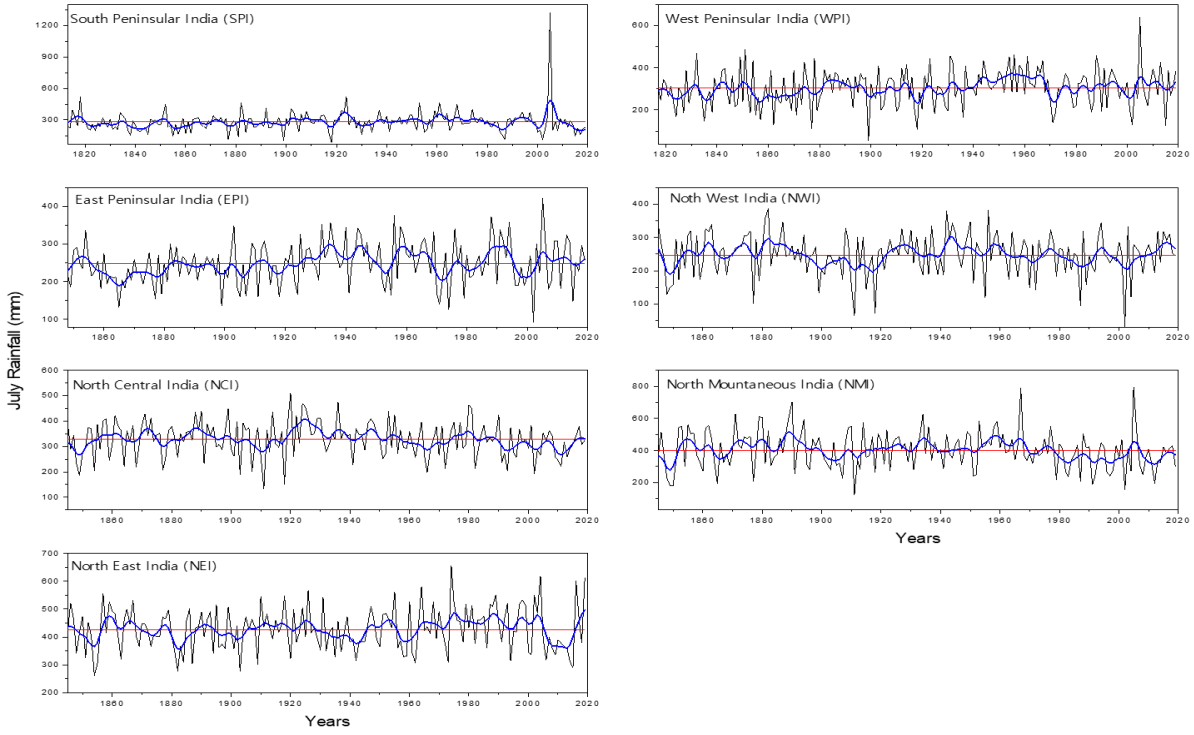

Fig 2.12. Inter-annual variations in July rainfall of seven homogeneous rainfall zones

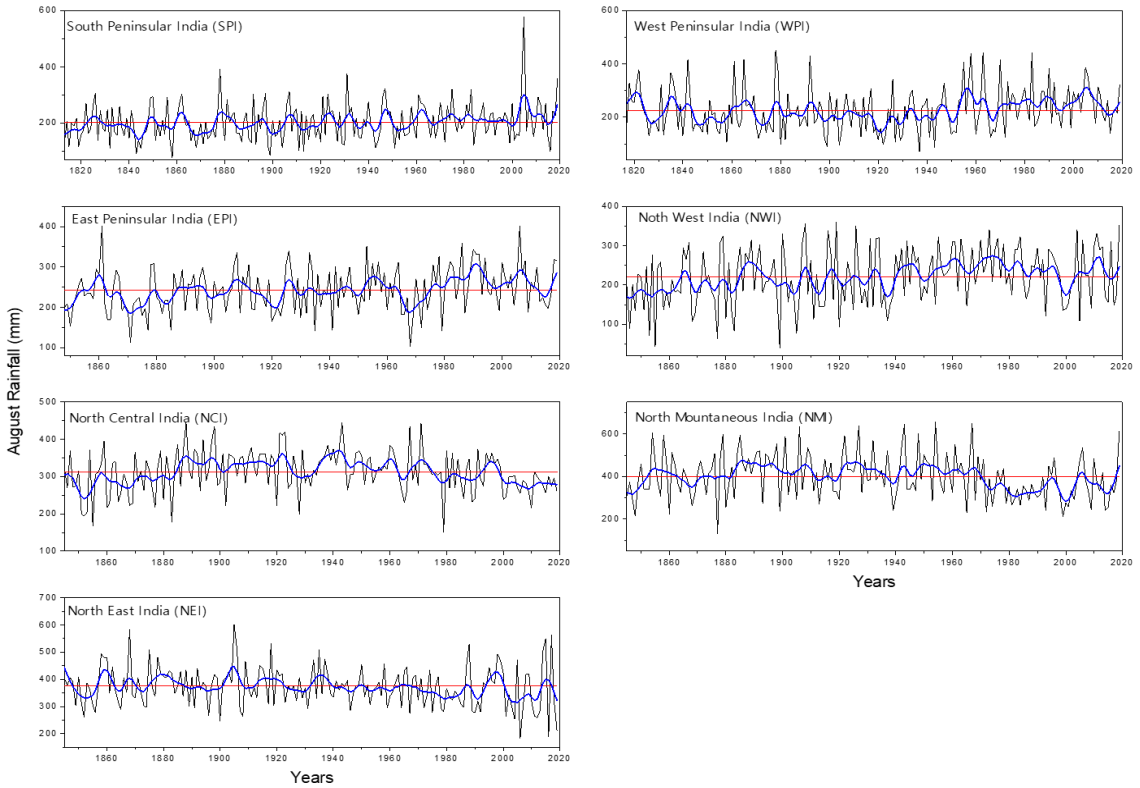

Fig 2.13. Inter-annual variations in August rainfall of seven homogeneous rainfall zones

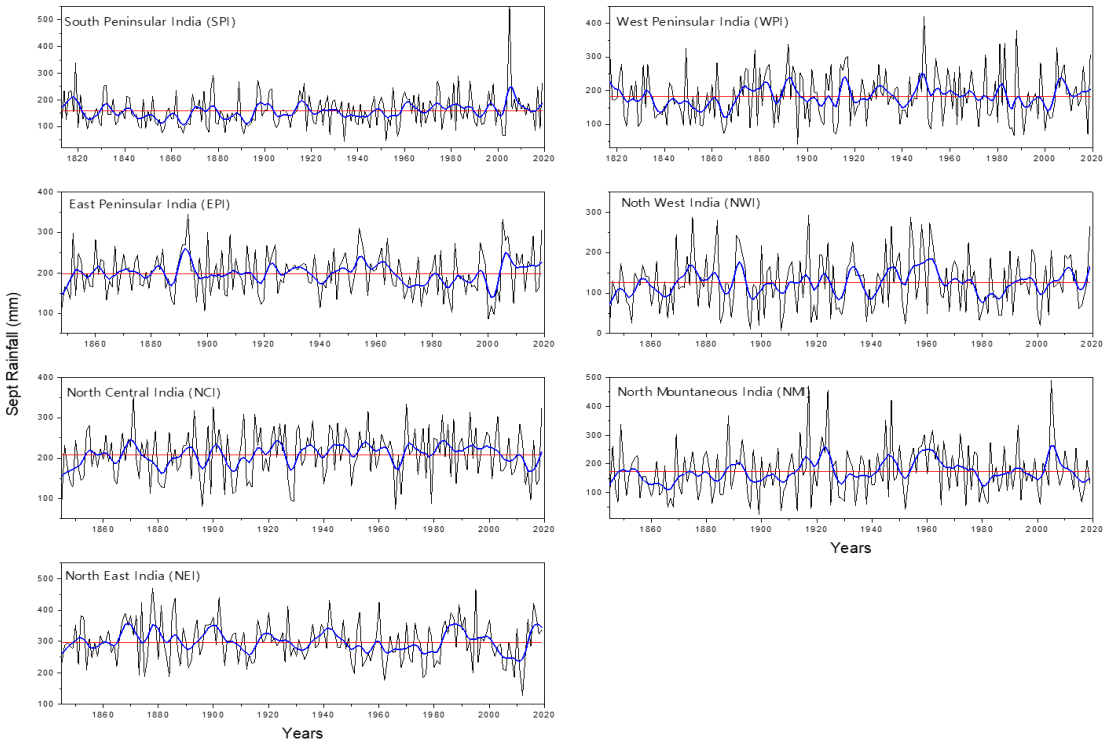

Fig 2.14. Inter-annual variations in September rainfall of seven homogeneous rainfall zones

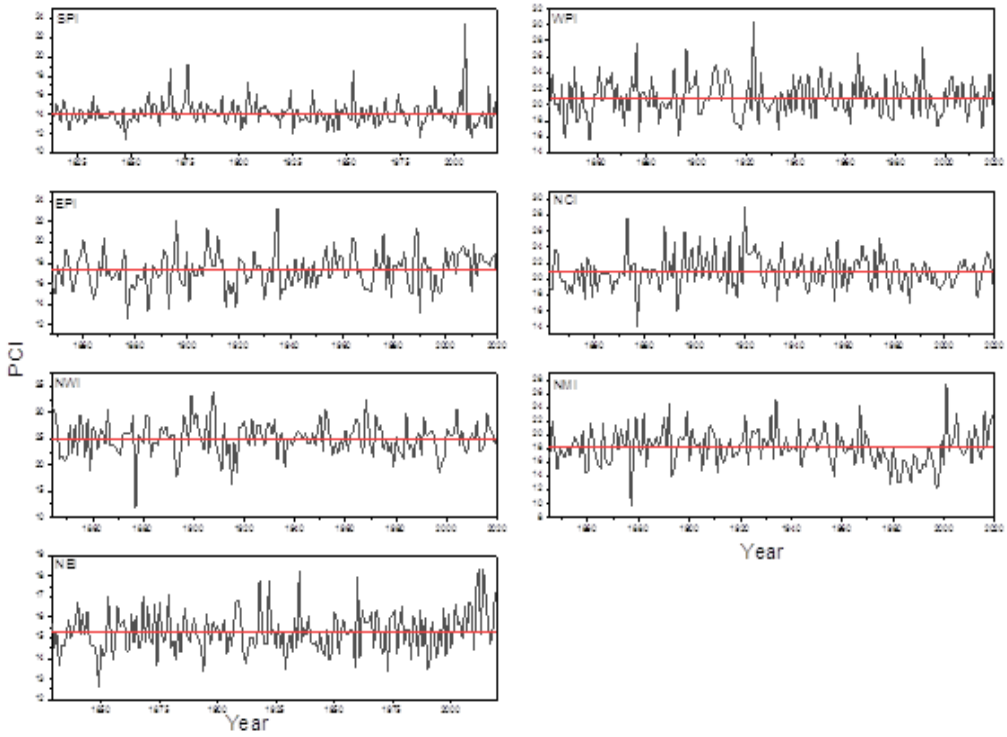

Fig 2.15 Long-term variations in annual precipitation concentration Index (PCI) of seven homogeneous zones

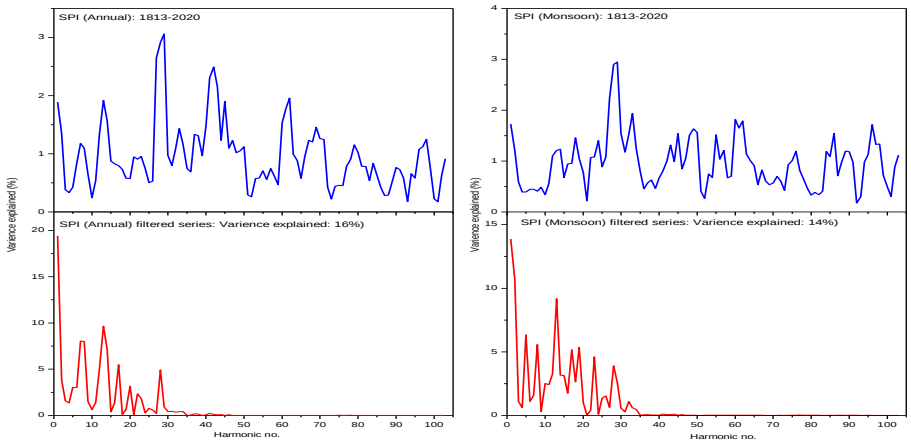

Fig. 2.16 Power spectra of annual and monsoonal rainfall (smoothed with 3-term running mean) and that of 9- point filtered rainfall series of South Peninsular India during 1813-2020

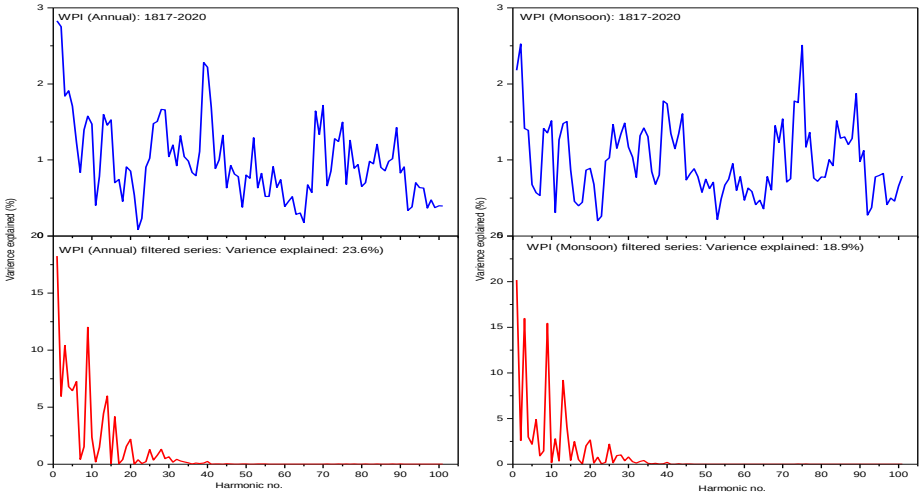

Fig. 2.17 Power spectra of annual and monsoonal rainfall (smoothed with 3-term running mean) and that of 9- point filtered rainfall series of West Peninsular India during 1817-2020

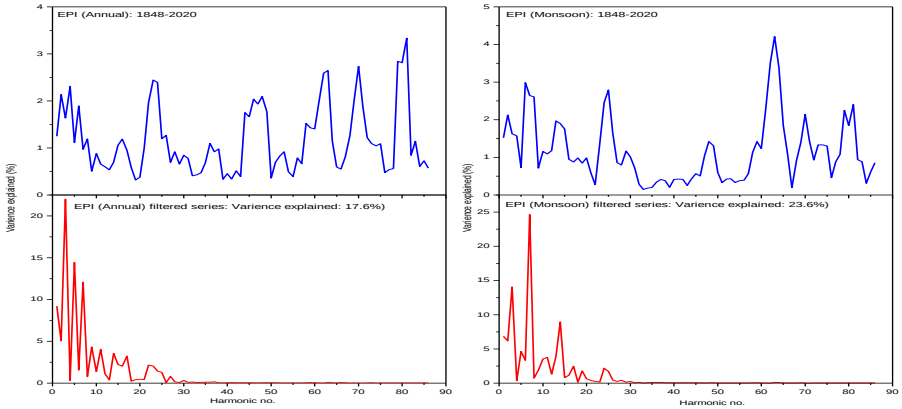

Fig. 2.18 Power spectra of annual and monsoonal rainfall (smoothed with 3-term running mean) and that of 9- point filtered rainfall series of East Peninsular India during 1848-2020

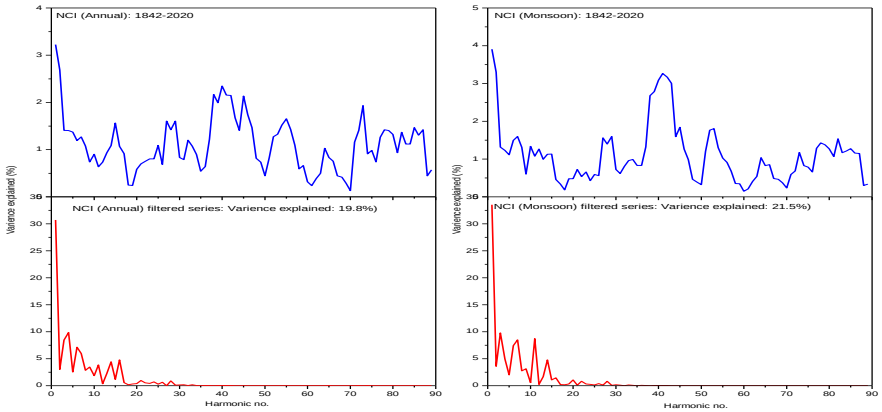

Fig. 2.19 Power spectra of annual and monsoonal rainfall (smoothed with 3-term running mean) and that of 9- point filtered rainfall series of North Central India during 1842-2020

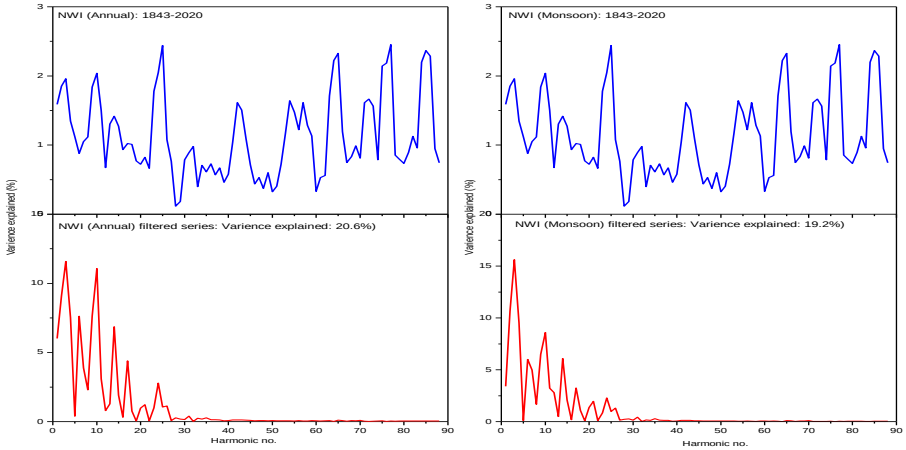

Fig. 2.20 Power spectra of annual and monsoonal rainfall (smoothed with 3-term running mean) and that of 9- point filtered rainfall series of North West India during 1843-2020

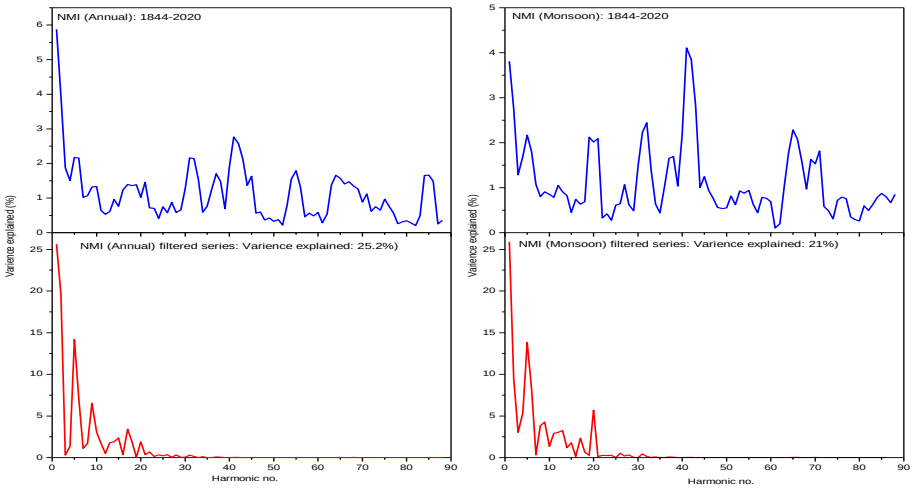

Fig. 2.21 Power spectra of annual and monsoonal rainfall (smoothed with 3-term running mean) and that of 9- point filtered rainfall series of North Mountainous India during 1844-2020

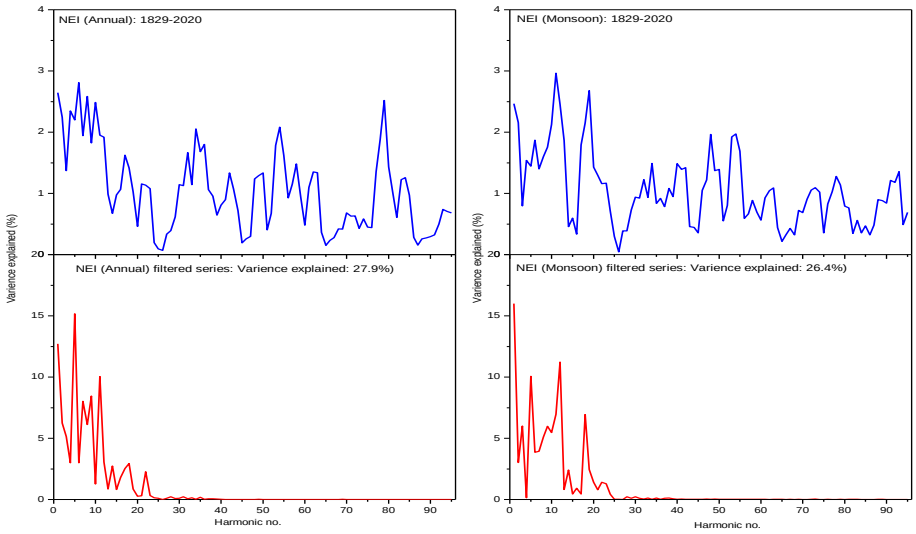

Fig. 2.22 Power spectra of annual and monsoonal rainfall (smoothed with 3-term running mean) and that of 9- point filtered rainfall series of North East India during 1829-2020

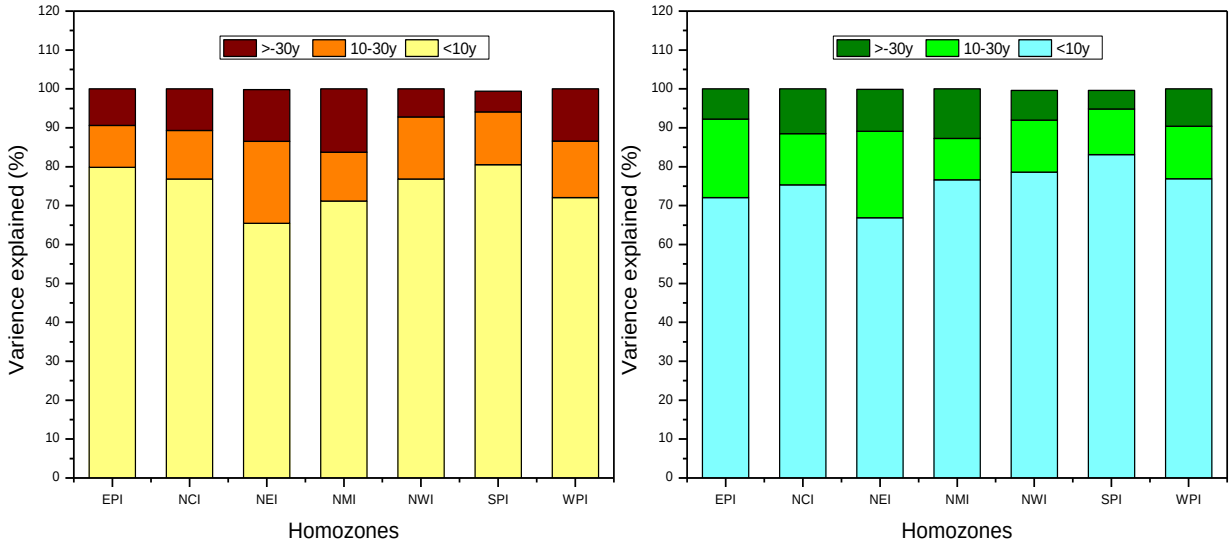

Fig. 2.23 Distribution of percentage of variance in short-term, decadal, and long-term variability of annual and monsoonal rainfall of seven homogeneous zones

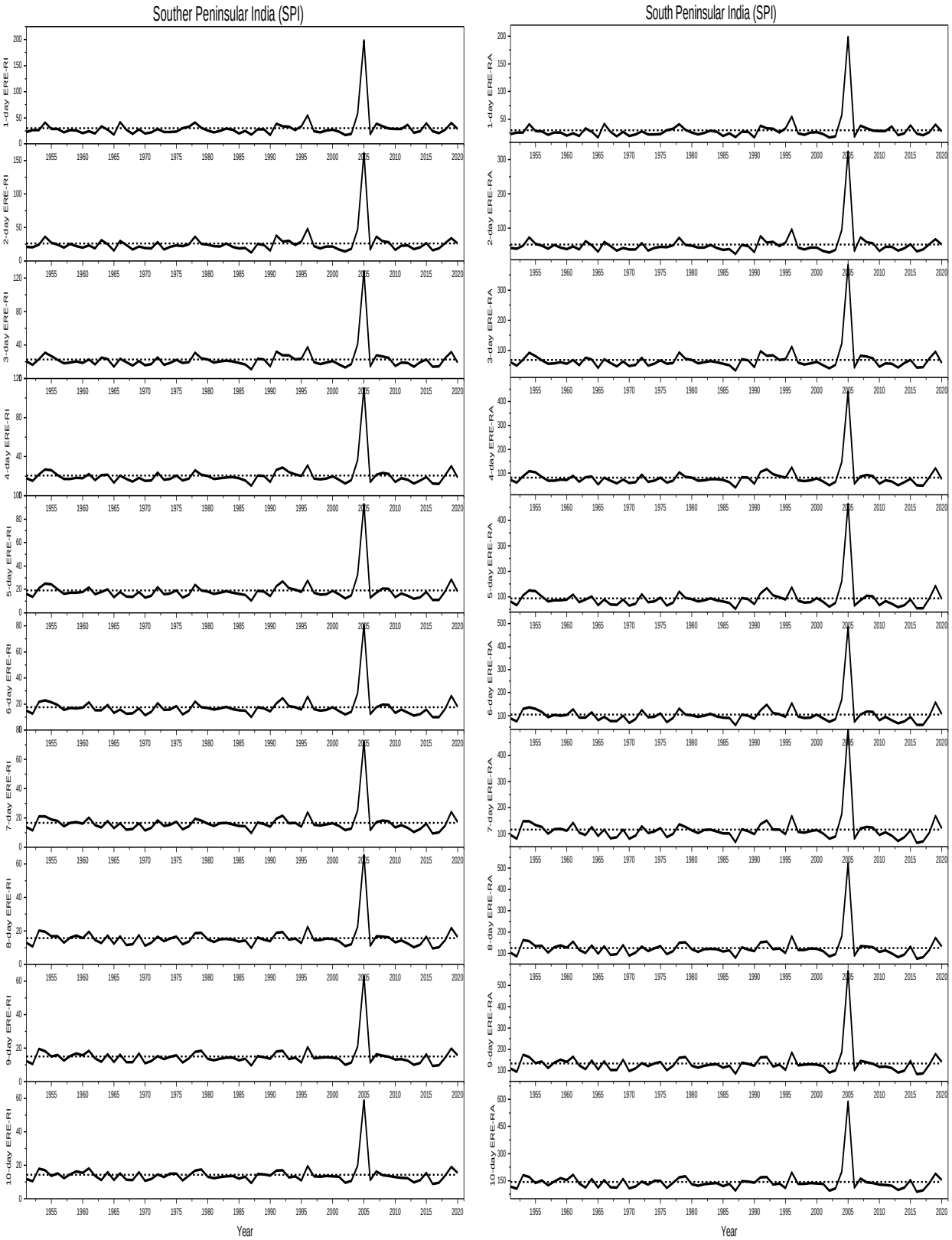

Fig 3.1 Interannual variations in rainfall intensity and rainfall amount of 1- to 10-day extreme rain event over southern peninsular India

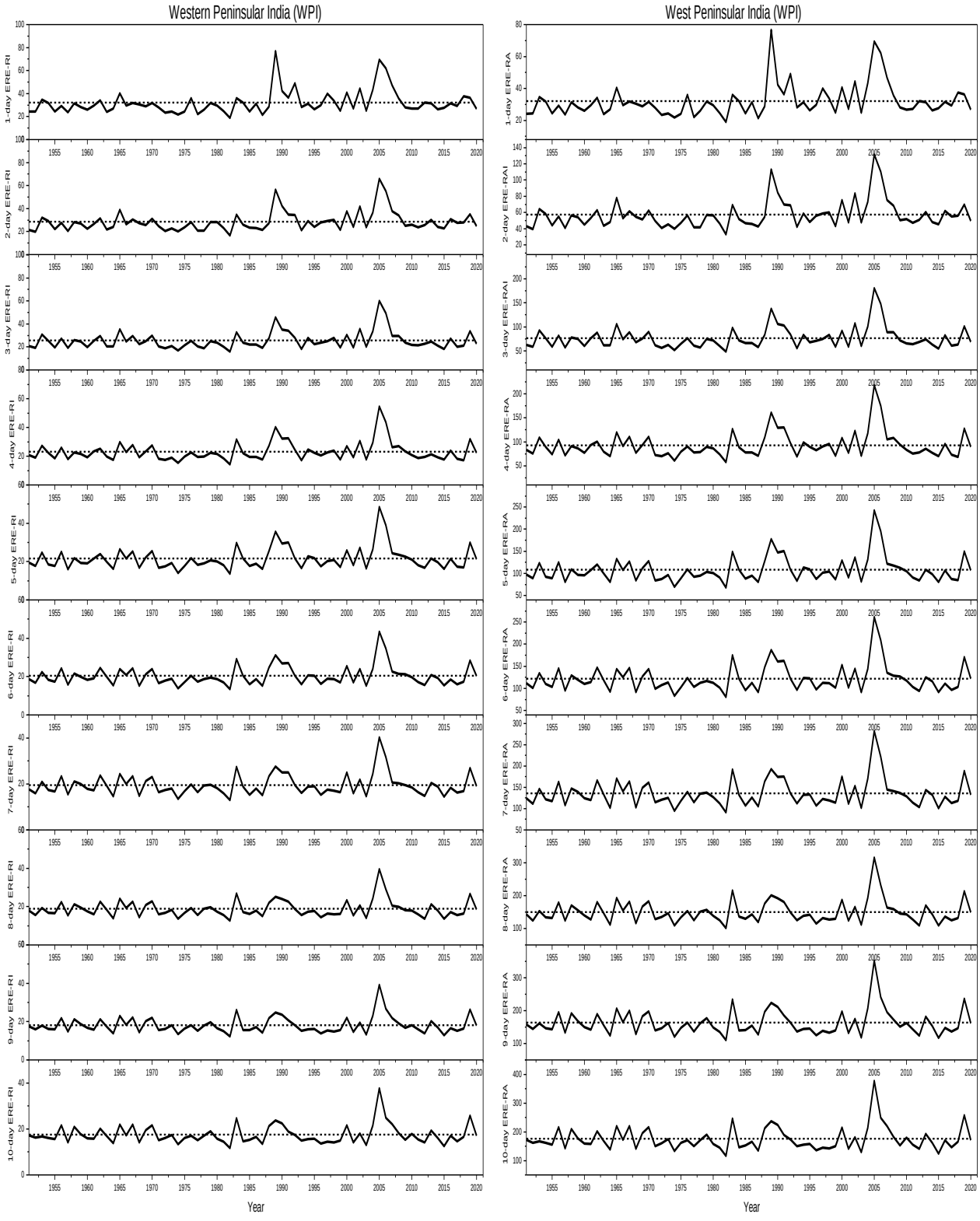

Fig 3.2. Interannual variations in rainfall intensity and rainfall amount of 1- to 10-day extreme rain event over western peninsular India

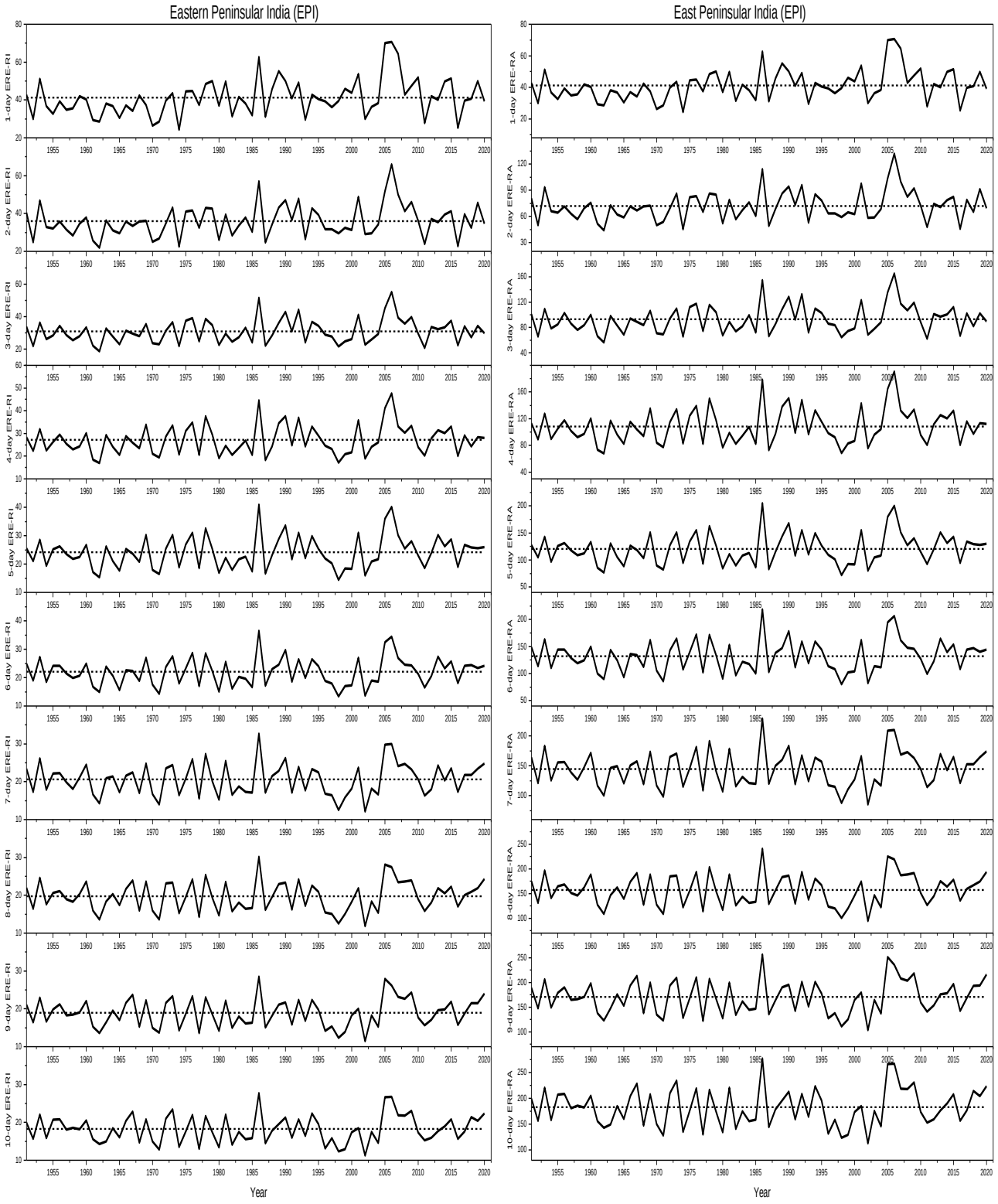

Fig 3.3. Interannual variations in rainfall intensity and rainfall amount of 1- to 10-day extreme rain event over eastern peninsular India

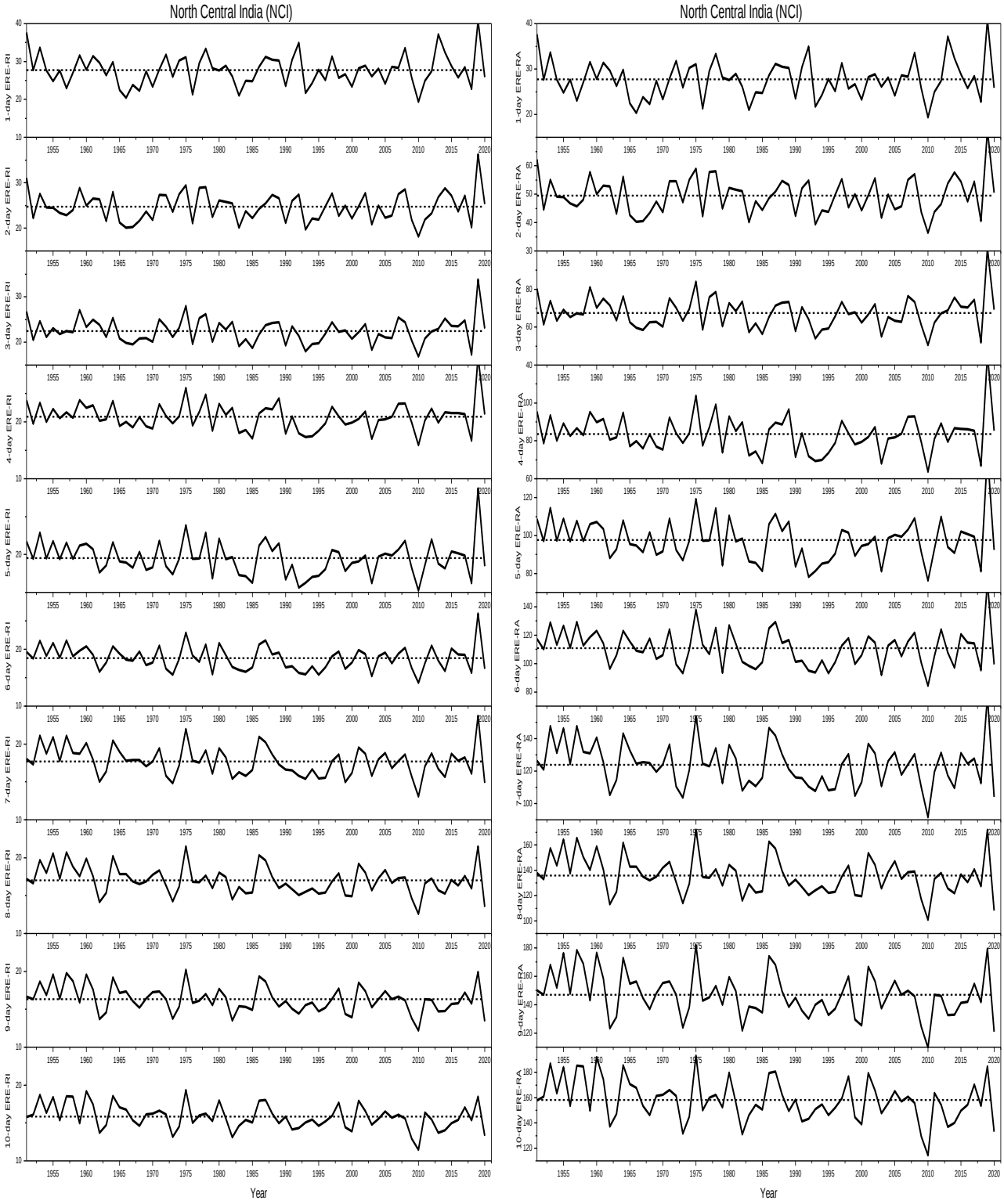

Fig 3.4. Interannual variations in rainfall intensity and rainfall amount of 1- to 10-day extreme rain event North Central India

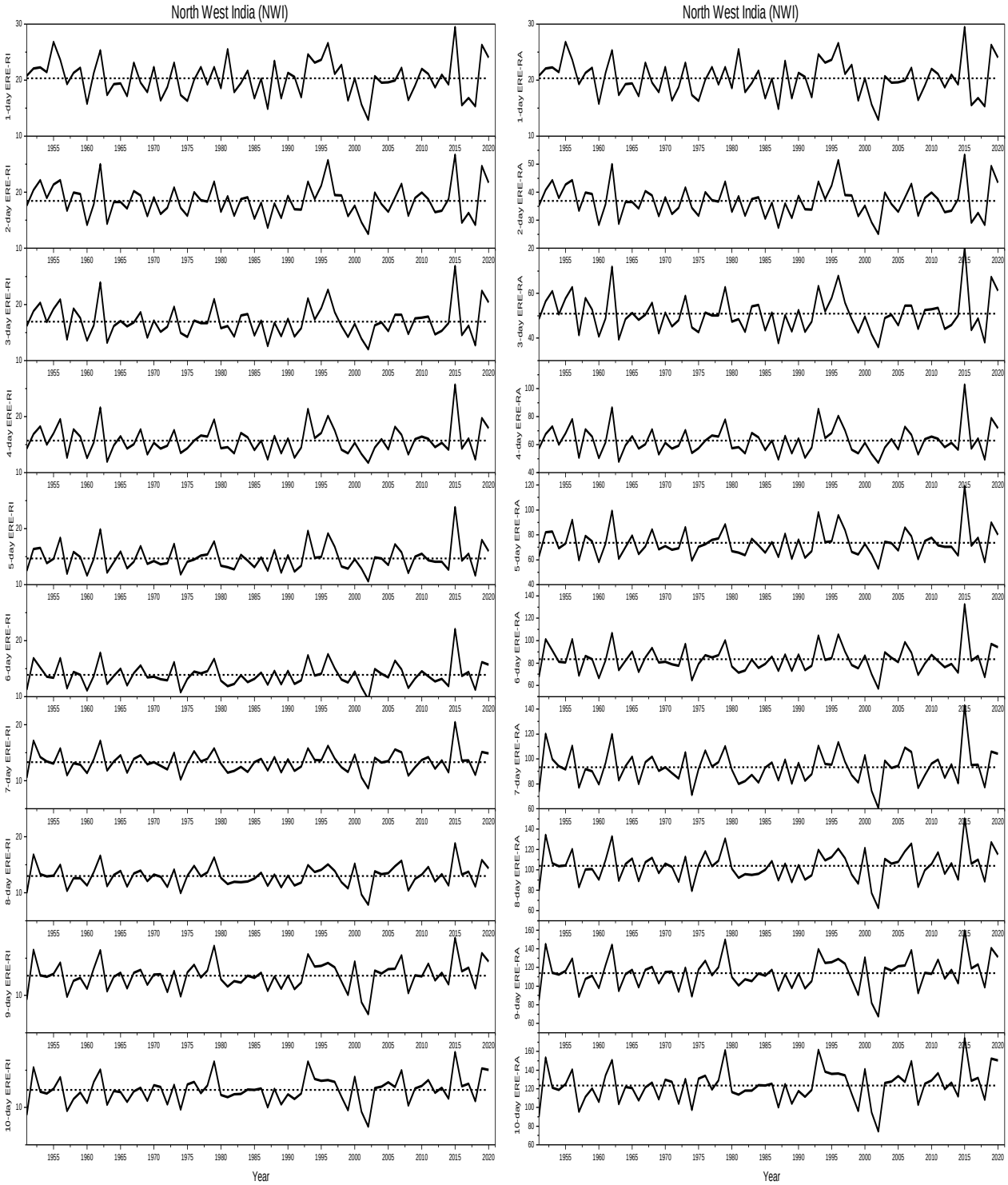

Fig 3.5. Interannual variations in rainfall intensity and rainfall amount of 1- to 10-day extreme rain event North West India

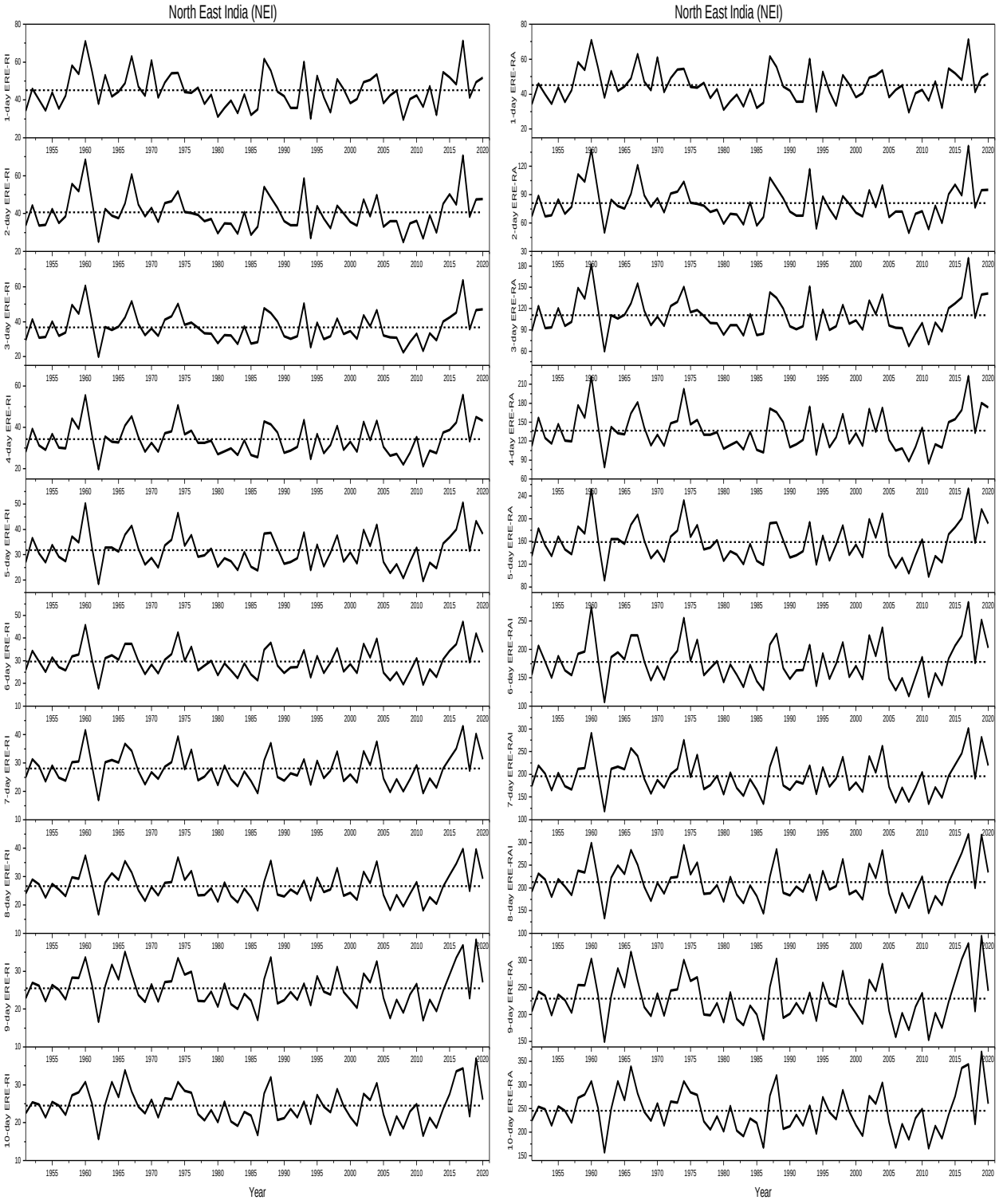

Fig 3.6. Interannual variations in rainfall intensity and rainfall amount of 1- to 10-day extreme rain event North East India

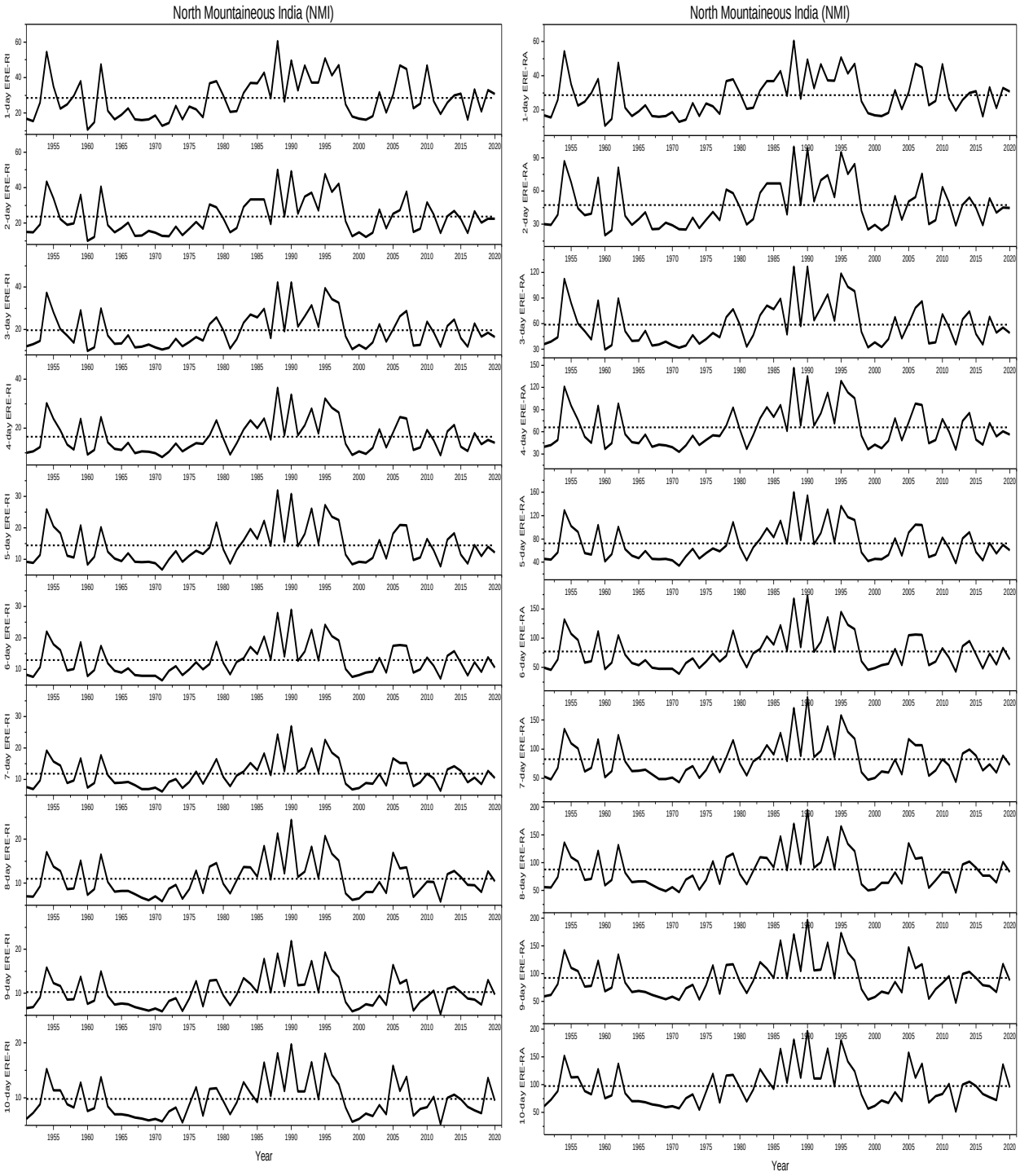

Fig 3.7. Interannual variations in rainfall intensity and rainfall amount of 1- to 10-day extreme rain event North Mountainous India

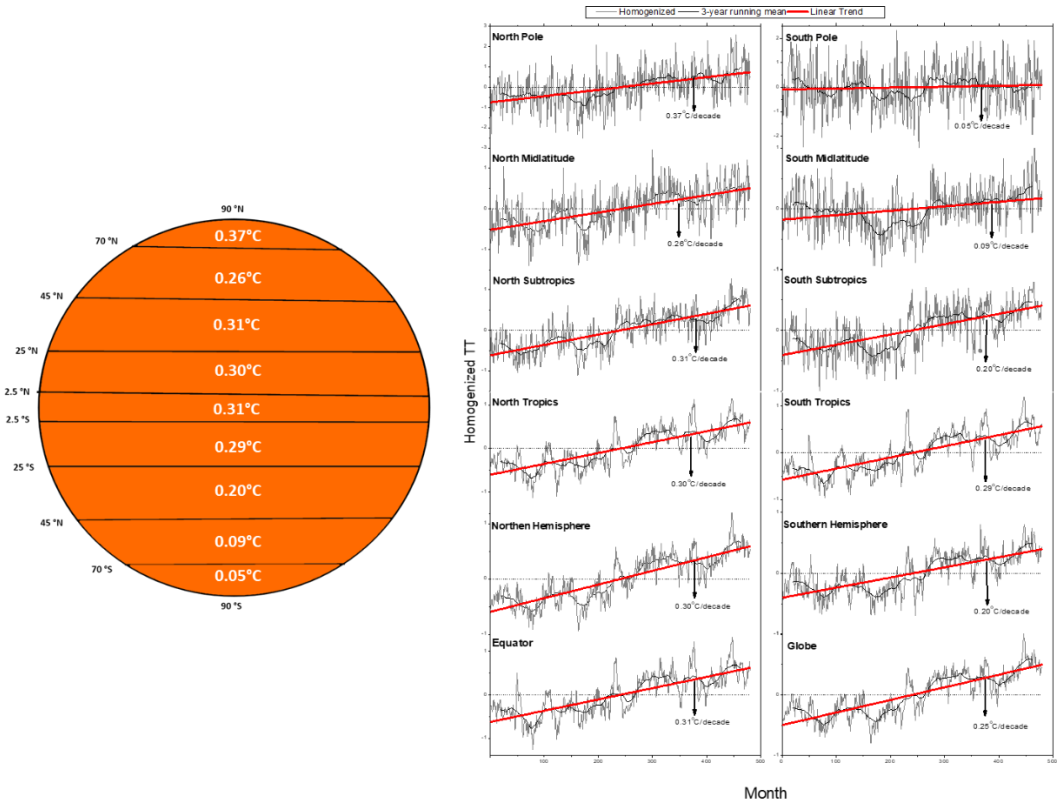

Fig 4.1 Linear trend (°C/10-yr) in Tropospheric Temperature (TT) during 1979-2018

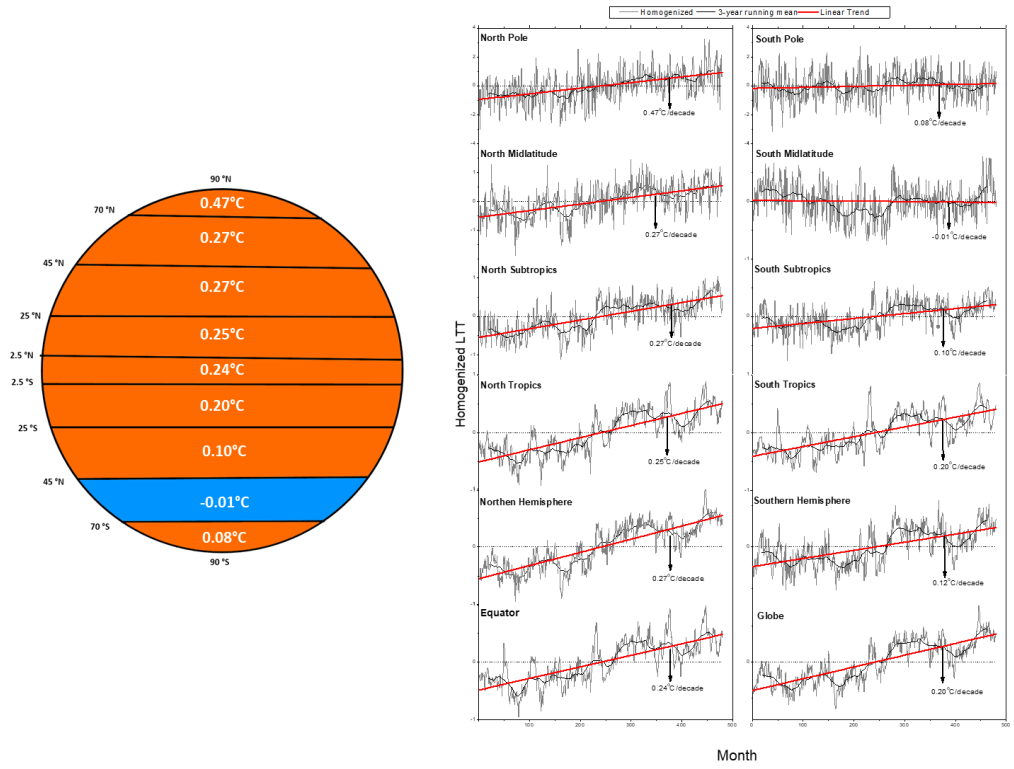

Fig 4.2 Linear trend (°C/10-yr) in Lower Tropospheric Temperature (LTT) during 1979-2018

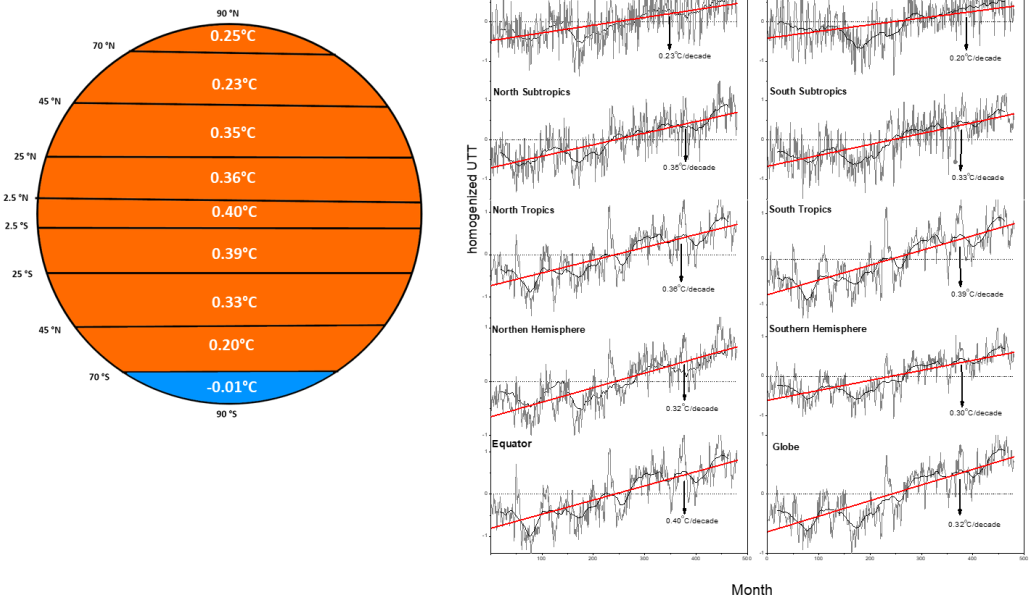

Fig 4.3 Linear trend (°C/10-yr) in Upper Tropospheric Temperature (UTT) during 1979-2018

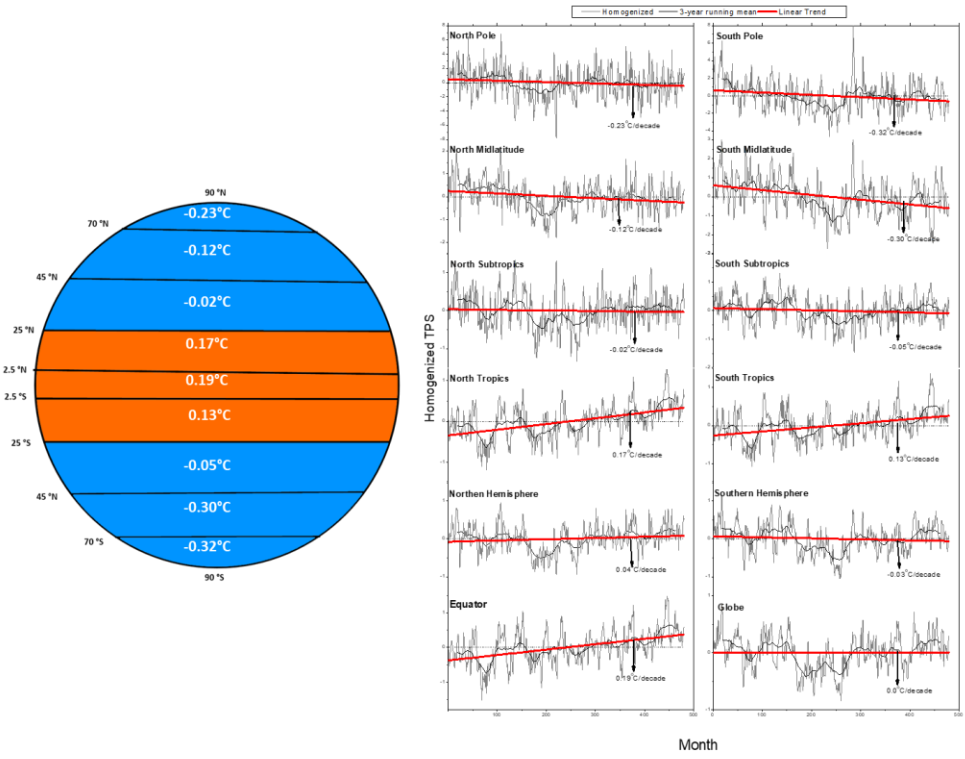

Fig 4.4 Linear trend (°C/10-yr) in Tropopause temperature (TPS) during 1979-2018

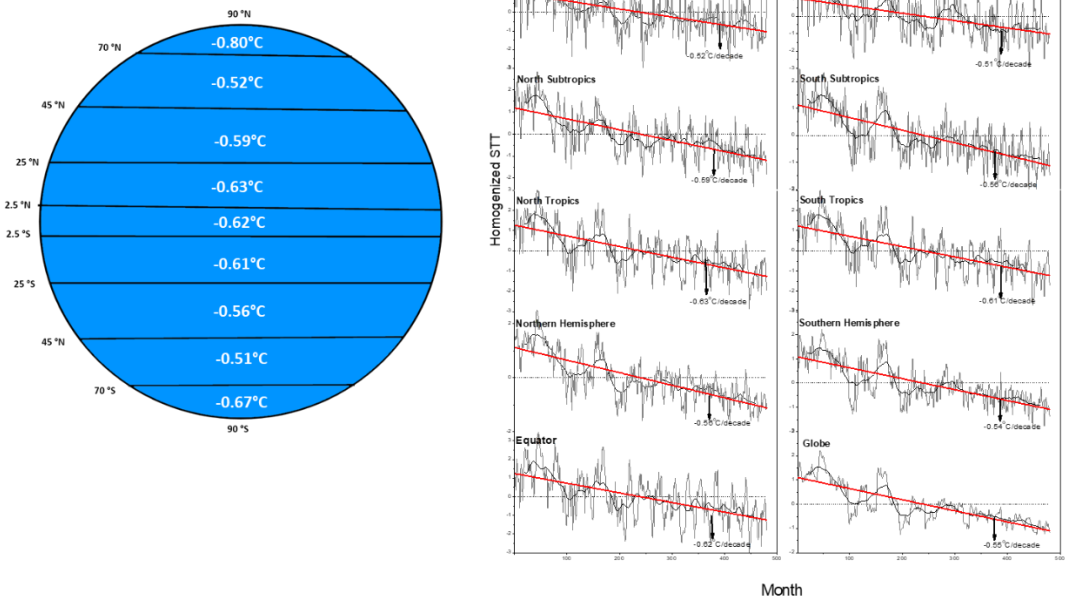

Fig 4.5 Linear trend (°C/10-yr) in Stratospheric Temperature (STT) during 1979-2018

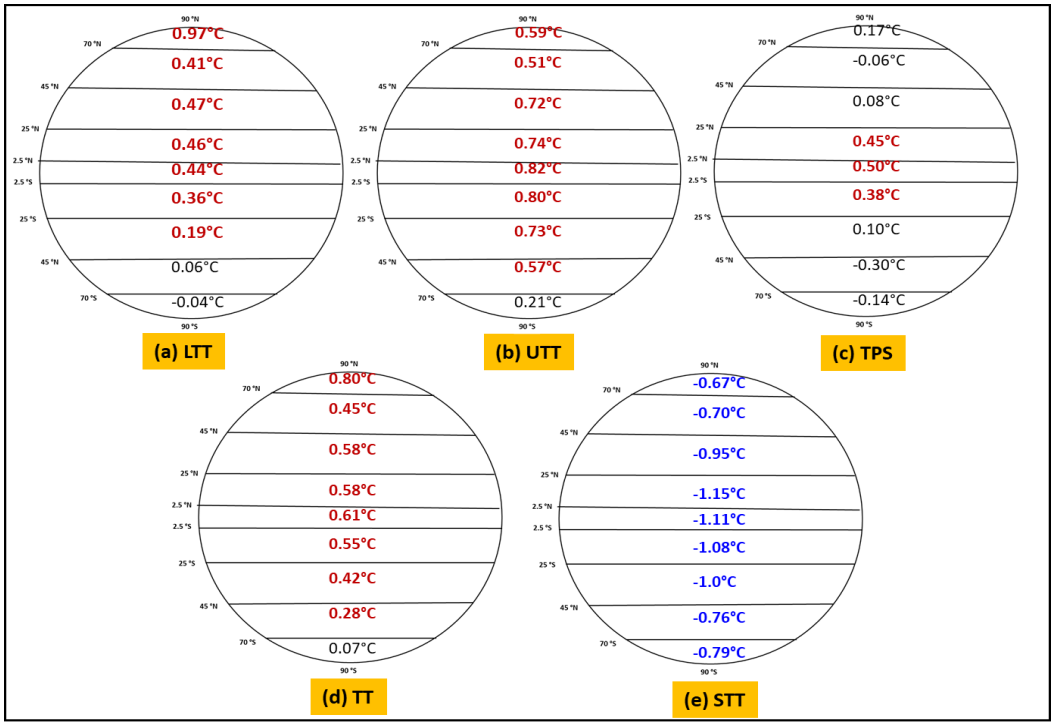

Fig 4.6 Annual Temperature Change during Recent 10-yr (2009-2018) of the 5 Layers over 9 Climatic Zones (bold figures indicate significant changes)

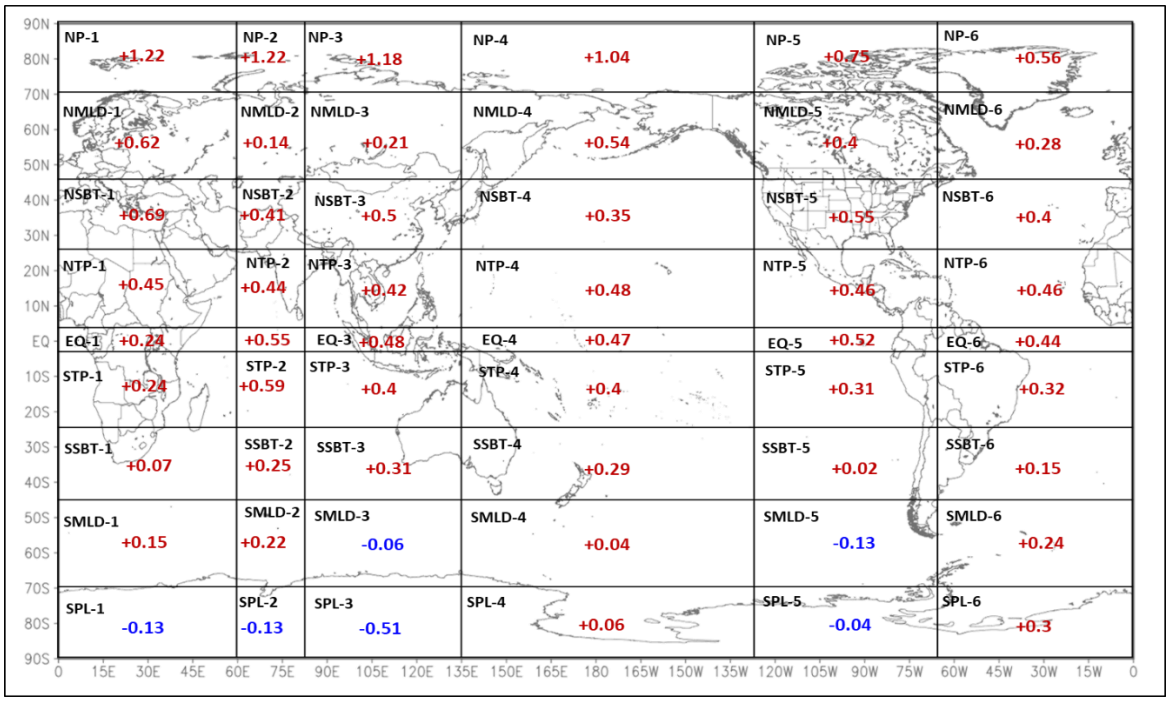

Fig 4.7 Recent 10-yr (2009-2018) changes in annual lower tropospheric temperature(LTT) across 54 geo-subdomains

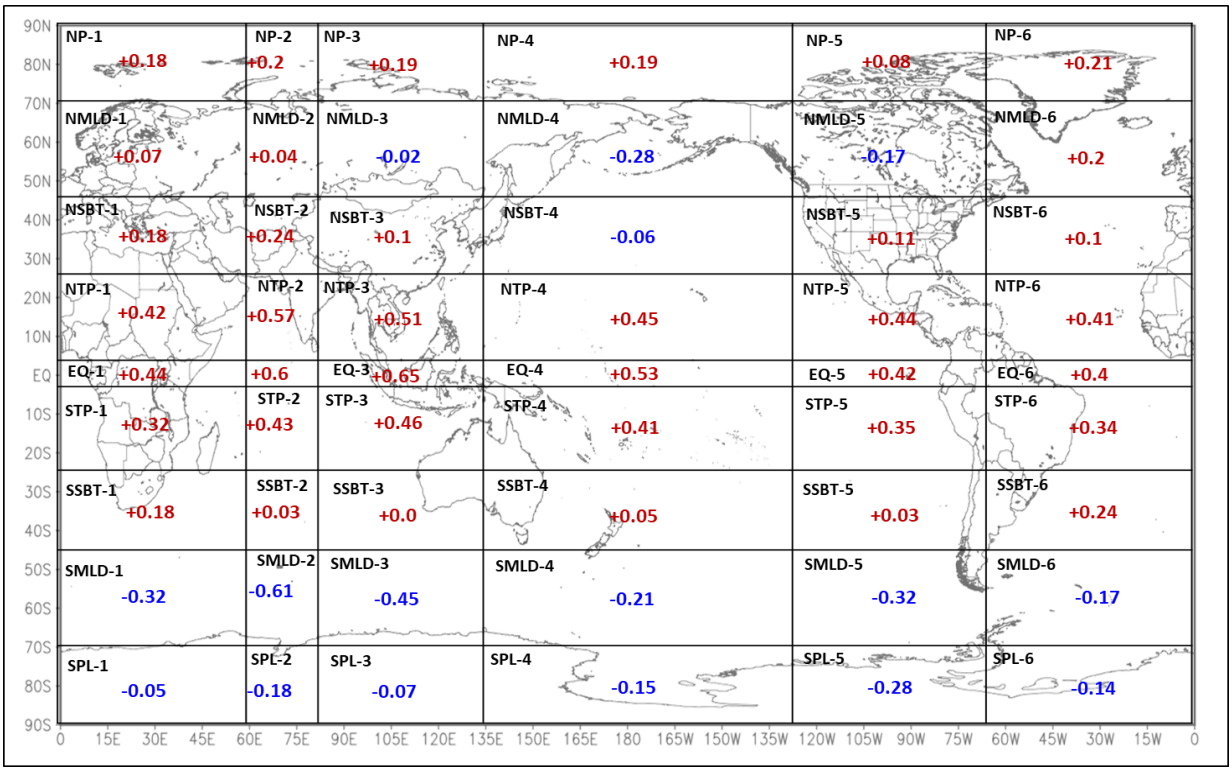

Fig 4.8 Recent 10-yr (2009-2018) changes in annual tropopause temperature(TPS) across 54 geo-subdomains

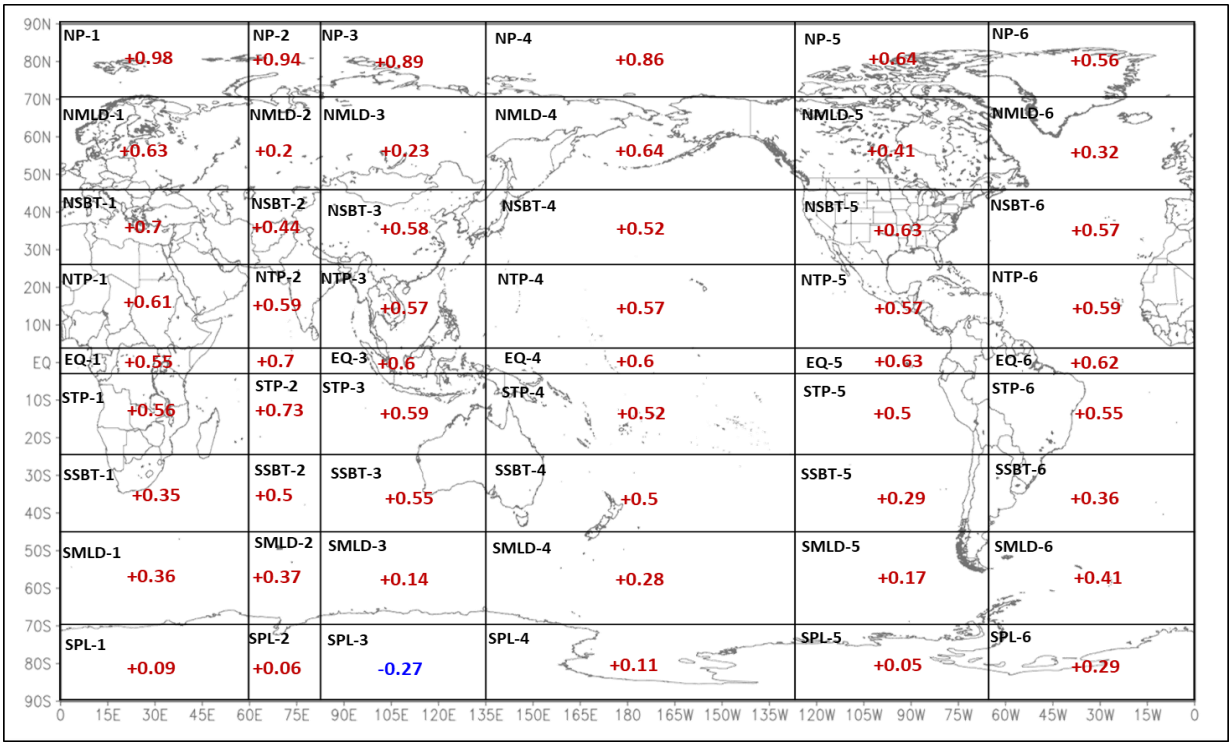

Fig 4.9 Recent 10-yr (2009-2018) changes in annual tropospheric temperature(TT) across 54 geo-subdomains

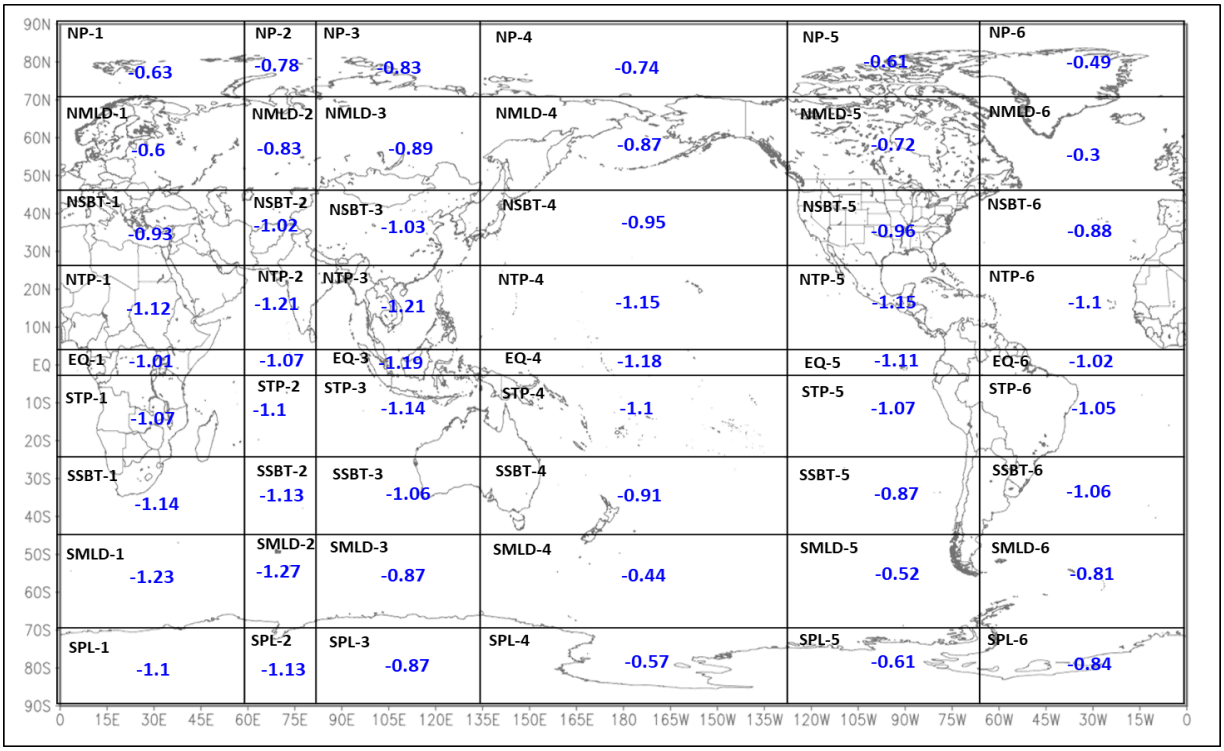

Fig 4.10 Recent 10-yr (2009-2018) changes in annual stratospheric temperature(STT) across 54 geo-subdomains

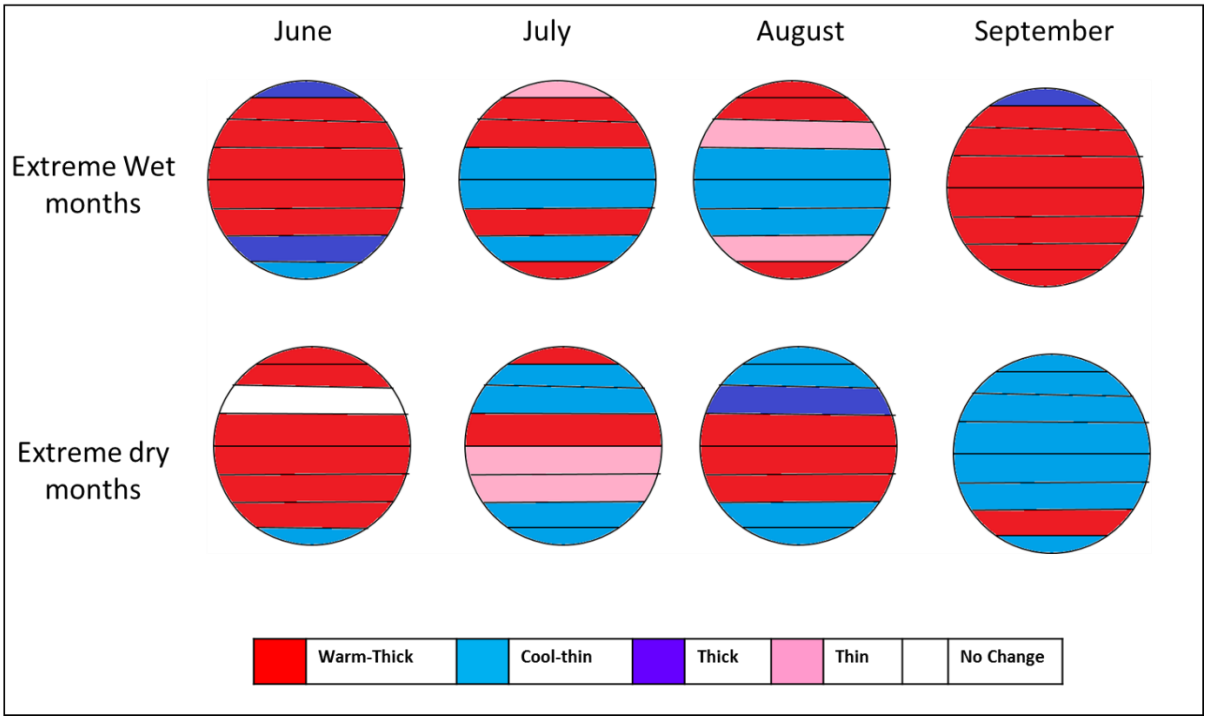

Figure 4.11. Combined tropospheric temperature and geopotential thickness anomalies over global climatic zones during extreme wet and dry months in monsoon season.

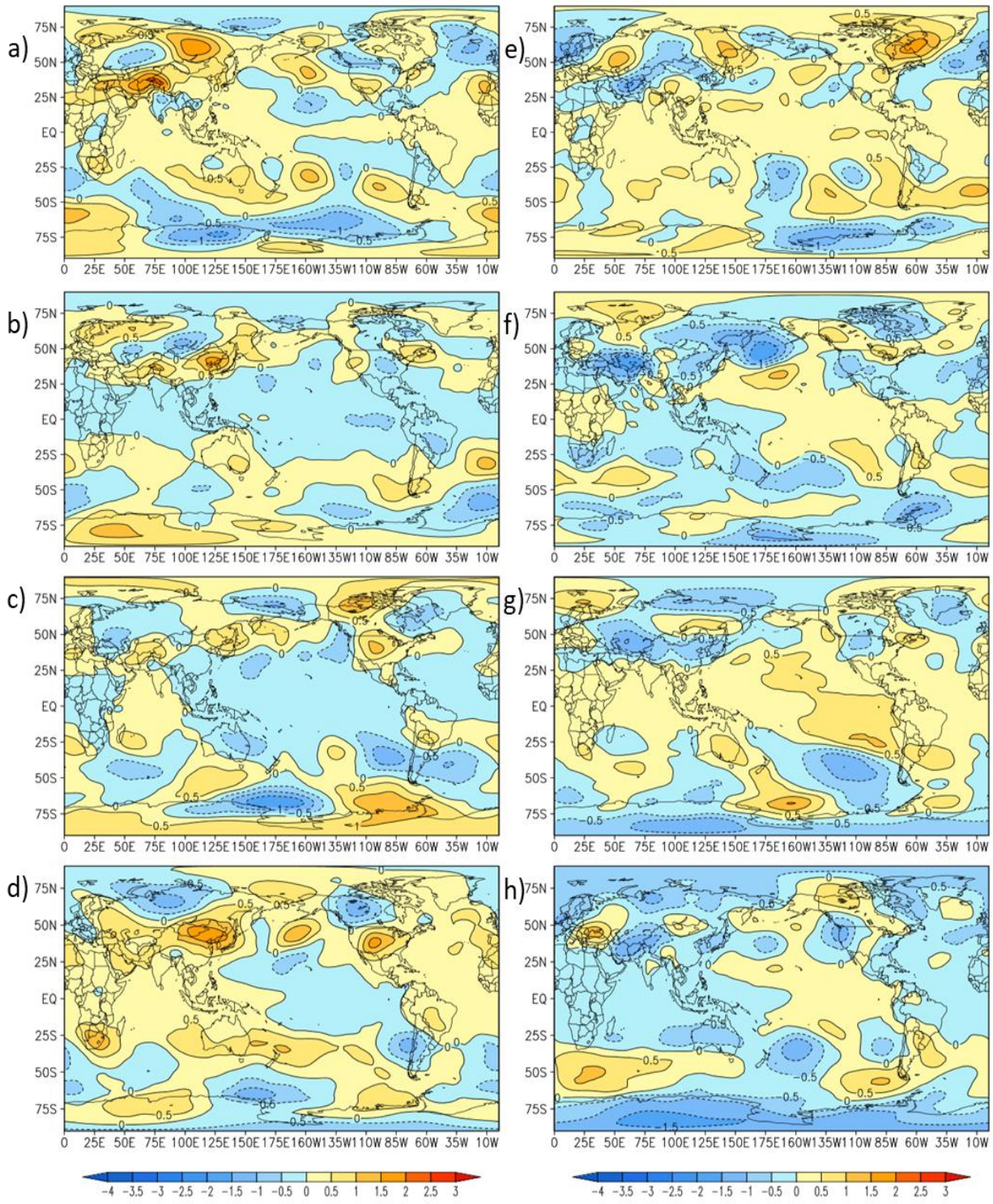

Fig.4.12 Global distribution of tropospheric temperature anomaly during extreme wet and dry months in order a & e) June, b & f) July c & g) Aug and d & h)Sept.

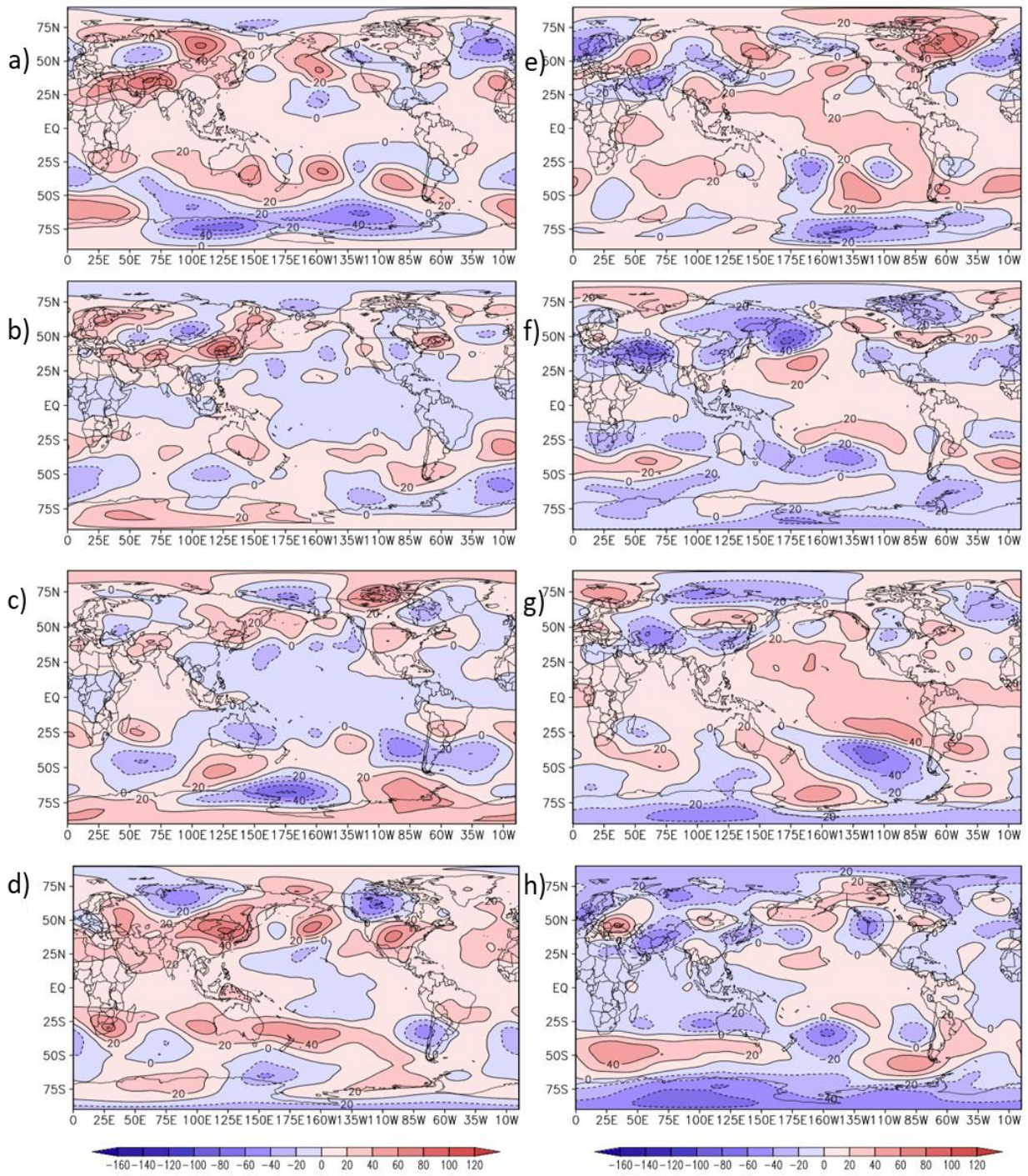

Fig.4.13 Global distribution of tropospheric thickness anomaly during extreme wet and dry months in order a & e) June, b & f) July c & g) Aug and d & h)Sept.

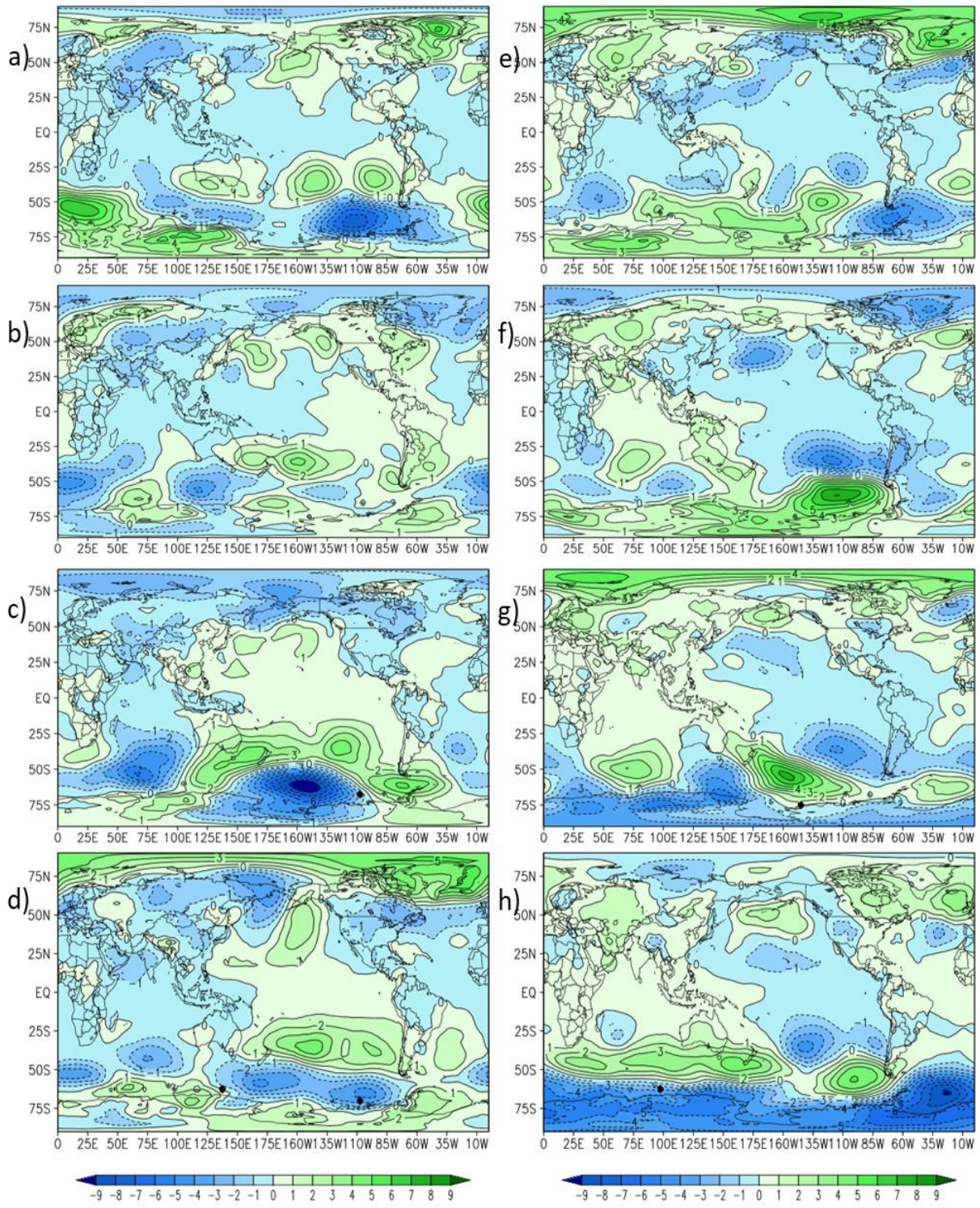

Fig.4.14 Global distribution of mean sea level pressure anomaly during extreme wet and dry months in order a) June, b)July c) Aug and d) Sept.

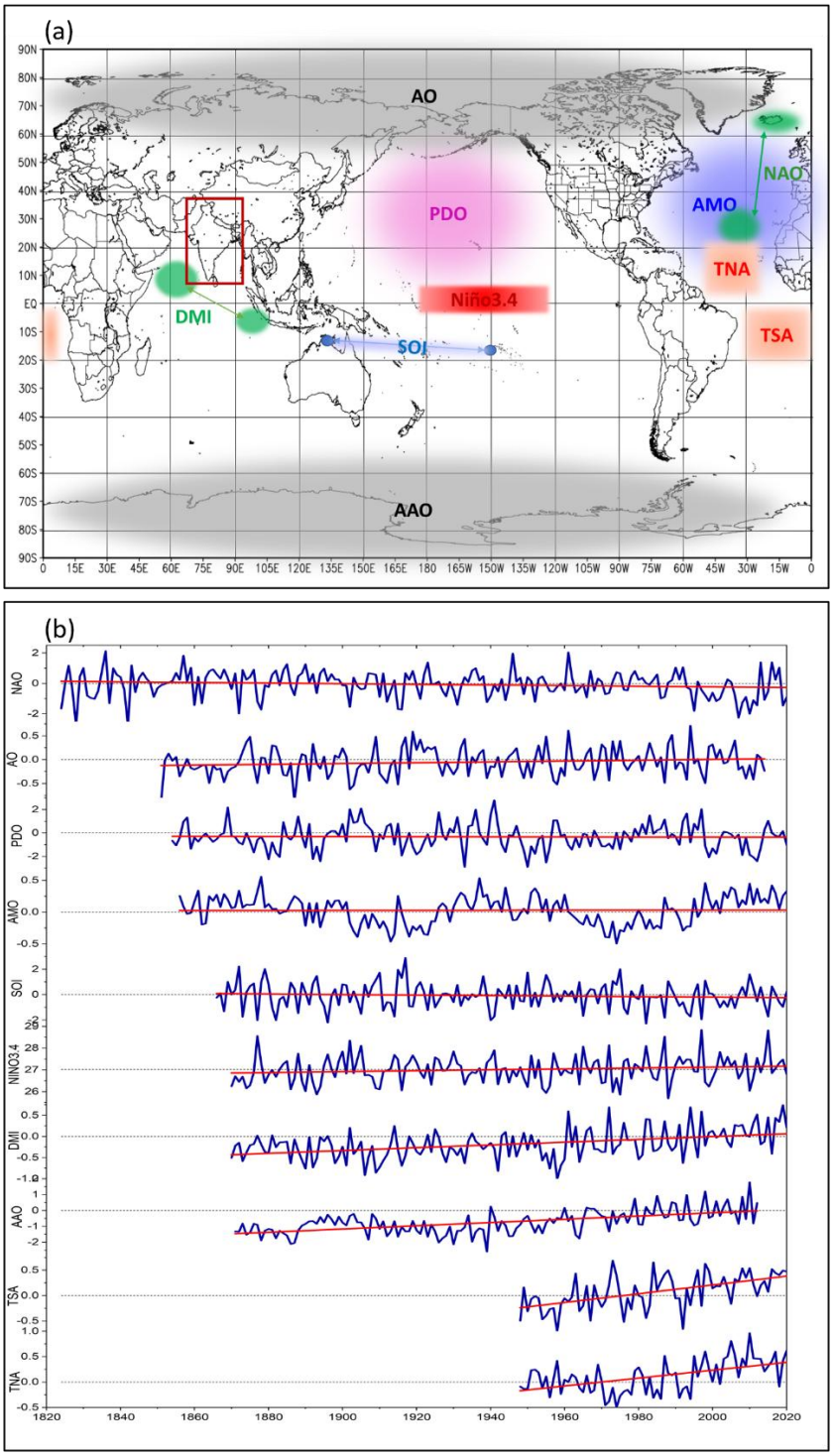

Fig 5.1 Locations/areal coverage of ten selected global climatic Indices surrounding Indian Subcontinent (red square box indicate the study area) shown in top panel. Interannual variations in different global climatic indices during JJAS (red line indicate linear trend) shown in bottom panel

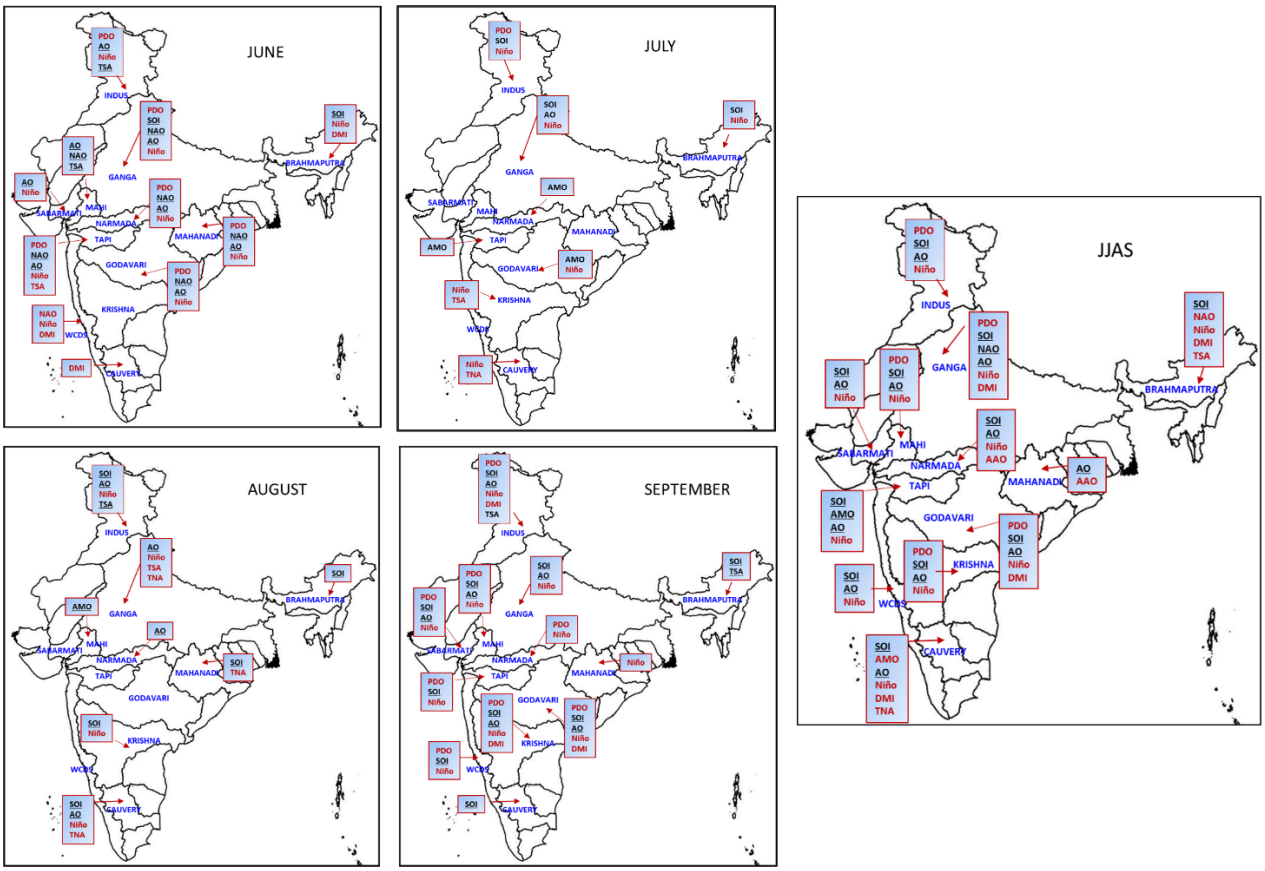

Fig 5.2 Schematic showing spatial distribution of significantly correlated (5% or 1% level of significance) climatic indices with monthly and monsoon rainfall over river basins of India (underlined label indicates +ve and red indicates –ve correlation)

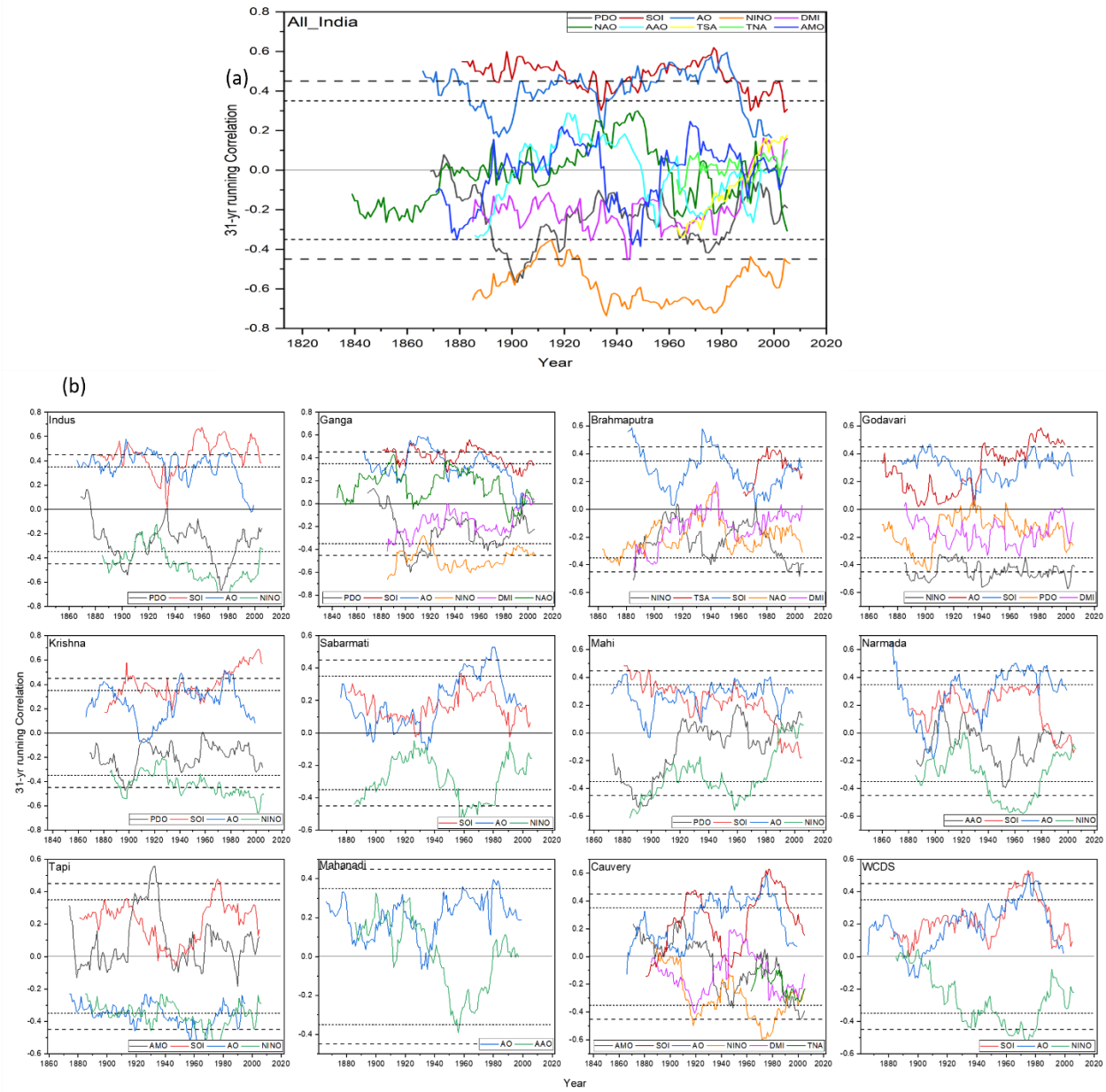

Fig 5.3 31-year running correlations between All India monsoon rainfall and 10 selected climatic indices (Dotted and dashed lines represent significance at 5% and 1% level of significance respectively.) shown in top panel. Bottom panel is for 11 river basins and WCDS and selected climatic indices that are significantly related on long-term basis.

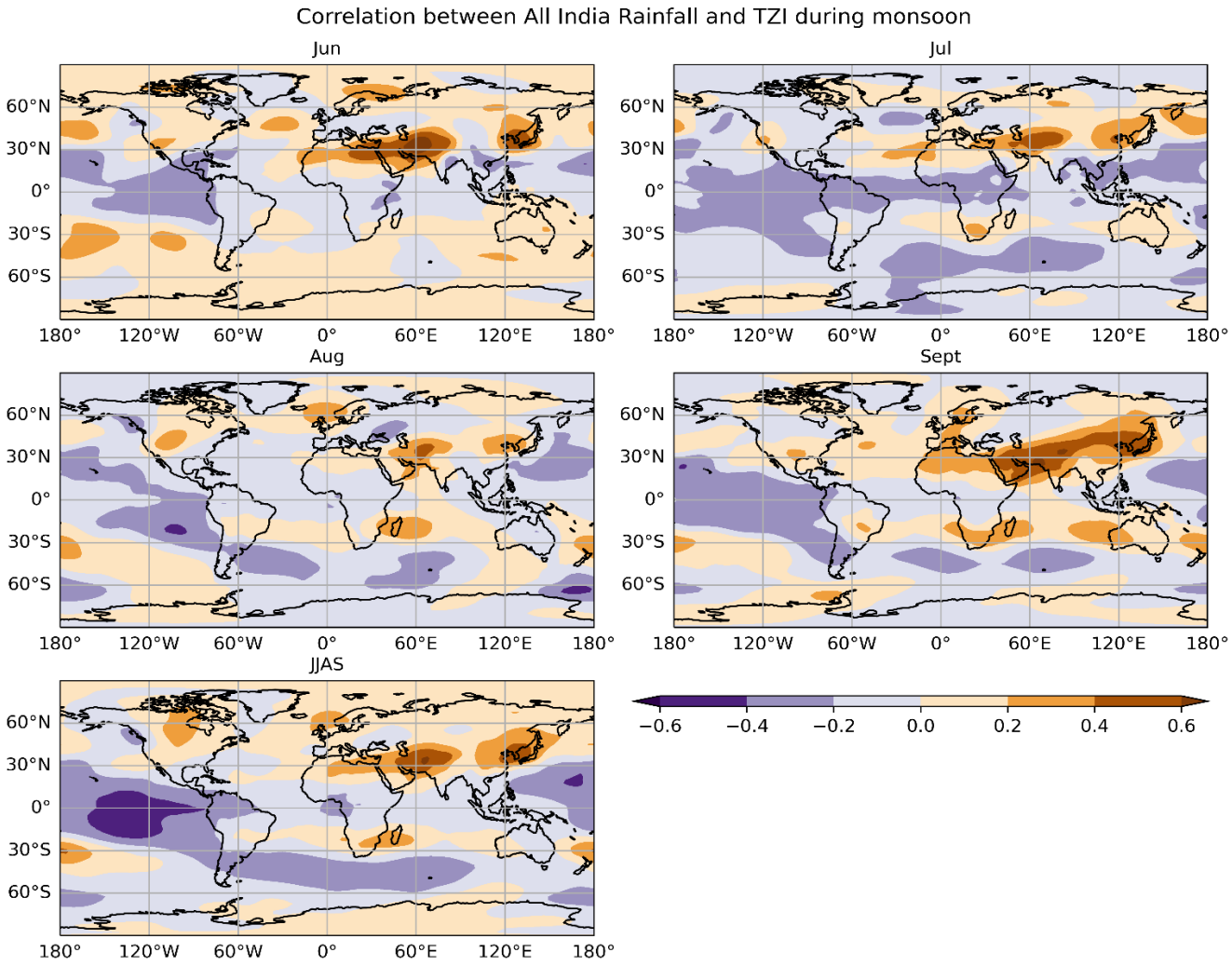

Fig 5.4 Spatial distribution of CC between All India rainfall and TZI index during June, July August, September and whole monsoon season.

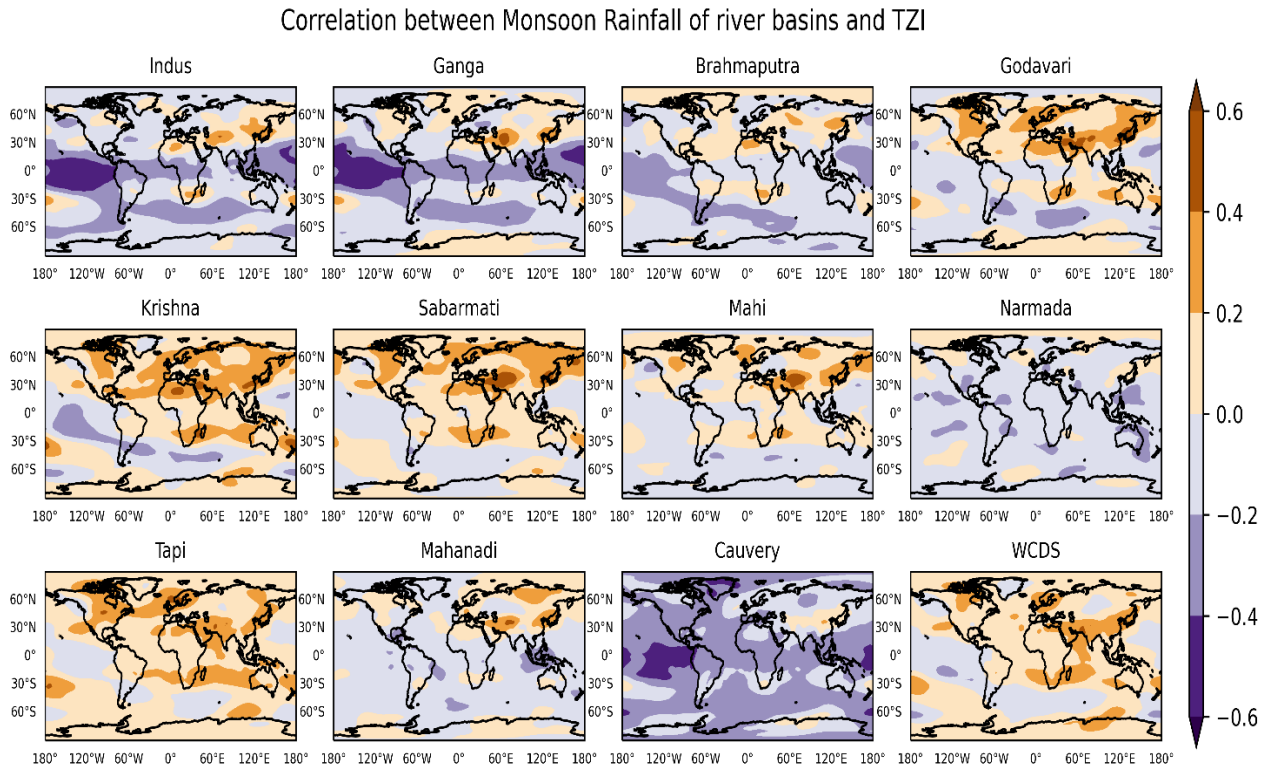

Fig 5.5. Spatial distribution of CC between monsoon rainfall of river basins and TZI index